A STUDY OF THE AXON INITIAL SEGMENT AND PROXIMAL AXON OF NEURONS IN THE PRIMATE MOTOR AND SOMATIC SENSORY CORTICES

By J. J. SLOPER and T. P. S. POWELL†
Department of Human Anatomy, University of Oxford, South Parks Road, Oxford OX1 3QX, U.K.

(*Communicated by C. G. Phillips, F.R.S. – Received* 21 *February* 1978)

[Plates 1–11]

CONTENTS

PAGE

Introduction 174

Material and methods 174

Results 174
- Qualitative features of initial segments and a comparison of the different cell types 174
- Cisternal organs 176
- Spines 177
- The axon beyond the initial segment 178
- The staining of axon initial segments by ethanolic phosphotungstic acid 180
- Quantitative aspects of complete initial segments 184
- Quantitative aspects of stellate initial segments 189

Discussion 190

References 193

Appendix 194

The axon initial segments of pyramidal cells and large and small stellate cells in the primate sensori-motor cortex have a typical membrane undercoating and bundles of neurotubules. Those of pyramidal cells are directed towards the white matter whereas those of large and small stellate cells often run obliquely or towards the cortical surface and may be curved. Cisternal organs in these initial segments are related to symmetrical axon terminals, frequently coming into close apposition to the non-synaptic part of these terminals adjacent to the synapse between the axon terminal and initial segment. The dense plates of cisternal organs and the membrane undercoating of the initial segment are specifically stained by ethanolic phosphotungstic acid (ethanolic PTA). Pyramidal initial segments have spines which receive only symmetrical synapses, as do the shafts of the initial segments of each cell type. The full length of the initial segment was studied for fourteen pyramidal and two large stellate cells. All gave rise to myelinated axons although two pyramidal cells had lengths of unmyelinated axon between the initial segment and myelinated

† Elected F.R.S. 16 March 1978.

axon. One of these lengths of unmyelinated axon made an asymmetric synapse on to a dendrite just after losing its initial segment features. Quantitative analysis of these complete initial segments showed that whereas the diameter of the initial segment and the axon it gave rise to were approximately proportional to the size of the parent cell soma over a considerable range of cell diameters, the length of the initial segment appeared to be unrelated to either its diameter or the size of its parent soma but varied between 30 and 55 μm apparently at random. Synapses were evenly distributed along the full length of the complete pyramidal initial segments, but the density of synapses on the initial segments of supragranular pyramids was about three times that on those of infragranular pyramids and cisternal organs were similarly more frequent in the initial segments of supragranular pyramids.

Introduction

The axon initial segment is thought to be the point at which all the influences acting upon a typical neuron are finally integrated and its output determined and so the structure of this region of the cell is of particular interest. The fine structure of the axon initial segment has been studied with the electron microscope (e.m.) in a number of sites (Conradi 1966, 1969; Palay, Sotelo, Peters & Orkand 1968; Peters, Proskauer & Kaiserman-Abramof 1968; Jones & Powell 1969; Westrum 1970; Kemp & Powell 1971 *a*, *b*) and it has been shown that the initial segment may be recognized by its membrane undercoating and bundles of neurotubules. A large number of initial segments belonging to the different types of neocortical neuron have here been studied mainly in the motor cortex and certain differences between those of the different cell types noted. The distribution of synapses along the length of the initial segment has been determined and in a number of examples the complete length of the initial segment has been studied which has enabled certain quantitative observations to be made. Extensive use of serial sections has made it possible to obtain information about the axon beyond the initial segment and to trace the origin of the most proximal axon collaterals. The ultrastructure of the initial segment has also been studied in material stained in the block with ethanolic PTA and certain specific staining properties of the initial segment noted.

Material and methods

All observations were made on material from the motor cortex (area 4 of Brodmann) or area 3*b* of the somatic sensory cortex of 21 young adult rhesus monkeys (*Macaca mulatta*). These were perfused under hypothermia with a mixture of 4 % paraformaldehyde and 1 % glutaraldehyde following a washout with buffered salt solution. The methods used for the preparation of material for electron microscopy both routinely and using ethanolic PTA staining have been given in detail in a previous paper (Sloper & Powell 1979).

Results

Qualitative features of initial segments and a comparison of the different cell types

The membrane undercoating and bundles of neurotubules in the axon initial segments of cells of the motor and somatic sensory cortices of the monkey have the same appearance as those described in sensory cortical areas of other species (Peters *et al.* 1968; Jones & Powell

1969; Westrum 1970) and these features allow an initial segment to be identified when seen in isolation in the neuropil. Initial segments of pyramidal cells arise from the base of the perikaryon (figures 1–3, plate 1) or from a basal dendrite and one cell was found where the initial segment arose from a dendrite 30 μm from the soma. Pyramidal initial segments are often very straight, although the first part may taper slightly, and they are always directed towards the white matter. They are closely aligned with the 'grain' of the cortex so that continuous long lengths of initial segment are mostly found in sections which are cut accurately perpendicular to the cortical surface and contain very long lengths of apical dendrite. There is often, however, a kink in the initial segment, usually towards the lower end, but the part of the axon below the kink is generally in line with that above so that in a single section an otherwise continuous initial segment has a short break and serial sections are required to establish the continuity. A similar kink is often present in initial segments of pyramidal cells which have been impregnated by the Golgi technique. Pyramidal initial segments usually give rise to myelinated axons and in one instance the axon was traced to its first node of Ranvier where it gave rise to two collaterals (figures 1–13, plates 1 and 2). The initial segments of Betz cells are similarly orientated to those of smaller pyramids (figures 14 and 15, plate 3) but in the larger pyramids the first part of the initial segment often arches away from the soma before becoming straight. The typical undercoating and bundles of neurotubules are present but are much less obvious than in smaller pyramids because of the much greater overall size of the initial segment (figures 14–19, plates 3 and 4).

The initial segments of large stellate cells may arise from the cell soma (figures 20–22, plate 5) or from a dendrite; those of small stellate cells have only been found arising directly from the cell soma but it is possible that this is because of the relative infrequency with which dendrites of this cell type are cut in continuity with the cell soma (Sloper, Hiorns & Powell 1979). The initial segments of both stellate cell types have a more pinched-off origin than those of pyramids. They do not have a single preferred orientation and consequently long lengths of them are cut in continuity with the cell soma less frequently than with pyramidal cells. The initial segments of large stellate cells in particular are also often curved, which reduces the chance of long lengths being found in a single section. Because of these factors, the isolated vertical lengths of initial segment often seen in the cortical neuropil probably arise mainly from pyramidal cells.

The membrane undercoating of the initial segment appears to be the same in the different types of neuron in the neocortex. When an initial segment gives rise to a myelinated axon (e.g. figure 3), the undercoating stops at this point; in two examples where the initial segment gave rise to an unmyelinated axon the undercoating extended for a similar distance from the soma and then stopped in a somewhat ragged fashion and the bundles of neurotubules became dispersed approximately at, or just proximal to, the end of the undercoating. Complex vesicles are often seen in the cytoplasm of initial segments and often appear to be budding from the surface membrane. They may be seen to be taking in cytoplasm from adjacent structures, this presumably giving rise to the double walled complex vesicle sometimes seen. The initial segments of pyramidal cells and both large and small stellate cells receive symmetrical synapses from axon terminals and these terminals may in addition make a synapse on to other components of the neuropil such as dendrites. The synapses on to pyramidal initial segments are evenly distributed along the whole length of the initial segment (see below) and those on to large stellate initial segments may occur right up to the beginning of the

myelin sheath. Qualitatively large stellate initial segments appear to receive fewer synapses than pyramidal initial segments and those of small stellate cells fewer than either.

Cisternal organs

Cisternal organs consist of an alternating arrangement of membranous sacs and plates of dense material. In single sections they may be very large and extend for a considerable distance along the initial segment (figure 23, plate 6) and serial sections show that their position in the initial segment may vary between the periphery and centre. They often become closely apposed to the plasma membrane and although any component of the neocortical neuropil may be found adjacent to an initial segment, this close apposition is found almost exclusively opposite the non-synaptic region of a symmetrical axon terminal and this terminal usually makes a synapse with the initial segment elsewhere (figures 23–28). This specificity of apposition was confirmed quantitatively; of the large number of cisternal organs studied, 62 were found to come into close apposition with the plasma membrane of the initial segment in a single section. This apposition occurred opposite the non-synaptic part of a symmetrical axon terminal in 56 examples (90 %), with five being opposite glia and one opposite an unmyelinated axon. Six of the 56 examples opposite symmetrical terminals also extended opposite glia and

---

Description of plate 1

Figures 1–13 show a pyramidal axon initial segment traced in continuity from the cell soma to the first node of Ranvier of its myelinated axon.

Figure 1. Pyramidal cell soma (P) in layer III of motor cortex with the first part of its axon initial segment (is) directed towards the white matter and receives two synapses (two arrowheads). (Section 45; magn. × 4600.)

Figure 2. Serial section to figure 1 showing the continuation of the axon initial segment and three further synapses upon it (two arrowheads). The same dendrite (d) is marked on both sections; this and other landmarks could be followed through the intervening sections. (Section 36; magn. × 8400.)

Figure 3. Axon initial segment of figures 1 and 2 traced to the beginning of its myelin sheath (large arrowheads) in a serial section. The same axon, a, is marked in both figures 2 and 3; this and other landmarks were traced through the intervening sections. Note the large number of synapses received by the initial segment right up to the beginning of the myelin sheath (two arrowheads). (Section 26; Magn. × 8400.)

Description of plate 2

Figures 4–13 show the myelinated axon of the cell seen in figures 1–3 traced in continuity to its first node of Ranvier where it gives rise to two collaterals, the second of which was myelinated. In all the figures the proximal end of the axon is to the left.

Figure 4. The axon (a) emerging from the myelin sheath of its first internode. The unmyelinated continuation of the axon (u) was traced in continuity with the proximal (left) end of the axon in figure 9 where the next myelin sheath started. Note that the unmyelinated continuation of the main axon is well past dendrite (d). (Section 44; magn. × 29000.)

Figures 5–8. Serial sections 34, 33, 31 and 29 respectively of the same axon as figure 4. Note how in progressing to the lower numbered sections the collateral (b) becomes separated from the parent axon. The continuation of the parent axon (u) was followed in serial sections of increasing number. (Magn. × 22000.)

Figure 9. This shows the continuation of the parent axon (u) which was traced in continuity through the sections between 44 (figure 4) and 65. The parent axon has now become myelinated again (a′). Note the cisternal organ-like structure (arrowhead) in the expansion from which the second collateral (b′) arises. (Section 65; magn. × 29000.)

Figures 10–13. Sections 69, 73, 74 and 81 respectively show the second axon collateral (b′) becoming separated off from the continuation of the parent axon (a′). The collateral can be seen to become myelinated as it is traced through these serial sections. (Magn. × 22000.)

FIGURES 1–3. For description see opposite.

(*Facing p.* 176)

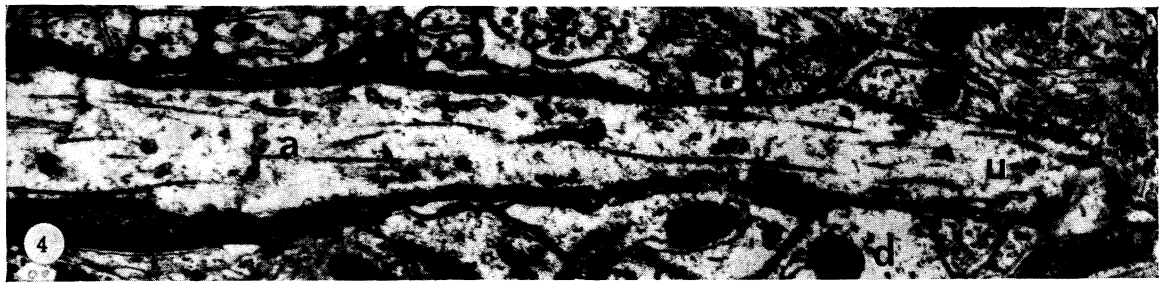

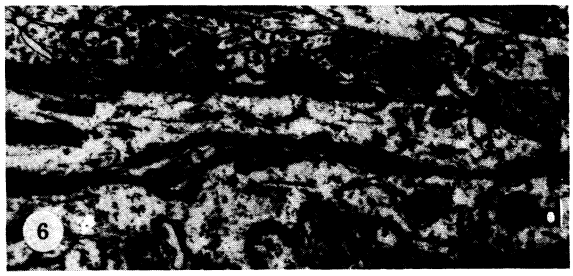

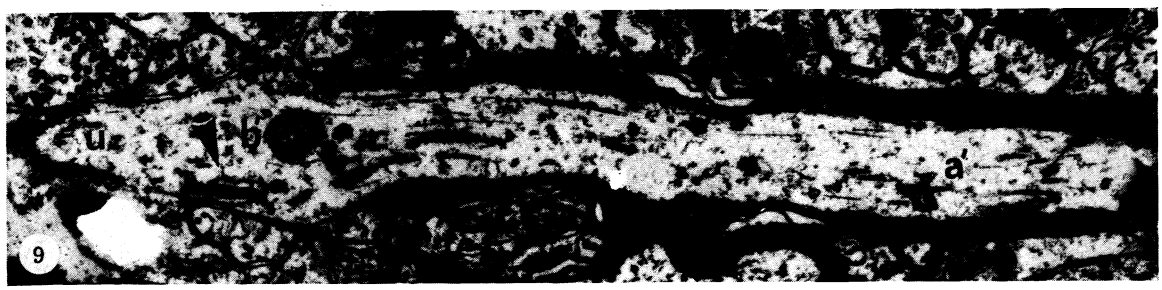

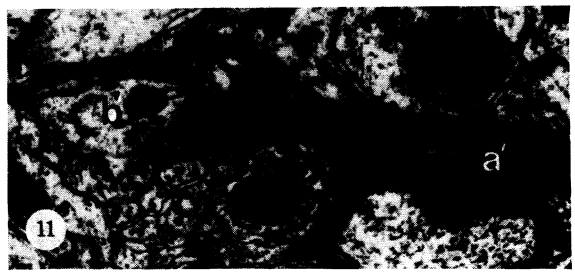

FIGURES 4–13. For description see page 176.

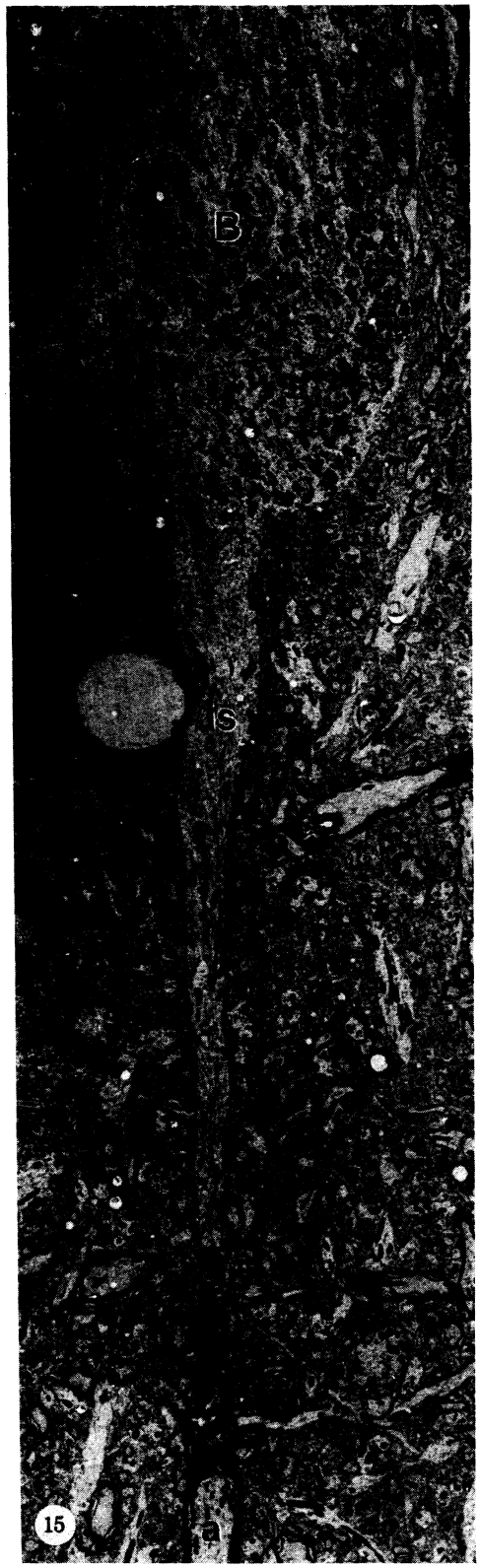

FIGURE 14. A Betz cell (B) with apical dendrite (ad) in layer V of the motor cortex. In serial sections this cell was shown to give rise to the axon initial segment of figures 15–19. (Magn. × 1300.)

FIGURE 15. Axon initial segment (is) of the Betz cell of figure 14 in a serial section. The nucleus of the cell is no longer in the plane of the section although a considerable amount of cytoplasm is still seen. Much of the apparent tapering of the initial segment is due to its not being parallel to the plane of the section. The continuity of the initial segment with the myelinated axon (a) was confirmed in serial sections (e.g. figure 19). (Magn. × 3000.)

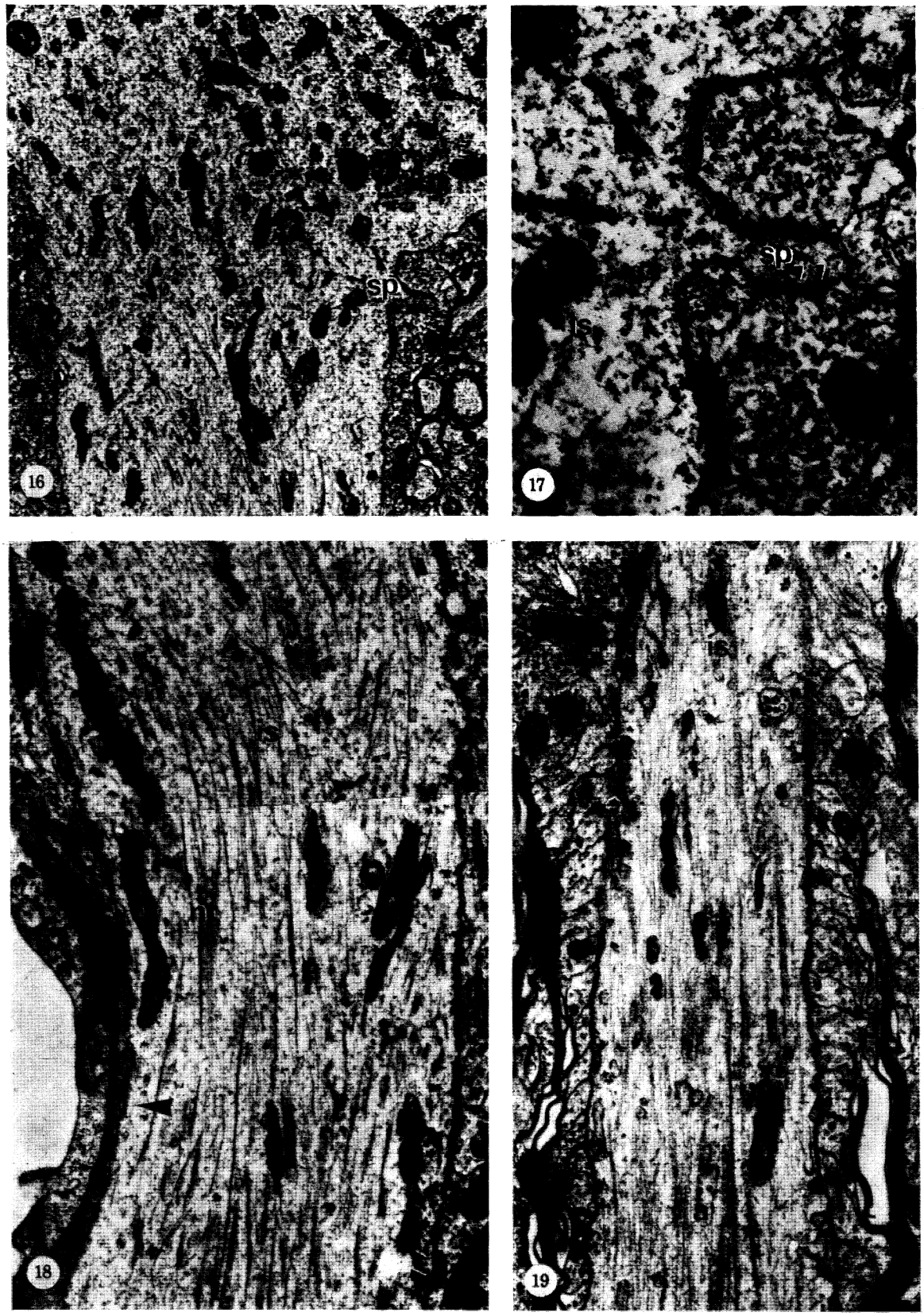

FIGURES 16–19. For description see opposite.

examples found opposite glia were shown to be related to symmetrical terminals in adjoining serial sections. The neuropil apposed to the initial segment was analysed in a single section of two of the complete supragranular and one of the infragranular pyramidal initial segments; the non-synaptic part of symmetrical axon terminals was found to occupy 31, 28 and 23% of the outlines of these three initial segments with glia occupying 40, 26 and 25%. Ninety per cent of the cisternal organs were therefore found closely apposed to the plasma membrane opposite a profile that occupied only about 30% of the outline of the initial segment and it seems likely that those found opposite other structures in single sections are related to terminals in serial sections. The close apposition does not extend beneath the synaptic membrane complex itself although the cisternal organ may, this being seen particularly well in transverse section (figures 24–27). A single cisternal organ has been found to come into close apposition with the non-synaptic parts of as many as three symmetrical axon terminals. The cisternal organ may also be closely associated with a mitochondrion (figure 23). In a number of examples the membranes of both the initial segment and symmetrical terminal appear denser over the area of apposition of the cisternal organ and there is granular material in the extracellular cleft between them, but in the majority the membranes are unspecialized. There is no aggregation of vesicles in the terminal opposite the area of apposition.

An exposed postsynaptic membrane specialization has occasionally been found apposed to an axon initial segment (figures 29, 30) and in these examples a subsurface cistern has been found in the initial segment immediately apposed to the exposed thickening.

Spines

Some initial segments in the neocortex are found to have spines (figures 31–37, plate 7) and when cut in continuity with their cell somata, these initial segments have arisen from pyramidal cells in all cases; one was found on the first part of the initial segment of a Betz cell (figures 16 and 17). The form of the spine varies considerably with most of them being small sessile pegs, but there is a complete range of forms from these pegs through to large pedunculated spines (figure 38). Spines have been found to receive synapses from one or two axon terminals and these have been of the symmetrical type. A terminal may make a synapse both on to a spine and directly on to the shaft of the parent initial segment and a terminal may make synapses on to two adjacent spines on the same initial segment (figure 37). Two or more spines are frequently found close together on an initial segment. The undercoating

---

Description of plate 4

Figure 16. Part of the axon hillock and the proximal part of the Betz cell axon initial segment of figure 14. There is a spine (sp) on the initial segment (is) which receives synapses from two axon terminals. (Magn. × 9000.)

Figure 17. High power of the axonal spine of figure 16. The lower synapse is clearly of the symmetrical type (two arrowheads) and in adjacent serial sections the other synapse was symmetrical; both terminals also made synapses on to the shaft of the initial segment as well as on to the spine. No other synapses were present on the spine. (Magn. × 32000.)

Figure 18. High power of part of the shaft of the Betz cell initial segment of figure 15. Note the membrane undercoating (e.g. single arrowhead) and bundle of neurotubules (nt); both of these features are less striking than usual because of the large diameter of the initial segment. Note also the two synapses it receives (two arrowheads). (Magn. × 14000.)

Figure 19. High power of the last part of the Betz cell initial segment and the beginning of the myelinated axon (a) in a serial section to figure 15. (Magn. × 24000.)

of the initial segment usually continues into the spine and sometimes appears to be giving rise to a complex vesicle within the spine. A cisternal organ may extend into a sessile spine (figures 33 and 35) and particularly in the longer spines, it may closely resemble the spine apparatus of dendritic spines (Gray 1959).

The axon beyond the initial segment

Twelve of the fourteen pyramids and both of the large stellate cells in which the whole length of the initial segment was obtained gave rise to typical myelinated axons of similar diameter to the parent initial segment. The first part of the myelinated axon contains a greater concentration of mitochondria and ribosomes than do most myelinated axons and may therefore be recognized when cut in isolation. In one pyramidal cell (figures 1–13) the myelinated axon was followed towards the white matter and the myelin sheath of the first internode was found to finish 120 μm from the soma, the length of the myelinated internode being

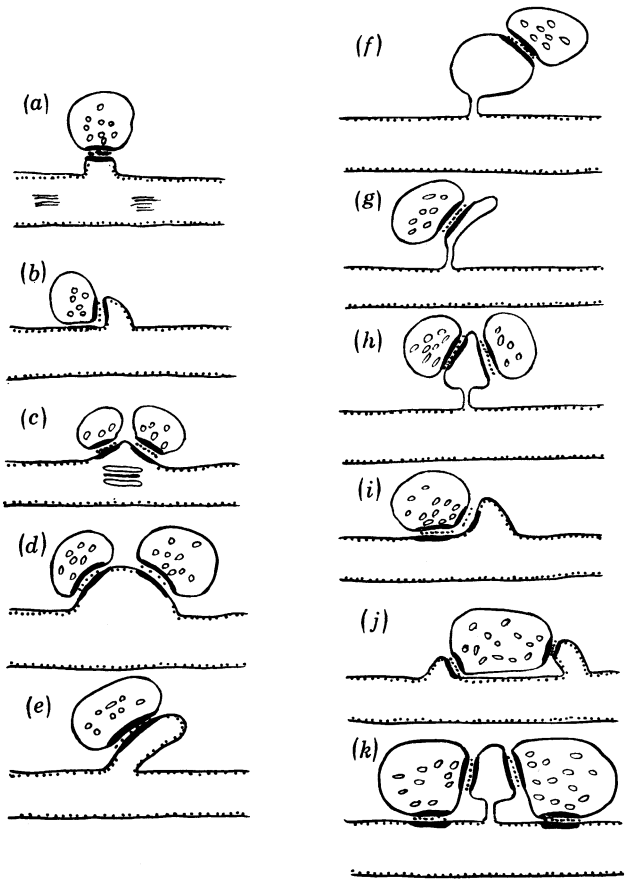

FIGURE 38. Diagrams showing the variety of shapes and synaptic relations of the spines found on axon initial segments. (*a*), (*b*) small sessile spines receiving a single synapse; (*c*), (*d*) large sessile spines of differing shapes, each receiving two synapses; (*e*) oblique elongated peg-like spine; (*f*) spine with a narrow neck and expanded spherical head receiving one synapse; (*g*) spine with narrow neck and elongated head receiving one synapse; (*h*) conical spine with narrow neck which receives two synapses; (*i*) sessile spine receiving a synapse from an axon terminal which also makes a synapse on to the adjacent shaft of the initial segment; (*j*) a single axon terminal which makes synapses on to two adjacent sessile spines; (*k*) a spine with a conical head and narrow stalk which receives two synapses, each from a terminal which also makes a synapse directly on to the shaft of the initial segment.

approximately 80 μm and of the initial segment 42 μm; the mean diameter of the parent cell was 17 μm and the axon diameter was 1.3 μm. The axon gave off a collateral immediately beyond the end of the myelin sheath, continued unmyelinated and gave off a second collateral 5 μm more distally; the main axon became myelinated beyond this point. The first collateral left the main axon at approximately a right angle and was unmyelinated for the 1.5 μm for which it could be followed and it had a diameter of 0.4 μm at that point. The second collateral left the opposite side of the parent axon and was directed obliquely downwards. It became myelinated immediately, the myelin being contiguous, if not continuous, with that of the parent axon and had an external diameter of 0.55 μm.

In two of the pyramidal cells, both of 17 μm mean diameter and from layer II of the motor cortex, the initial segment gave rise to an unmyelinated axon which became myelinated considerably further from the cell soma. In one of these the cell gave rise to a typical descending initial segment which curved forward through a number of serial sections and then became parallel to the plane of the sections (figures 39–51, plates 8 to 10). Five spines were found on this region of the initial segment and also a number of synapses directly on its shaft. The membrane undercoating ended rather patchily at about 43 μm from the cell soma and the bundles of neurotubules became dispersed at about this level (figures 43–45). Two afferent symmetrical synapses were found on the initial segment distal to this point, the last at 52 μm from the cell soma. Immediately proximal to this last afferent synapse the initial segment/unmyelinated axon made an efferent synapse on to a dendrite (figures 43, 45, 47 and 48). This was within 0.5 μm of the last afferent synapse, proximal to it and about 3.5 μm from the next most proximal afferent symmetrical synapse so there was a serial axo-axonic synaptic arrangement within a small region. The membrane specialization of the efferent axo-dendritic synapse had the typical structure of an asymmetric synaptic complex, including presynaptic projections. The synaptic vesicles were round and were fairly clustered in the region of the membrane complex but were not as restricted as in a typical dendro-dendritic synapse in the motor cortex (Sloper & Powell 1978). The dendrite postsynaptic to this efferent synapse was followed through 41 serial sections and over a length of approximately 3 μm it received 8 synapses, a number of which were asymmetric (figures 45, 47–49). Its shape was slightly varicose and it contained prominent microtubules, a considerable number of ribosomes and a mitochondrion and so was typical of a dendrite of a large stellate cell (Sloper, Hiorns & Powell 1979). Beyond these afferent and efferent synapses the 'initial segment' continued as an unmyelinated axon with a diameter of approximately 0.6 μm. At 65 μm from the soma an exposed membrane thickening on a spine was apposed to the axon and had induced a small sac in the axon (cf. Pinching & Powell 1972). The axon had a bulbous expansion 75 μm from the soma and the serial sections showed this to be the origin of a collateral of 0.5 μm diameter. The junctional region contained ribosomes and scattered vesicles but the comparatively regular arrangement of the tubules of the axon became disorganized. At 95 μm from the soma the axon expanded and gave rise to a second collateral. The axonal membrane had an undercoating in this region which was not present above and below and the tubules again became scattered and could be seen to pass into both the main axon and the collateral, although individual tubules were not seen to branch. The main axon continued beyond the origin of the collateral for a further 8 μm and then acquired a typical myelin sheath and became a myelinated axon 0.5 μm diameter at 103 μm below the parent soma (figure 51). This cell and axon are shown diagrammatically in figure 50.

The second pyramidal cell also gave rise to a typical descending initial segment which received symmetrical synapses and had a spine. Its undercoating finished at approximately 40 μm from the soma, distal to the last afferent synapse, and the axon continued unmyelinated for 50 μm and then became myelinated at 90 μm from the cell soma. The cytological features of the unmyelinated part of the axon were very similar to the previous example and an exposed thickening on a dendrite had become apposed to this axon and had induced a sac in it as in the other example. A collateral was given off immediately proximal to its myelin sheath.

The staining of axon initial segments by ethanolic PTA

Examination of unstained sections from blocks stained with ethanolic PTA confirmed previous observations that this method stains specifically the membrane specializations of the synaptic complex (Bloom & Aghajanian 1968) and the dense plates of the spine apparatus (Adinolfi 1971) (figure 62, plate 11). In this material certain profiles were found which were outlined in black and stood out clearly from the rest of the neuropil. These were identified as axon initial segments by the typical way they emerged from cell somata, particularly from the bases of pyramidal cells (figure 52), by their shape and predominantly vertical orientation, by the faintly stained bundles of neurotubules they contained and by the synapses they received (figure 53); one example both received synapses and entered a myelin sheath (figure 56), a combination of features in the neocortex which only occurs on axon initial segments. Examples were also observed to arise from dendrites (figure 54).

The black outline of the initial segment was due to specific staining of a membrane undercoating by the PTA (figures 53 and 55). This undercoating is found immediately beneath the plasma membrane (electron lucent in PTA stained material) and corresponds in position and fine structure to that seen in normally prepared material. At high magnifications the undercoat can be seen to have a dentate appearance (figure 55 and 57) and when seen face on it has a discontinuous granular structure (figure 56). There is also a less densely stained layer of granular material immediately outside the plasma membrane of the initial segment (figure 55), (Peters *et al.* 1968); this is particularly well shown in this material where the membrane itself is unstained. The membrane undercoating starts a short distance from the cell soma and continues to the beginning of the myelin sheath and into at least some spines (figure 60) but stops immediately adjacent to the postsynaptic specializations of synapses. Complex vesicles can be seen both in axon initial segments and apparently budding from their surfaces (figure 61).

Description of plate 5

Large stellate cell initial segment. The relative positions of figures 20 to 22 are given by the axons a and x marked in all three serial sections.

Figure 20. Large stellate cell (LS) from layer IV of the motor cortex with an axon initial segment (is) directed toward the pial surface. Note the large size of the cell soma, its abundant cytoplasm full of organelles and the large number of synapses it receives (arrows). The large arrowhead indicates the first part of the myelinated axon of this cell as shown by serial sections. (Section 1; magn. × 4000.)

Figure 21. Serial section showing the first part of the initial segment of the large stellate cell in figure 20. Note the lack of synapses on the initial segment although synapses are present on the immediately adjacent cell soma. (Section 7; magn. × 9000.)

Figure 22. The initial segment of the large stellate cell of figure 20 showing it entering its myelin sheath. (Section 8; magn. × 9000.)

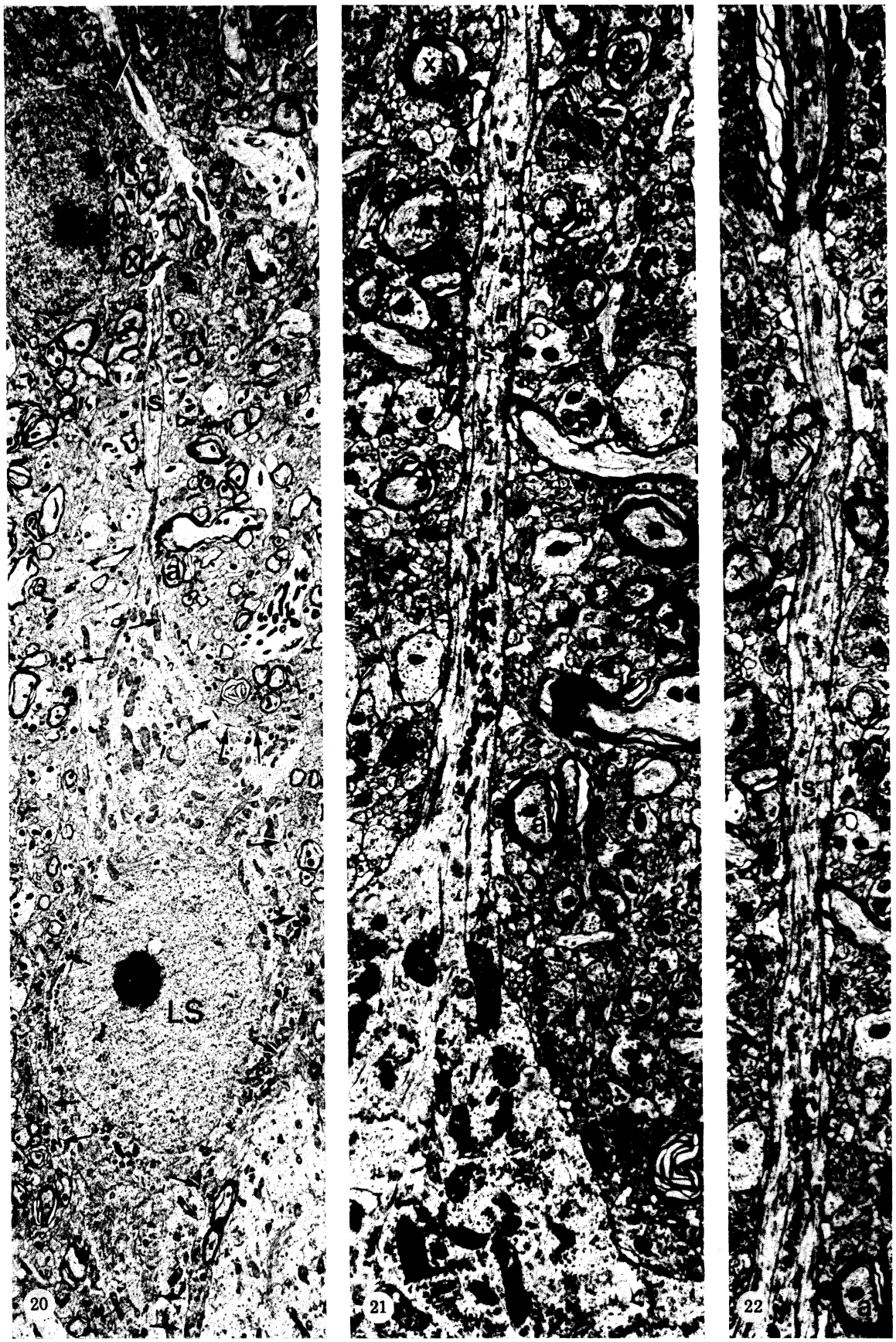

FIGURES 20–22. For description see opposite.

(*Facing p.* 180)

Description of plate 6

Cisternal organs and subsurface cisternae in initial segments.

Figure 23. Cisternal organ (co) in a pyramidal axon initial segment (is). Note how it becomes closely apposed to the plasma membrane of the initial segment opposite the non-synaptic regions of two axon terminals t_1 and t_2, but avoids the synaptic membrane complex. Terminal t_2 made a symmetrical synapse on to the initial segment in the region of the large arrowhead in an adjacent section. Note also the associated mitochondrion (m). (Magn. × 29 000.)

Figures 24–27. Adjacent serial sections showing an axon initial segment and cisternal organ cut transversely in sections parallel to the pial surface. Note how the cisternal organ is closely applied to the initial segment membrane opposite the non-synaptic part of the axon terminal (arrow) but consistently avoids the synaptic region itself, where the terminal makes a symmetrical synapse on to the initial segment. (Magn. × 48 000.)

Figure 28. A cisternal organ showing its close apposition to the plasma membrane of the axon initial segment opposite the non-synaptic region (arrow) of the axon terminal which makes a symmetrical synapse on to the initial segment. (Magn. × 53 000.)

Figure 29. An exposed membrane thickening on a small dendrite (d). This has become apposed to an axon initial segment in which there is an associated subsurface cistern (sc). This association is the same as that seen when exposed membrane thickenings become apposed to dendrites or cell somata. Note the mitochondrion (m) associated with the subsurface cistern, the membrane undercoating and neurotubules of the initial segment and the synapse it receives (two arrowheads). (Magn. × 29 000.)

Figure 30. The exposed membrane thickening and associated subsurface cistern (sc) of figure 29 at a greater magnification. (Magn. × 67 000.)

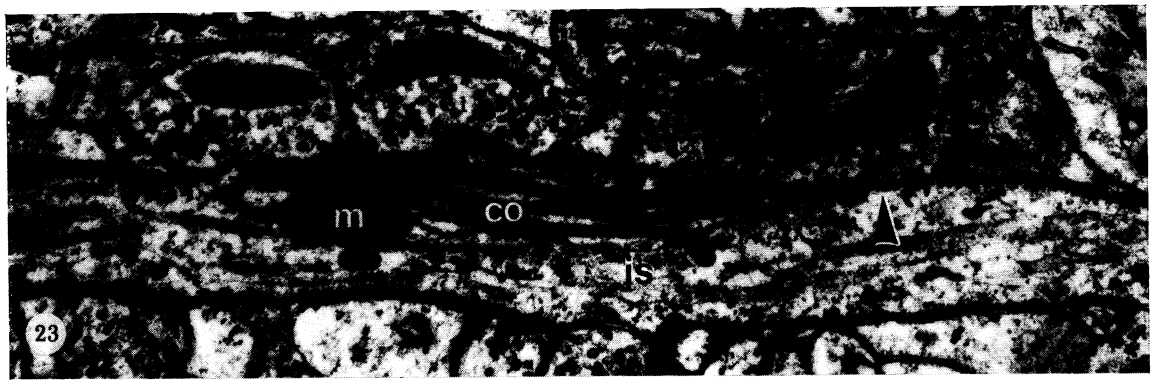

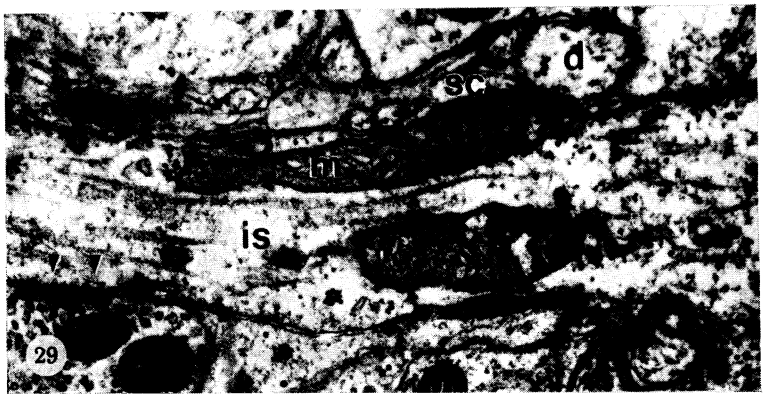

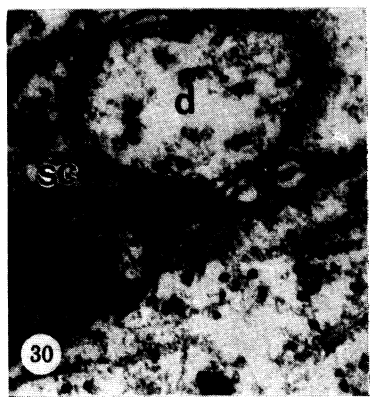

FIGURES 23–30. For description see opposite.

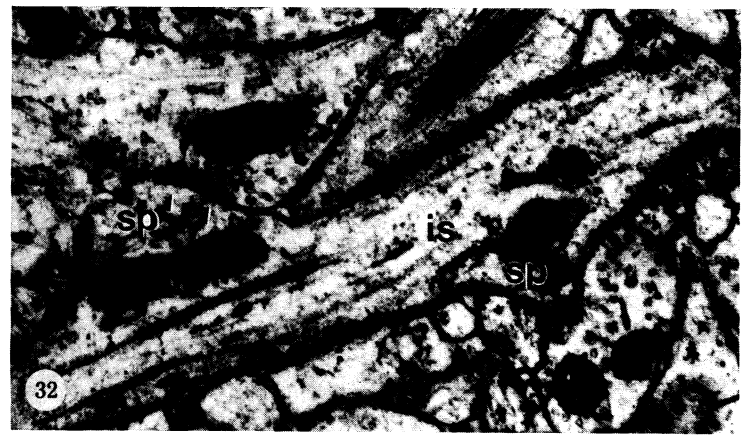

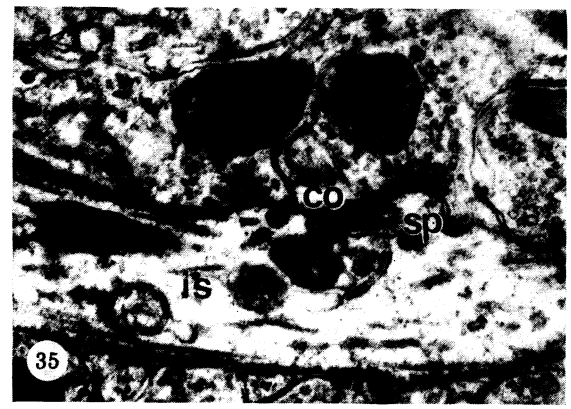

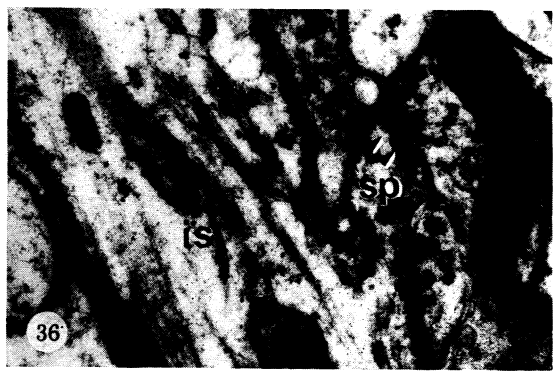

FIGURES 31–37. For description see opposite.

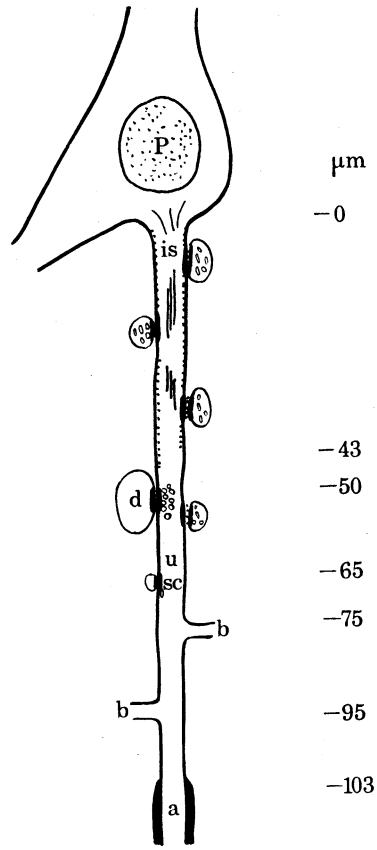

FIGURE 50. Diagrammatic representation of the pyramidal cell (P) and axon initial segment (is) of figures 39–49, and 51. The initial segment has the typical features of membrane undercoating and bundles of neurotubules from its origin to approximately 50 μm from the cell soma. It then loses these and makes a synapse on to a dendrite (d) but receives a further afferent synapse immediately distal to this. The initial segment then continues as an unmyelinated axon (u). It contains a subsurface cistern (sc) opposite an exposed membrane thickening on a dendritic spine at 65 μm and gives off two collateral branches (b) at 75 and 95 μm before becoming a myelinated axon at 103 μm from the cell soma (a).

DESCRIPTION OF PLATE 7

Spines on axon initial segments.

FIGURE 31. Part of an axon initial segment (is) having a large sessile spine (sp_1) which receives a symmetrical synapse (two arrowheads) and a second spine (sp_2) which does not receive a synapse in this particular section but does in an adjacent one. (Magn. × 32 000.)

FIGURE 32. A length of axon initial segment with a large and small sessile spine (sp), both of which receive synapses, one of which is clearly symmetrical (two arrowheads). (Magn. × 29 000.)

FIGURE 33. Peg-like sessile spine (sp) on an axon initial segment. Note that it receives a synapse and contains a small cisternal organ (co) which appears remarkably like a spine apparatus. (Magn. × 29 000.)

FIGURE 34. Example of an initial segment spine with a narrow stem and an expanded head which receives a symmetrical synapse (two arrowheads). (Magn. × 32 000.)

FIGURE 35. A small sessile spine on an axon initial segment. Note the cisternal organ immediately adjacent to the spine which receives a symmetrical synapse. (Magn. × 29 000.)

FIGURE 36. A small initial segment spine with an expanded head receiving a symmetrical synapse (two arrowheads). (Magn. × 29 000.)

FIGURE 37. An example of an axon initial segment which has two spines, both of which receive synapses from the same axon terminal (t). (Magn. × 18 000.)

In sections cut both perpendicular and parallel to the pial surface from material block-stained by ethanolic PTA the initial segments frequently contained a single or several parallel plates of electron dense material which resemble the appearance of the spine apparatus in this material (figures 53, 57, 59 and 60) and which correspond in size and position to the dense plates of the cisternal organ (figures 23–28).

The myelin sheaths of axons are not stained by ethanolic PTA but show up as white against the general granularity of the background. This enables nodes of Ranvier to be identified and these show a similar undercoating to that of the initial segment as has previously been described in conventionally stained axons (Peters 1966) and they also have a granular layer outside the plasma membrane in this material like that of the initial segment. Patches of what appear to be a membrane undercoating similar to that at the nodes of Ranvier may also be seen below the plasma membrane of axons within their myelin sheath but the significance of this is unclear.

The effect of pre-osmification on this staining by ethanolic PTA was studied in blocks prepared by Method 2 (Sloper & Powell 1979). This gave much better tissue preservation

---

Description of plate 8

Figures 39–51 show the initial segment of a pyramidal cell which was shown in serial sections to give rise to an unmyelinated and then myelinated axon and to make an efferent synapse on to a dendrite.

Figure 39. A pyramidal cell (P) in layer II of the motor cortex giving rise to its initial segment (is). (Section 3; magn. × 5000.)

Figure 40. Serial section to show the immediate continuation of the pyramidal cell initial segment from figure 39. Note the part of the cell (P) still present at the top of the figure (Section 14; magn. × 8400.)

Figure 41. The continuation of the initial segment (is) from figures 39 and 40 in a further serial section. Note the same dendrite is (d) present in all three sections. The proximal part of the initial segment is now to the left of the figure. (Section 22; magn. × 9000.)

Description of plate 9

Figures 42 and 43. The continuation in a further serial section of the axon initial segment (is) of the pyramidal cell shown in figure 39. Note the axons a and a′ and the dendrite d′ present in both figures 41 and 42. Figures 42 and 43 are continuous at the black bars; the continuity of the two narrowed regions of this length of initial segment was unequivocally confirmed in serial sections, one of which is shown in figure 46. In figure 43 the initial segment loses its characteristic features and makes an efferent synapse on to a dendrite (large arrowhead). (Section 17; magn. × 9000.)

Figures 44 and 45. The distal (right hand) region of the initial segment (is) of figure 43 at a greater magnification and in the next serial section, figures 44 and 45 being continuous at the black bar. In figure 44 note the membrane undercoating (e.g. between the arrows) and the bundle of neurotubules (nt), both characteristics of an axon initial segment. In figure 45 both these features are lost and the unmyelinated axon (u) makes an asymmetric synapse (large arrowhead) on to the dendrite d. Note however the afferent symmetrical synapse on to the initial segment/unmyelinated axon immediately *distal* to the efferent synapse (arrow). (Section 18; magn. × 29000.)

Figure 46. Serial section of the initial segment confirming its continuity at the proximal narrowed segment in figure 42. (Section 14; magn. × 8400.)

Figure 47. The efferent synapse (large arrowhead) of figure 45 in a serial section confirming its clearly asymmetric character. (Section 17; magn. × 29000.)

Figure 48. A further serial section of the efferent synapse (large arrowhead) of figures 45 and 47. Note how the synaptic vesicles are scattered in contrast to the close packed vesicles of a dendrodendritic synapse. (Section 20; magn. × 29000.)

Figure 49. The post-synaptic dendrite in a further serial section. Note the number of synapses it receives, including one clearly asymmetrical one (small arrowhead) and its smaller diameter compared to figures 47 and 48. (Section 5; magn. × 29000.)

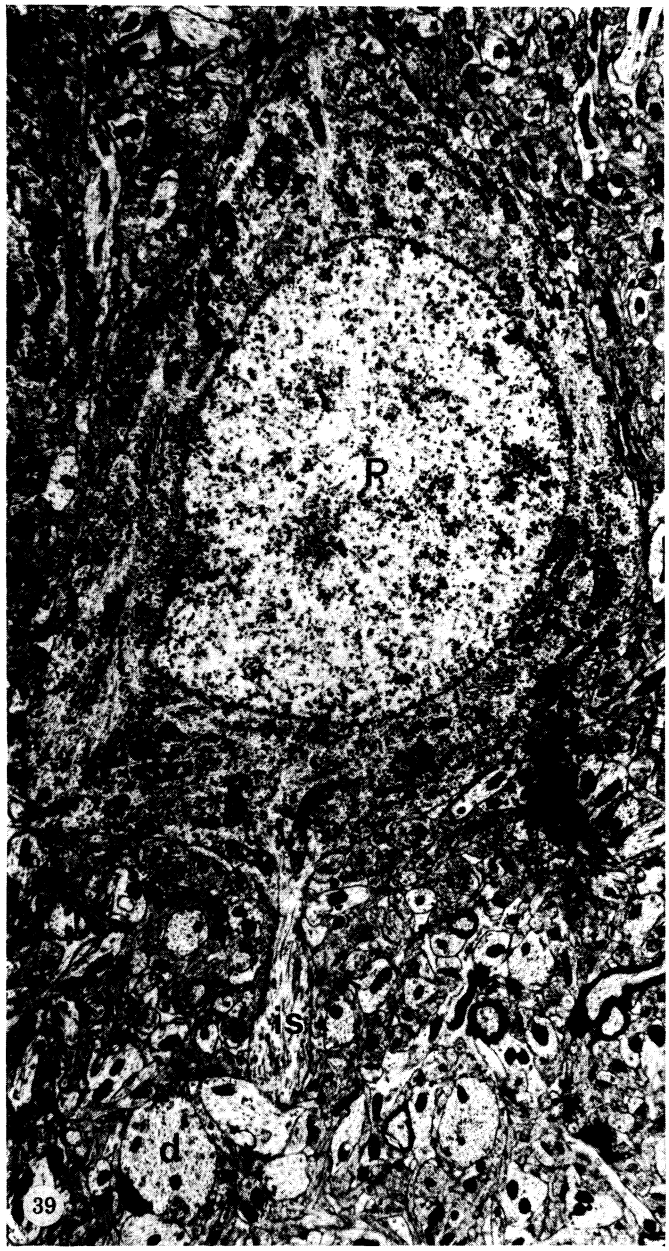

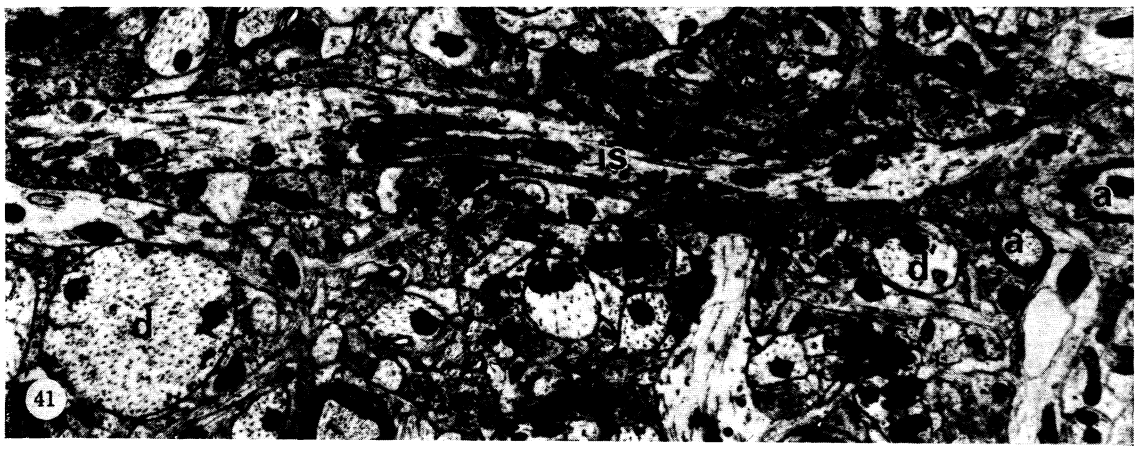

FIGURES 39–41. For description see opposite.

(*Facing p.* 182)

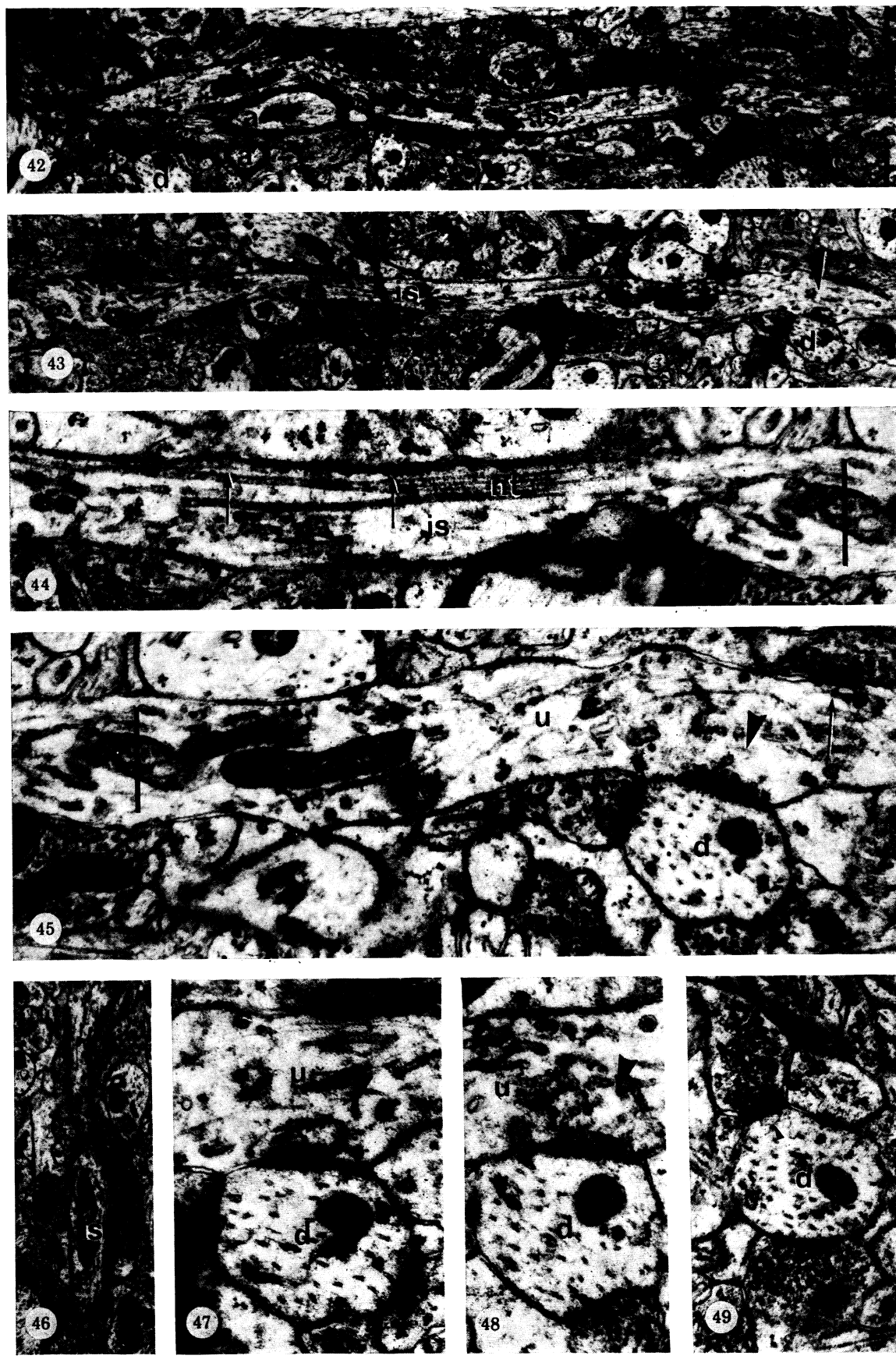

FIGURES 42–49. For description see page 182.

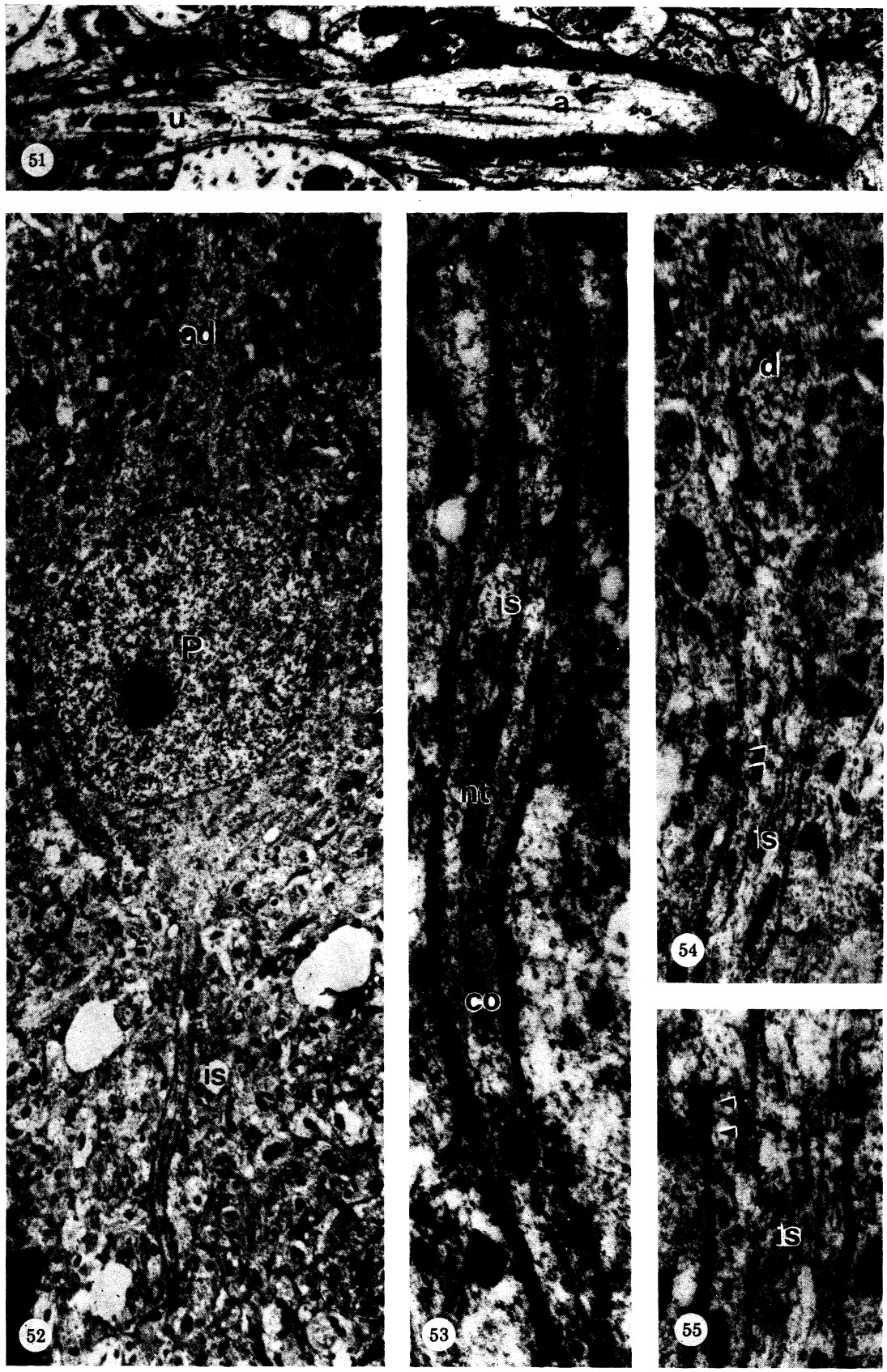

FIGURES 51–55. For description see page 183.

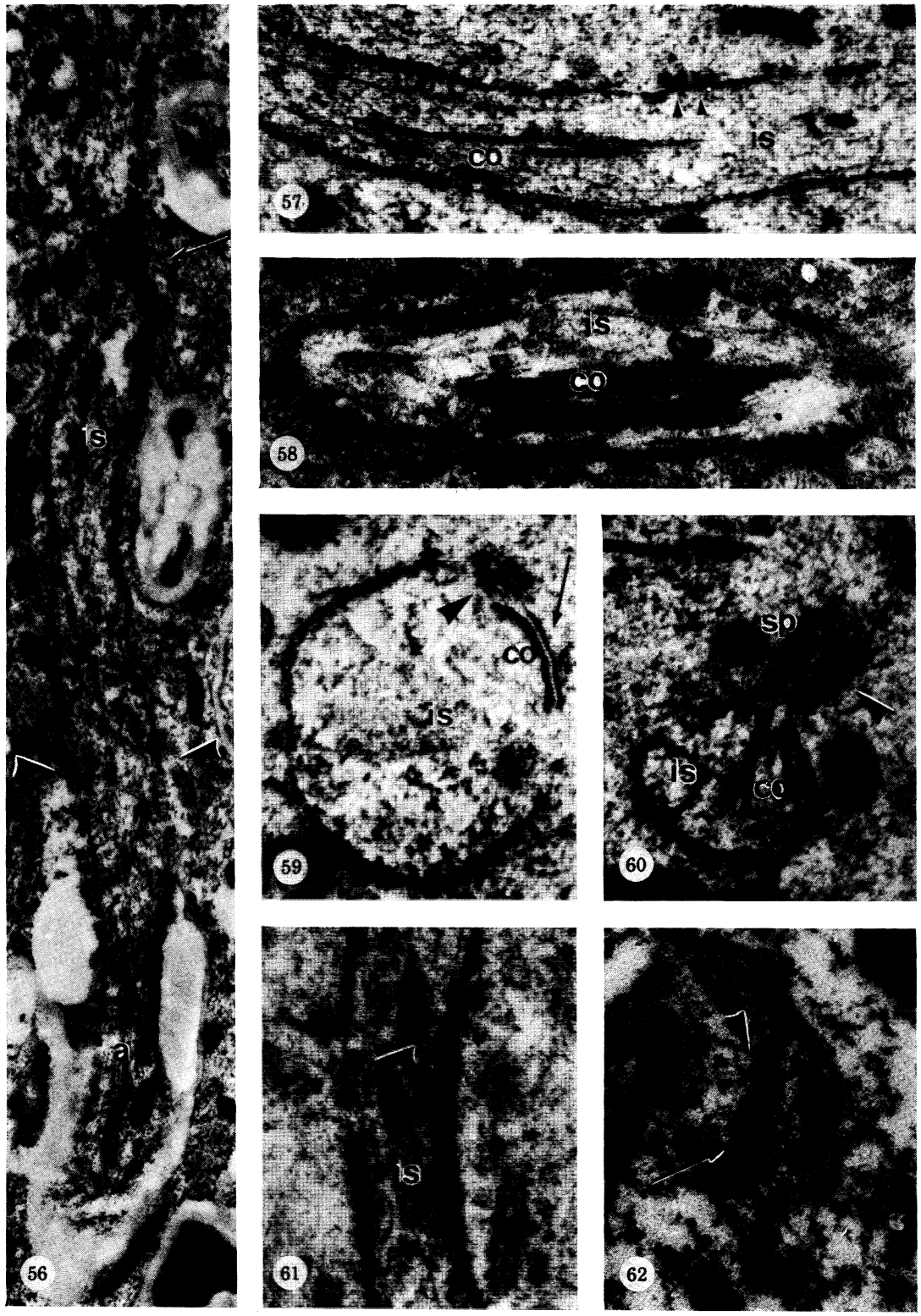

FIGURES 56–62. For description see opposite.

than PTA alone and in particular it showed up the plasma membranes. However, although the synaptic complexes were still specifically stained by the ethanolic PTA to at least some extent, the specific staining of the membrane undercoating and the dense plates of the cisternal organ was inhibited by this treatment (figure 58) in regions of the blocks which were comparable to those well stained by ethanolic PTA alone. It would therefore seem that pre-treatment with osmium tetroxide inhibits the binding of PTA to these structures, possibly by competing with it for the same binding sites.

As a control, to ensure that the electron density of the membrane undercoating and dense plates of the cisternal organ in ethanolic PTA stained material was due to the ethanolic PTA treatment, unstained sections from unosmicated, unstained blocks (Method 3, Sloper & Powell 1979) were examined. Neither of these two structures could be found and so this confirmed

---

Description of plate 10

Figure 51. The continuation of the unmyelinated axon (u) formed from the initial segment of figures 39–48 showing it becoming a myelinated axon (a). The whole of this initial segment/axon is shown diagrammatically in figure 50. (Section 59; magn. × 29000.)

Figure 52. A pyramidal cell (P) with its axon initial segment (is) and apical dendrite (ad) in material block stained with ethanolic PTA. Note how the initial segment stands out from the neuropil because of the specific staining of its membrane undercoating. (Magn. × 6000.)

Figure 53. The initial segment of figure 52 at a greater magnification showing the staining of the membrane undercoating but not of the membrane itself. Note also the bundle of neurotubules (nt) and the cisternal organ (co). (Magn. × 29000.)

Figure 54. An initial segment arising from a dendrite (d) in ethanolic PTA stained material. Note the staining of the membrane undercoating of the initial segment and the symmetrical synapse it receives (two arrowheads). (Magn. × 18000.)

Figure 55. Part of the initial segment of figure 54 at a greater magnification. Note the staining of the membrane undercoating, the lack of staining of the plasma membrane itself and the staining of a thin layer of extracellular material outside it. Note also the symmetrical synapse (two arrowheads) on to the initial segment. (Magn. × 39000.)

Description of plate 11

Figure 56. An axon initial segment (is) giving rise to a myelinated axon (a) in material block stained with ethanolic PTA. Note how the stained membrane undercoating stops at the beginning of the myelin sheath (large arrowheads). Note also the granular appearance of the membrane undercoating where it is cut obliquely (arrow). (Magn. × 18000.)

Figure 57. Initial segment in material block stained with ethanolic PTA to show the specific staining of the dense plates of the cisternal organ (co). Note also the synapse on to the initial segment (two arrowheads). (Magn. × 29000.)

Figure 58. Initial segment and cisternal organ in material stained with ethanolic PTA *after* osmification. Note how the staining of the dense plates of the subsurface cistern is inhibited. (Magn. × 29000.)

Figure 59. Transverse section of an axon initial segment containing a cisternal organ in material block stained with ethanolic PTA. Note how the dense plate of the cisternal organ is closely applied to the surface of the initial segment adjacent to the synapse complex (arrow) but becomes separated opposite the synaptic complex itself (large arrowhead). (Magn. × 53000.)

Figure 60. Transverse section of an axon initial segment in material block stained with ethanolic PTA. The initial segment has a spine (sp) which receives a symmetrical synapse (large arrowhead) and it contains a cisternal organ. (Magn. × 53000.)

Figure 61. Part of an axon initial segment in material stained with ethanolic PTA showing a vesicle arising from the membrane undercoating (large arrowhead). (Magn. × 48000.)

Figure 62. Synaptic membrane complex (arrow) and desmosome (large arrowhead) stained with ethanolic PTA. Note that the synaptic complex has discrete presynaptic projections whereas the dense material of the desmosome is continuous on both sides of the membranes. (Magn. × 53000.)

that the specific staining was due to the PTA and that the structures were not naturally electron dense.

Quantitative aspects of complete initial segments

The initial segments of 14 pyramidal cells, including Betz cells, and 2 large stellate cells were cut in continuity from the cell soma to the end of the initial segment in single or serial sections (figures 1–15 and figures 20–22). The initial segments of both the large stellate cells and 12 of the pyramidal cells gave rise to myelinated axons immediately and the other 2 pyramidal cells to unmyelinated axons by loss of the membrane undercoating and dispersion of the bundles of neurotubules; both of these unmyelinated axons became myelinated considerably further from the cell soma. For each of these cells the mean diameter of the cell soma was measured by the method described previously (Sloper, Hiorns & Powell 1979); the length of the initial segment was measured from its origin at the soma to the point where it became myelinated or, in the two examples having a length of unmyelinated axon, to the end of the undercoating membrane or last afferent synapse if this was further from the soma. The diameter of the myelinated or unmyelinated axon was also measured, as was that of the initial segment at about 10–15 μm from the soma, beyond any initial tapering. The distance of each afferent synapse from the cell soma was determined and the presence of cisternal organs noted.

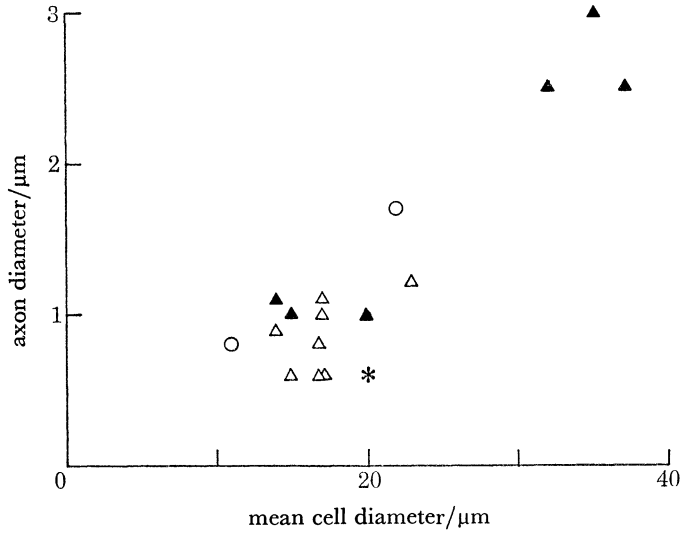

FIGURE 63. Graph showing the relation between mean diameter of a cell soma and the diameter of its axon. There is an approximately linear relation with large cells giving rise to proportionately wider axons. △, Supragranular pyramidal cell; ▲, infragranular pyramidal cell; ○, large stellate cell; *, ?Martinotti cell.

The relation of the *mean diameter of the cell soma* to the *diameter* of its myelinated or unmyelinated axon for these cells is shown in figure 63. There is a clear relationship between these two parameters with the cells of larger mean diameter giving rise to larger diameter axons, at least for that part of the axon closest to the cell soma. The same is not true when the *length* of the initial segment is plotted against the *mean cell diameter* (figure 64); all the initial segments of the 14 pyramidal cells are between 30 and 55 μm in length and although no initial segments of larger cells were found at the lowest end of the length range, there is no tendency comparable to that for the axon diameter for the larger cells to have longer initial segments. The length of the initial segment would therefore appear to be largely independent of the diameter

of the cell soma. Similarly, there is no clear relationship between the *length* of the initial segment and the *diameter* of the axon to which it gives rise and over a five-fold range of axon diameter the length of the initial segment of some examples was almost identical (figure 65).

This independence of the length of the initial segment from the diameters of the cell soma and axon is also true for the two large stellate cells (figures 64 and 65). However, the initial segments of both large stellate cells are considerably shorter (23 and 24 μm) than any of those of the pyramidal cells and are only just over half of the mean of the lengths of all the pyramidal initial segments (43 μm, see table 1), although they do not differ greatly in the diameters of soma or axon. There would therefore appear to be a difference in the length of initial segment between these two cell types which cannot be explained by difference in cell size.

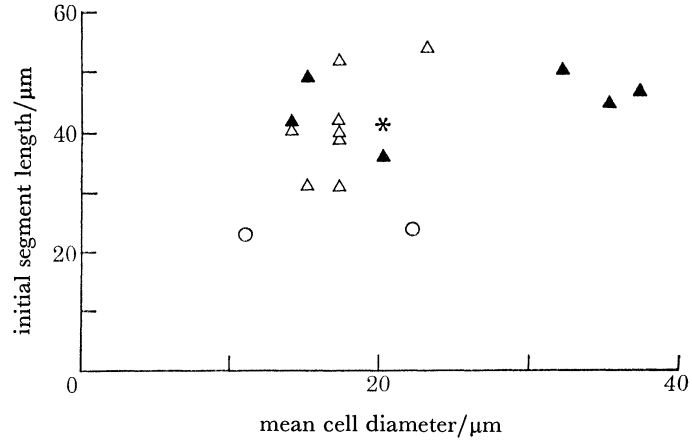

FIGURE 64. Graph showing the relation between the mean diameter of a cell soma and the length of its axon initial segment. Note that although the two large stellate initial segments are shorter than those of the pyramidal cells, there is no tendency for larger cells to have longer initial segments within one cell type comparable to the increase in initial segment diameter (figure 63). △, Supragranular pyramidal cell; ▲, infragranular pyramidal cells; ○, large stellate cell; *, ?Martinotti cell.

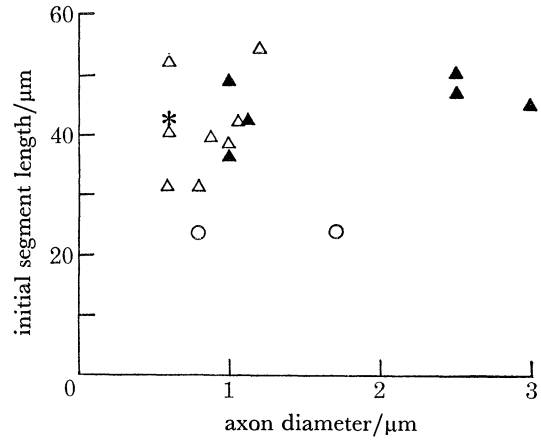

FIGURE 65. Graph showing the relation between the length of the axon initial segment and the diameter of the axon to which it gives rise. As with mean cell diameter (figure 64) larger diameter axons do not arise from proportionately longer axon initial segments. △, Supragranular pyramidal cell; ▲, infragranular pyramidal cell; ○, large stellate cell; *, ?Martinotti cell.

The distribution of the distances from the cell soma of afferent synapses on to the 14 pyramidal initial segments is shown in figure 66. The synapses are evenly distributed for the first 35 μm from the cell soma and then fall off progressively in density. This falling off, however, corresponds to the myelination of the shorter initial segments which starts at about 35 μm. If the length of each initial segment is divided into ten equal parts and the numbers of synapses in each tenth plotted in order to compensate for this inequality of length, it can be seen (figure 67) that synapses occur with equal frequency along the entire length of the initial segment. Insufficient synapses were found on the two large stellate initial segments to give a comparable distribution but synapses occur right up to the point of myelination in this cell type as well.

TABLE 1. COMPLETE PYRAMIDAL INITIAL SEGMENTS

cell number	layer	mean cell diameter μm	axon diameter μm	initial segment diameter μm	initial segment length μm	number of synapses found	number of cisternal organs	synaptic density	estimated total number of synapses
supragranular									
1	II/III	17	0.8	0.8	31	14	1	0.65	50
2	II/III	17	1.0	1.1	39	12	3	0.44	59
3	II/III	17	0.6†	0.9	52	9	2	0.25	36
4	II	23	1.2	1.7	54	19	0	0.50	145
5	II/III	17	1.1	1.2	42	14	2	0.48	76
6	III	14	0.9	1.1	40	15	1	0.54	74
11	III	15	0.6	0.8	31	12	1	0.55	43
14	II/III	17	0.6†	0.8	40	12	2	0.43	43
infragranular									
7	V	20	1.0	1.0	36	5	1	0.20	22
8	V	32	2.5	3.3	50	7	5	0.20	104
9	V	37	2.5	2.7	47	6	0	0.18	73
10	IV	14	1.1	1.2	42	2	0	0.07	11
12	V	15	1.0	1.0	49	7	1	0.20	31
13	V	35	3.0	3.2	45	2	1	0.06	29

Mean initial segment length/μm: overall 43, supragranular 41, infragranular 45.
Mean synaptic densities/synapses μm^{-2}: supragranular 0.48, infragranular 0.15.
† Gave rise to unmyelinated axons.

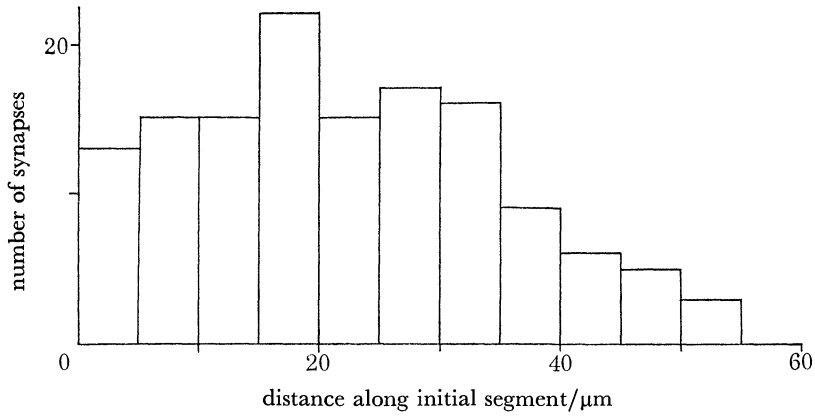

FIGURE 66. Histogram showing the distribution of synapses along the length of the complete pyramidal axon initial segments, each initial segment being divided into 5 μm segments.

Although the three largest of these fourteen pyramids occurred in layer V, there are no systematic differences between the pyramids of the supra- and infragranular layers in the length of the initial segment (figures 64 and 65; table 1) or the distribution of synapses along it (figure 67). There is however a clear difference in the number of synapses found on the initial segments of these two groups of pyramids (tables 1 and 2); on average the total length of an initial segment of a supragranular pyramid receives 13.4 synapses in a single section,

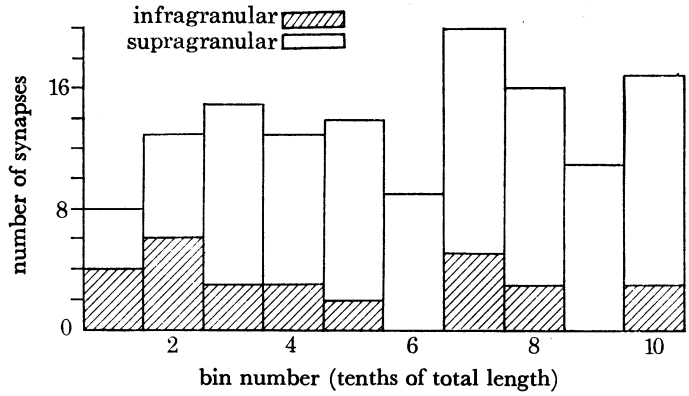

FIGURE 67. Histogram showing the distribution of synapses along the length of the complete pyramidal initial segments, each initial segment being divided into ten equal parts.

TABLE 2. COMPARISON OF FREQUENCIES OF SYNAPSES AND CISTERNAL ORGANS OF INITIAL SEGMENTS OF THE DIFFERENT CELL TYPES

cell type	number of cells	total initial segment length μm	total initial segment area μm²	number of synapses	average synaptic spacing μm	number of cisternal organs	average cisternal organ length μm	average cisternal spacing area μm²
pyramids								
overall	14	598	929	136	4.5	20	30	46
supragranular	8	329	358	107	3.1	12	27	30
infragranular	6	269	571	29	9.3	8	34	78
large stellate	14	129	117	13	9.9	0	—	—
small stellate	10	54	24	3	18.0	0	—	—

one every 3.1 μm, whereas that of an infragranular pyramid receives only 4.8, one every 9.3 μm; this difference in the number of synapses found occurs irrespective of the diameter of the initial segments (figure 68). Using the formulae derived in the Appendix, the density of synapses on the surface of each initial segment and the estimated total number of synapses received by each initial segment may be calculated (table 1). On average the infragranular pyramids receive a smaller total number of synapses, with a mean of 45 compared to 65 for the supragranular pyramids. This difference is less than that found in single sections but when the total number of synapses is plotted against the diameter of the initial segment (figure 69) or cell soma (figure 70) this is seen to be due to the three large pyramids in the infragranular group. The measurement of the density of synapses on the surface membrane of the initial segment compensates for these size differences and overall the density of synapses on the initial segments of supragranular pyramids is more than three times that of synapses on those of infragranular pyramids.

Whereas synapses occur only on the surface of an initial segment and the number found is proportional to its length, the cisternal organs may be found anywhere in the cytoplasm of the initial segment and the chance of finding one will be proportional to the area of initial segment cytoplasm found on a given section. The frequency of cisternal organs was therefore measured both in relation to the length of the initial segment and to the area on the section of the initial segment profiles, this being calculated as the product of length and diameter and so the total areas of supra and infragranular initial segments were obtained for these fourteen pyramids. In the initial segments of supragranular pyramids there were 12 cisternal organs in 358 μm^2, one every 30 μm^2 of initial segment profile, and in the initial segments of infragranular pyramids there were 8 in 571 μm^2, an average of one every 78 μm^2 (table 2). Cisternal organs were thus 2.6 times as frequent per unit area in the initial segments of supragranular pyramids.

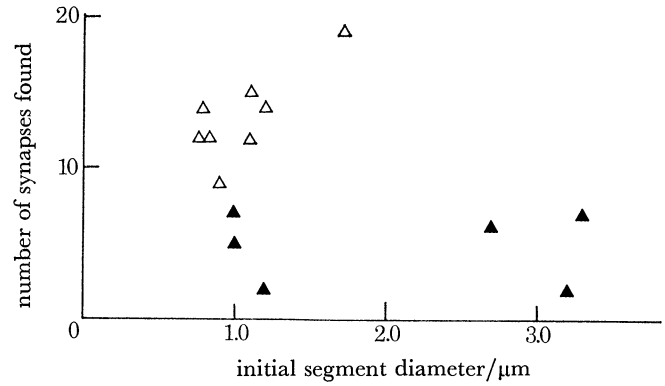

FIGURE 68. Graph showing the number of synapses found on each complete pyramidal initial segment against the initial segment diameter. Initial segments of supragranular (△) pyramids can be seen consistently to receive more synapses than those of infragranular (▲) pyramids and no more synapses were found on large diameter initial segments of infragranular pyramids than on small ones, thus indicating a similar synaptic density (see Appendix).

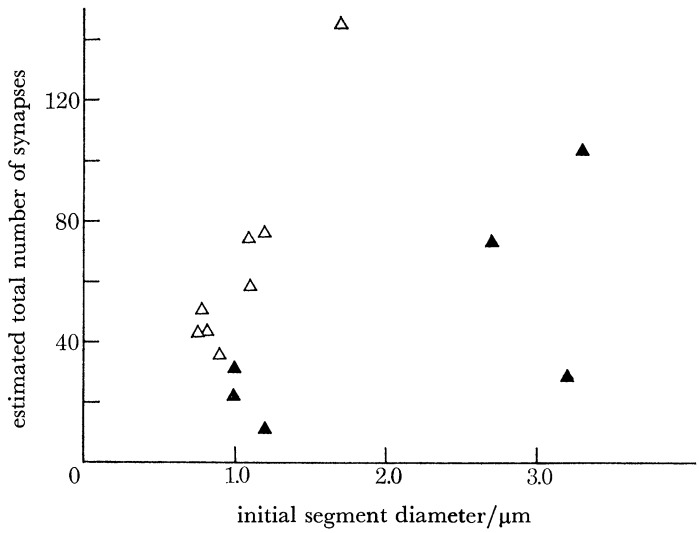

FIGURE 69. Graph showing the calculated total number of synapses received by each full length pyramidal initial segment against its diameter. Note the separation of supragranular (△) and infragranular (▲) pyramids.

Quantitative aspects of stellate initial segments

In addition to the two complete stellate initial segments described above, a considerable number of stellate cells have been observed giving rise to lengths of axon initial segment and certain limited quantitative conclusions may be drawn from these. The relationship of the mean diameter of the cell soma to the diameter of the initial segment is shown for large and small stellate cells in figure 71 where they are compared with the 14 complete pyramidal initial

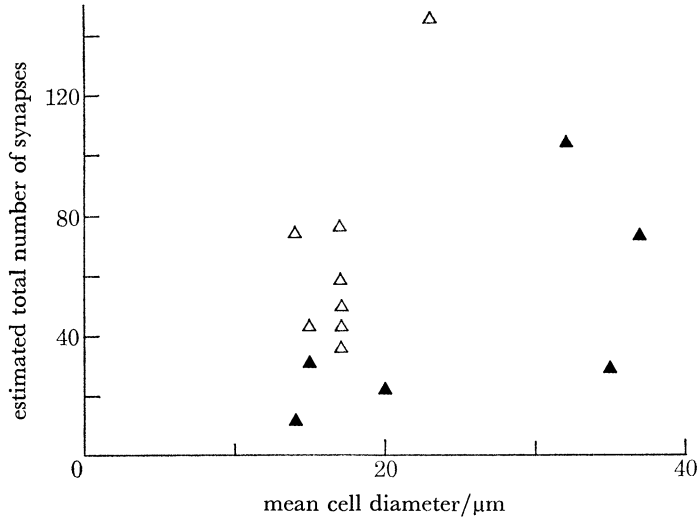

FIGURE 70. Graph showing the calculated total number of synapses received by each full length pyramidal initial segment against the mean diameter of its cell soma. Note the separation of supragranular (△) and infragranular (▲) pyramids.

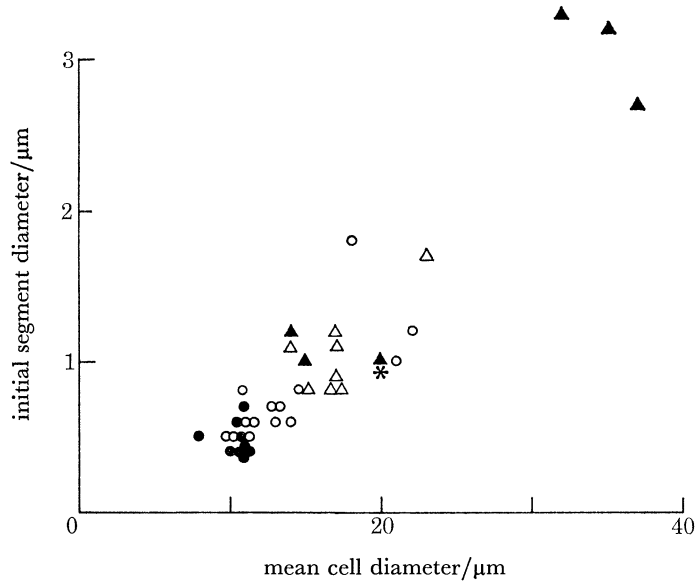

FIGURE 71. Graph showing the relationship of diameters of the cell soma and axon initial segment for the various cell types. In general larger diameter cells give rise to larger diameter axon initial segments with there being no marked difference between cells of similar size but different types. △, Supragranular pyramidal cell; ▲, infragranular pyramidal cell; ○, large stellate cell; ●, small stellate cell; *, ?Martinotti cell.

segments. Both dimensions are in general slightly smaller than for pyramidal cells, particularly in the case of small stellate cells, but the relationship between them is similar for all three cell types. Lengths of initial segment cut in continuity with the somata of a number of large and small stellate cells were measured and the number of synapses on them seen in a single section counted (table 2). This will give a sample in which that part of the initial segment nearest to the soma is most heavily represented. Comparison with the complete pyramidal initial segments, in which the synapses were shown to be evenly distributed along the length of the initial segment, showed that the synapses on all the pyramidal initial segments taken together occurred with an average spacing of 4.5 μm, those on large stellate initial segments at an average spacing of 9.9 μm and those on small stellate initial segments at an average spacing of 18 μm (table 2). However, when pyramidal cells are divided into supra and infragranular groups most of the difference in density is in fact between supragranular pyramids and large stellate cells. For at least their proximal part the initial segments of large stellate cells receive less than a third of the linear density of synapses of supragranular pyramidal cells and since there was no concentration of synapses in the distal part of the two complete large stellate initial segments, it is likely that this difference in synaptic density is present for the whole length of the initial segment. Although the synaptic density on the initial segments of infragranular pyramids and large stellate cells is similar, however, the two full length initial segments of large stellate cells are only just over half as long as those of the infragranular pyramids and so they will receive only about half the total number of synapses that initial segments of the same diameter arising from infragranular pyramids receive.

Discussion

The possibility of an association of cisternal organs with synapses has been discussed by a number of previous authors without any definite conclusions being reached. Although Westrum (1970) and Kemp & Powell (1971 *b*) thought that there was some association, Peters *et al.* (1968) did not. The fact that cisternal organ profiles occurred with a higher density in the initial segments of supragranular pyramids, which receive more synapses, is indirect evidence of an association but close study shows that the association is not in fact with the synapse itself but with the symmetrical axon terminal at a site away from the membrane complex. The close apposition of cisternal organs to the non-synaptic region of symmetrical axon terminals occurs much too frequently to be a chance finding and has in fact been illustrated previously (Westrum 1970, figures 3 and 9; Peters *et al.* 1968, figure 9); in the rare examples where apposition occurs opposite another profile in a single section it seems likely that this is due to an extension of a cistern from a region of apposition to a symmetrical terminal. The specificity of the relationship of cisternal organs to symmetrical terminals is also shown by the fact that a proportion show a degree of membrane specialization in this region of apposition which has not been seen elsewhere. The relationship of the cisternal organ to symmetrical synapses is very similar to that of somatic subsurface cisternae to them and is also analogous to the relation of the spine apparatus to asymmetric synapses. The structure of all three organelles is similar, the dense material of all three stains with PTA and all three are related to the reticulum of the cell (Peters & Kaiserman-Abramof 1970; Sloper & Powell 1979) and so it seems likely that they may all serve a similar function. The relationship of the cisternal organ to the non-synaptic region of the terminal suggests that this function is related

to some interaction between the terminal and cell and that it is not directly related to synaptic function.

Although spines have not been previously described on axon initial segments in the neocortex, they are similar to those found on the initial segments of neurons in the prepyriform cortex (Westrum 1970) and the caudate nucleus (Kemp & Powell 1971*a*, *b*). It is interesting that, where it was possible to identify the cell of origin, the axonic spines found were all on the initial segments of pyramidal cells, the dendrites of which give rise to many spines. These pyramidal initial segments also receive an unusually large number of synapses compared to initial segments of other types of neuron (Palay *et al.* 1968) and both these factors may be related to the presence of spines on their initial segment. There has been considerable speculation as to the function of dendritic spines (e.g. Diamond, Gray & Yasargil 1970) and some features of axonic spines noted here may be of relevance. Although dendritic spines always receive at least one synapse from an asymmetric axon terminal (see Sloper & Powell 1979), the axon initial segment receives only symmetrical synapses and this is equally true for spines on the initial segment, even when these are of the type with a narrow pedicle and expanded head. Such a spine may receive two symmetrical synapses and no asymmetric ones, this having been demonstrated in serial sections. Serial sections have also demonstrated that it is relatively frequent for a single terminal to make a synapse both on to an axonic spine and the shaft of an axon initial segment, an arrangement seen with dendritic spines (Harding & Powell 1977; Sloper & Powell 1979). Although there may be differences in the functioning of spines in these different locations, these factors should be taken into account in the consideration of their physiology.

Technical factors make it very difficult to follow the axon of a cell beyond the initial segment and to do this requires fortunate orientation of the section in relation to the axon and the extensive use of serial sections. The finding of an efferent synapse from the distal end of an initial segment was surprising and there appears to be no previous report of this (except cf. Pinching & Brooke 1973). The efferent synapse was proximal to the most distal afferent synapse on to the initial segment, although distal to the end of the membrane undercoating and bundles of neurotubules, so it is a matter of semantics as to whether it should be considered as arising from the end of the initial segment or the beginning of the unmyelinated axon, but in either case a serial axo-axonic synaptic arrangement was present. This serial axo-axonic synapse differed from the dendro-dendritic synapses in the motor cortex in the ultrastructural features of both the first and second synapses of the series and in its laminar location (Sloper & Powell 1978). There is, however, a previous report which described a few examples of serial axo-axonic synapses in the motor cortex of the rat (Artyukhina 1966). These were also found in the superficial cortical laminae and the efferent synapses were of type I of Gray (1959), with the afferent synapses being type II (equivalent to asymmetric and symmetrical synapses respectively in aldehyde-fixed material) and they may correspond to the appearance found here although they were not described as involving an initial segment.

The two initial segments described here where the axon did not become myelinated immediately distal to the initial segment both originated from cells in layer II and were of small diameter and it would appear that the absence of a myelin sheath on the first portion of the axon may be related to the superficial position of these cells in the cortex. Most of the other examples of complete initial segments were somewhat deeper in the cortex but all except one had axons of larger diameter. The presence of collaterals arising from the axons

of pyramidal cells is of course well known from Golgi studies (e.g. Cajal 1911) but this technique does not show their relation to the myelin sheath or initial segment. Although collaterals do not appear to arise from the initial segment itself, they were found proximal to the beginning of the myelin sheath in both examples where myelination did not occur immediately and two were found arising from the first node of Ranvier of the myelinated axon followed.

Few quantitative data are available on the dimensions of axon initial segments or about the synapses on them. The 14 pyramidal cells with complete initial segments provide such data and form an interesting group because the diameters of the cell somata vary over a considerable range in these cells of the same type; this allows the relation between the various dimensions of the soma and initial segment to be studied without complications due to differences between cell types.

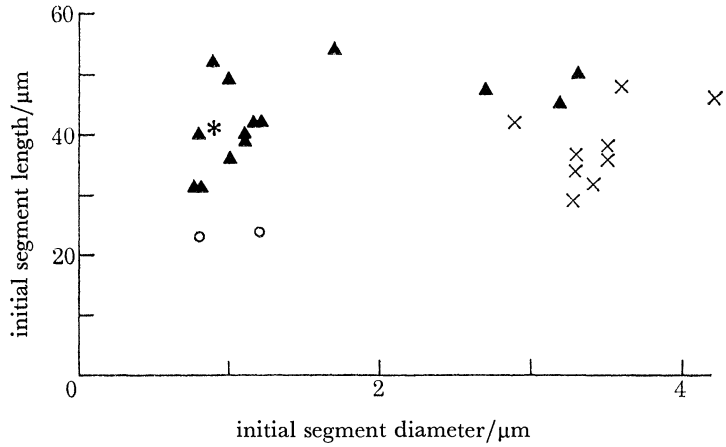

FIGURE 72. Graph showing the relation between the length and diameter of the complete axon initial segments studied here compared to those of spinal motor neurons studied by Conradi (1969). Note that initial segments of larger diameter are no longer than those of small diameter. ▲, Pyramidal cell; ○, large stellate cell; ×, motor neuron; *, ? Martinotti cell.

It has generally been accepted that larger cells give rise to initial segments and axons of larger *diameter* and this is borne out by measurements made on these pyramids and also by measurements on stellate cells (figures 63 and 71). However the *length* of the initial segment of pyramidal cells is not proportional to the diameter of the soma, as might be expected, but varies between 30 and 55 μm, apparently at random and independently of the diameters of both the cell soma and axon (figures 64 and 65). Conradi (1969) made similar measurements on spinal motoneurons and the distance from cell soma to the myelin sheath of these cells (his AH + IS in table 1) is plotted against initial segment diameter in figure 72 and compared to the measurements made here of initial segment length and diameter. (The initial segment diameter of the pyramids is used instead of the axon diameter used previously so that the results are directly comparable (table 1); the initial segment diameter was measured at about 10–15 μm from the soma and distal to any marked tapering of the initial segment and is generally slightly larger than the axon diameter of the same cell.) Although the initial segments of the spinal motor neurons have diameters considerably greater than those of the largest pyramids and there is a fivefold range of initial segment diameter overall, the lengths of all the initial segments fall within this same range (figure 72). It is also interesting that, in the

two pyramids which had lengths of unmyelinated axon between the initial segment and the myelinated axon, the length over which the undercoat and bundles of neurotubules were present was similar to that in the cells which gave rise to a myelinated axon directly. This suggests that this length, and so by present criteria the length of the initial segment, is determined by factors other than the proximity of the myelin sheath to the soma. What these factors may be is unclear but it is likely that the dimensions of the initial segment will have a considerable effect on its electrical properties. As the initial segment is the site of initiation of the action potential, the relative constancy of its length in contrast to the variation of the diameters of the soma and axon may have important implications for the understanding of the electrical properties of the neuron and of spike initiation. In this respect it may be significant that it is the length over which the undercoating and bundles of neurotubules extend which is constant rather than the distance from the soma to the beginning of the myelin sheath.

The synapses on the initial segments also only extend for this same distance from the cell soma even if myelination does not occur immediately and these synapses are likely to exert a powerful influence on the cell. The synapses are evenly distributed along the whole length of the initial segment of both supra- and infragranular pyramids and this would seem to indicate that they have some influence even when immediately adjacent to the myelin sheath. To determine this distribution only requires a sampling technique which is uniform along the length of the initial segment, a condition satisfied by the single longitudinal section used and having shown that this distribution is even, the density of synapses on the initial segment and the total number of synapses received by the initial segment may be calculated (see Appendix). It is not possible to determine whether it is the density of synapses or the total number received regardless of initial segment size which determines their effectiveness, but comparison of supra- and infragranular pyramids shows a clear difference both in the density of synapses on their initial segments and in the total numbers of synapses on initial segments of cells of comparable size. This difference appears to be restricted to the initial segment since the somata of pyramids of comparable sizes from the supra- and infragranular layers receive similar numbers of synapses in a section (Sloper, Hiorns & Powell 1979). The marked quantitative difference between the synapses on the initial segments of supra- and infragranular pyramids is likely to have an important influence on the function of these cells and this is of particular interest because they are now known to project to distinctly different sites, the supragranular pyramids projecting mainly to other cortical areas whereas the infragranular pyramids project predominantly to subcortical sites (Jones & Wise 1977).

This work was supported by grants from the Medical and Science Research Councils.

References

Adinolfi, A. M. 1971 The organisation of synaptic junctions in cat putamen. *Brain Res.* **32**, 53–67.

Artyukhina, N. I. 1966 Structure of synapses in rat motor cortex. *Fedn Proc. Fedn Am. Socs exp. Biol.* **25**, T559–564.

Bloom, F. E. & Aghajanian, G. K. 1968 Fine structural and cytochemical analysis of the staining of synaptic junctions with phosphotungstic acid. *J. Ultrastruct. Res.* **22**, 361–375.

Cajal, S. R. Y. 1911 *Histologie du système nerveux de l'Homme et des Vertébrés*, vol. II. Paris: Maloine.

Conradi, S. 1966 Ultrastructural specialisation of the initial axon segment of cat lumbar motoneurones. Preliminary observations. *Acta Soc. Med. upsal.* **71**, 281–284.

Conradi, S. 1969 Observations on the ultrastructure of the axon hillock and initial axon segment of lumbosacral motoneurons in the cat. *Acta physiol. scand.*, Suppl. **332**, 65–84.

Diamond, J., Gray, E. G. & Yasargil, G. M. 1970 The function of the dendritic spine: an hypothesis. In *Excitatory synaptic mechanisms*, (Proc. Fifth Int. Meet. Neurobiol.), (ed. P. Andersen & J. K. S. Jansen), pp. 213–222. Oslo: Scandinavian University Books.

Gray, E. G. 1959 Axo-somatic and axo-dendritic synapses of the cerebral cortex: an electron microscope study. *J. Anat.* **93**, 420–433.

Harding, B. N. & Powell, T. P. S. 1977 An electron microscopic study of the centre-median and ventro-lateral nuclei of the thalamus in the monkey. *Phil. Trans. R. Soc. Lond.* B **279**, 357–412.

Jones, E. G. & Powell, T. P. S. 1969 Synapses on the axon hillocks and initial segments of pyramidal cell axons in the cerebral cortex. *J. Cell Sci.* **5**, 495–507.

Jones, E. G. & Wise, S. P. 1977 Size, laminar and columnar distribution of efferent cells in the sensory-motor cortex of monkeys. *J. comp. Neurol.* **175**, 391–438.

Kemp, J. M. & Powell, T. P. S. 1971*a* The structure of the caudate nucleus of the cat: light and electron microscopy. *Phil. Trans. R. Soc. Lond.* B **262**, 383–401.

Kemp, J. M. & Powell, T. P. S. 1971*b* The synaptic organisation of the caudate nucleus. *Phil. Trans. R. Soc. Lond.* B **262**, 403–412.

Palay, S. L., Sotelo, C., Peters, A. & Orkand, P. M. 1968 The axon hillock and initial segment. *J. Cell Biol.* **38**, 193–201.

Peters, A. 1966 The node of Ranvier in the central nervous system. *Q. J. exp. Physiol.* **51**, 229–236.

Peters, A. & Kaiserman-Abramof, I. R. 1970 The small pyramidal neuron of rat cerebral cortex. The perikaryon, dendrites and spines. *Am. J. Anat.* **127**, 321–356.

Peters, A., Proskauer, C. C. & Kaiserman-Abramof, I. R. 1968 The small pyramidal neuron of the rat cerebral cortex. The axon hillock and initial segment. *J. Cell Biol.* **39**, 604–619.

Pinching, A. J. & Brooke, R. N. L. 1973 Electron microscopy of single cells in the olfactory bulb using Golgi impregnation. *J. Neurocytol.* **2**, 157–170.

Pinching, A. J. & Powell, T. P. S. 1972 A study of terminal degeneration in the olfactory bulb of the rat. *J. Cell Sci.* **10**, 585–619.

Sloper, J. J., Hiorns, R. W. & Powell, T. P. S. 1979 A qualitative and quantitative electron microscopic study of the neurons in the primate motor and somatic sensory cortices. *Phil. Trans. R. Soc. Lond.* B **285**, 141–171.

Sloper, J. J. & Powell, T. P. S. 1978 Dendro-dendritic and reciprocal synapses in the primate motor cortex. *Proc. R. Soc. Lond.* B **203**, 39–47.

Sloper, J. J. & Powell, T. P. S. 1979 Ultrastructural features of the sensori-motor cortex of the primate. *Phil. Trans. R. Soc. Lond.* B **285**, 123–139.

Westrum, L. E. 1970 Observations on initial segments of axons in the prepyriform cortex of the rat. *J. comp. Neurol.* **139**, 337–356.

Appendix. The relationship of the number of synapses seen in a single longitudinal section of an initial segment to the synaptic density and total number of synapses upon it.

A single section along the length of an initial segment will demonstrate only those synapses on it which extend into or through the plane of the section. The relationship of this number to the synaptic density and total number of synapses on the initial segment may be determined if the following approximations are made:

(1) That sufficient of the dense material of a synaptic membrane complex is present in a section to allow the synapse to be identified as such when the edge of the synaptic disk extends through at least half the thickness of the section. This is equivalent to a synapse touching or crossing the plane midway between the two surfaces of the section.

(2) The initial segment is treated as a cylinder.

(3) The plane of section is parallel to the long axis of the initial segment.

(4) Synapses are treated as disks of a constant diameter applied to the surface of the cylinder and distributed homogeneously round its circumference without overlap. (They have been shown here to be evenly spread along the length of the initial segment.)

Figure 73*a* shows a cross section of an initial segment with a longitudinal plane of section AA′ perpendicular to the page. Any synapse whose edge touches or crosses this plane will be seen in the section of which this is the plane midway between its two surfaces. Thus any synapses which lie at or between the extreme positions VX and XZ or vx and xz will be detected, that is any synapse whose centre lies between W and Y or w and y will be seen in the section AA′. This diagram is extended into three dimensions in figure 73*b* and it can be seen that any synapse whose centre is in the shaded area on the surface of the cylinder bounded by WYY′W′ will be seen in the section AA′ (extending back through X′) and there will be an identical area on the opposite side of the cylinder corresponding to the projection of wy.

Let T = total number of synapses on an initial segment;
D = density of synapses on the surface of an initial segment;
d = diameter of the initial segment;
l = length of the initial segment;
s = diameter of the synaptic disks.
WX = XY = W′X′ = X′Y′ = $\frac{1}{2}s$ (by definition).

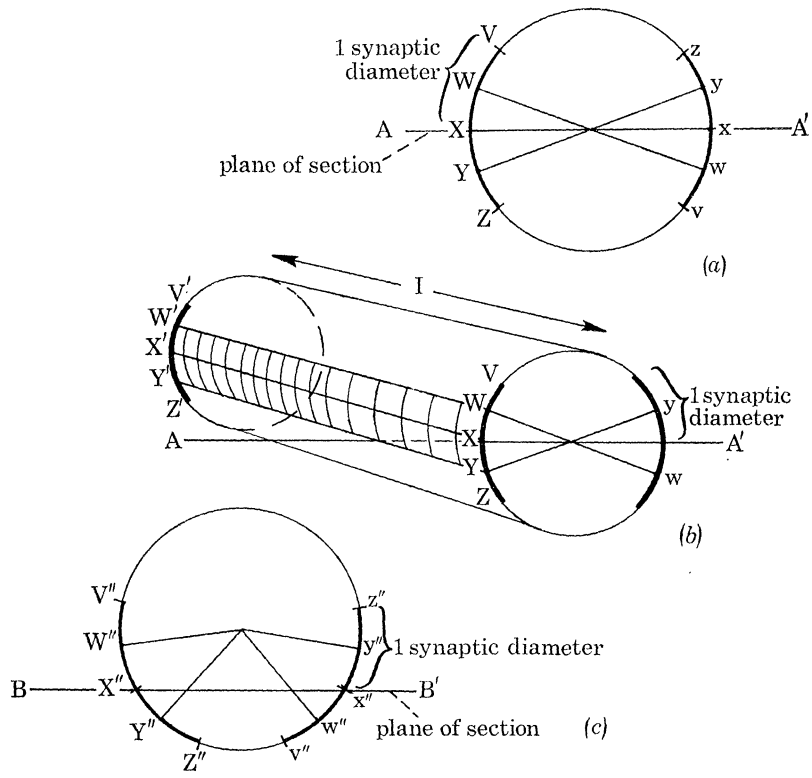

FIGURE 73. (*a*) Theoretical transverse section of an axon initial segment to show that synapses lying between the positions VX and XZ or vx and xz, and therefore having centres between W and Y or w and y, will be detected by the section AA′ and therefore the proportion of the total number of synapses detected by the section AA′ will be the distances WY plus wy, equal to two synaptic diameters, divided by the circumference of the initial segment πd (see text). (*b*) Three-dimensional expansion of the theoretical diagram of an initial segment of (*a*) showing that the proportion of synapses detected by the section AA′ is the area WYY′W′ plus the equal area on the opposite side of the cylinder (which is the projection of wy), divided by the total area of the curved surface of the cylinder (see text). (*c*) Theoretical transverse section of an axon initial segment to show that an off-centre section BB′ parallel to the long axis of the initial segment will detect the same proportion of synapses as the section AA′ through the centre of the initial segment (*a*) (see text).

The area of WYY'W' is therefore sl and the total area in which the synapses are detected (i.e. both sides of the cylinder) is $2sl$.

It is not necessary for the section to pass through the centre of the initial segment to obtain this result. Figure 73*c* shows an off-centre section BB'. This will detect all the synapses within one synaptic width of it, i.e. completely between V″ and Z″, and v″ and z″, and therefore with centres between W″ and Y″, and w″ and y″, and the area on the surface of the cylinder in which synapses are detected will be $W''Y'' \times l + w''y'' \times l$. Since $W''Y'' = w''y'' = s$, the area in which synapses are detected is $2sl$ (as above). This will be true for any off-centre section provided that Z″ and v″ or z″ and V″ do not meet or overlap when the total area in which detection occurs is reduced by the area of the overlap.

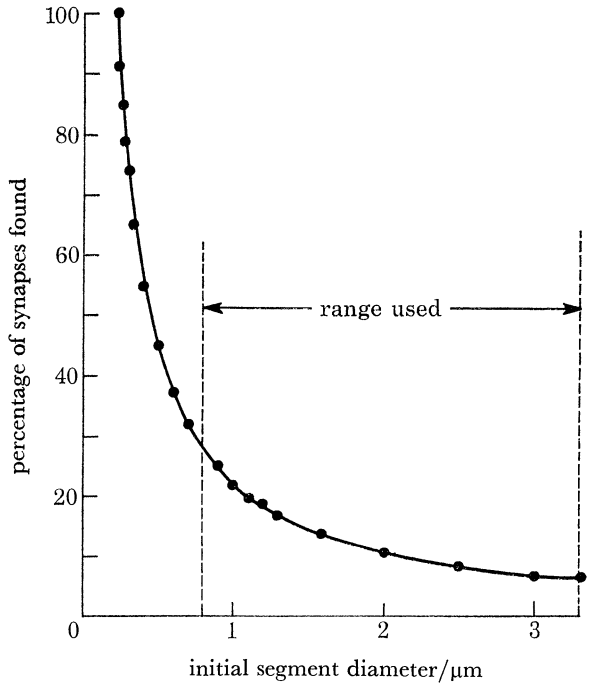

FIGURE 74. Graph to show the proportion of the total number of synapses on to an initial segment which will be found by a single longitudinal section through the initial segment. This curve is calculated on the basis of the model described in the Appendix using a synaptic diameter of 0.35 μm.

A section along the length of an initial segment will therefore detect all synapses on an area of $2sl$ on the surface of the initial segment and the number of synapses divided by this area will be the synaptic density (D) on this surface, i.e.

$$D = \frac{\text{number of synapses detected}}{2sl}.$$

The measurement of the synaptic density is therefore independent of the diameter of the initial segment; this is because the synapses detected by this method are contained in a constant width strip ($2s$) whatever the diameter of the initial segment. It is therefore only necessary to divide the number of synapses seen on an initial segment by its length in order to compare the synaptic density on different initial segments (provided that the synaptic diameter is constant).

The total number of synapses on an initial segment (T) may be calculated by multiplying the density (D) by the total area of the curved surface of the initial segment (πdl), i.e.

$$T = \pi dlD$$

and the proportion of the total number of synapses on an initial segment which is observed in a particular case is given by the area in which synapses were detected divided by the total area, i.e.

$$\text{proportion observed} = \frac{2sl}{\pi dl} = \frac{2s}{\pi d}.$$

The proportion of the total number of synapses observed is therefore inversely proportional to the diameter of the initial segment and this relation is shown graphically in figure 74. However, since more than the total number of synapses cannot be observed, πd must always be greater than, or equal to, $2s$. (When πd is less than $2s$ the same synapse may be counted on both sides of an initial segment and so the result invalidated.) In practice however the synaptic diameter is about 0.35 μm and the inequality may be solved:

$$\pi d \geqslant 2 \times 0.35 \text{ μm},$$

$$d \geqslant \frac{0.7}{\pi} \text{ μm},$$

$$d \geqslant 0.22 \text{ μm}.$$

The expression therefore holds for initial segments of diameter 0.22 μm and above, which includes all those in this study.

The total number of synapses on an initial segment may also be calculated as the number seen multiplied by the reciprocal of the proportion observed at that diameter, i.e.

$$T = \frac{\pi d}{2s} \times \text{number seen}.$$

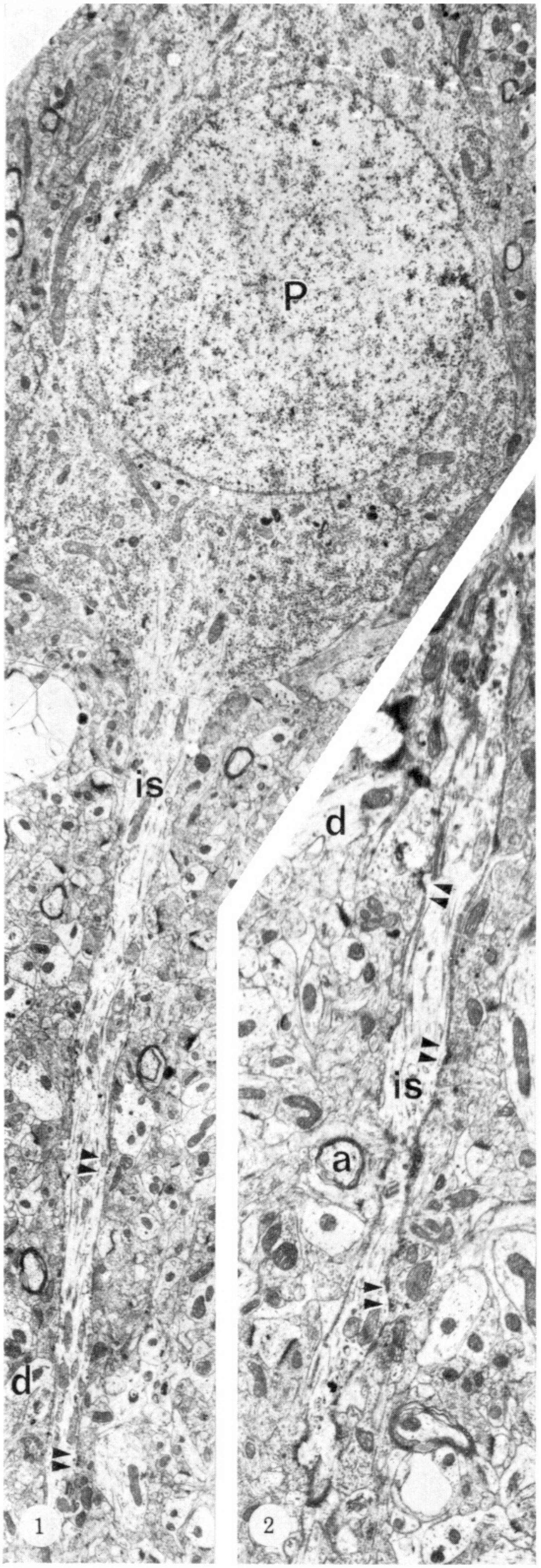

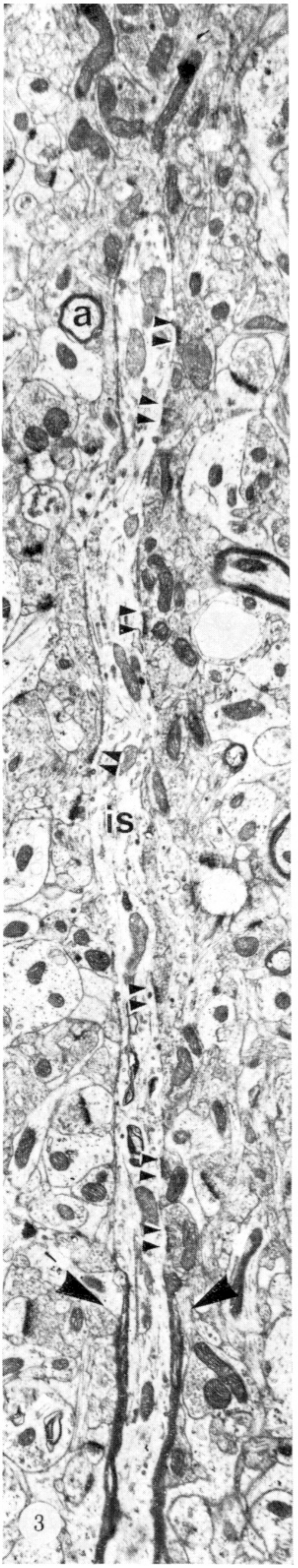

FIGURES 1–3. For description see opposite.

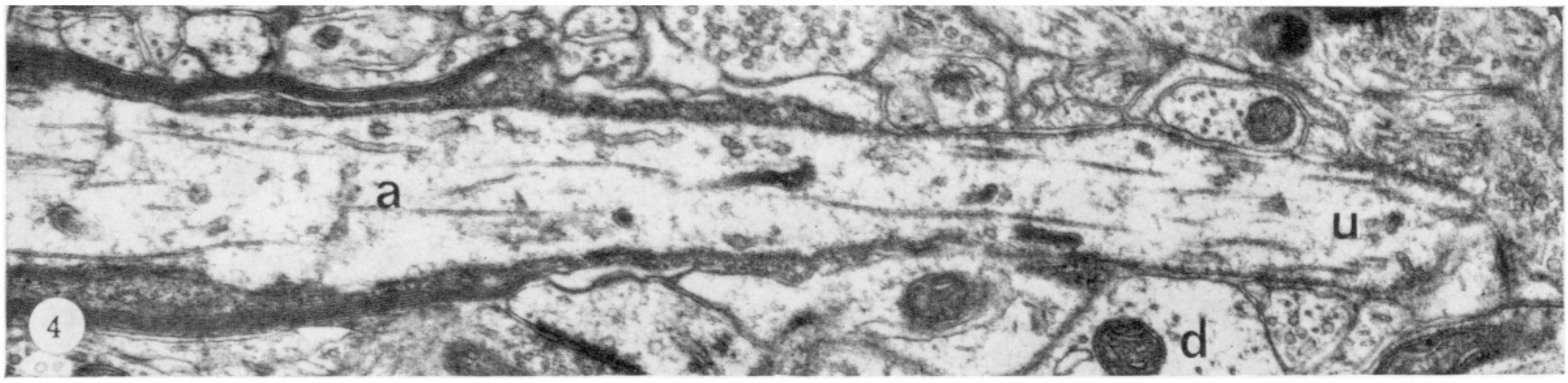

4

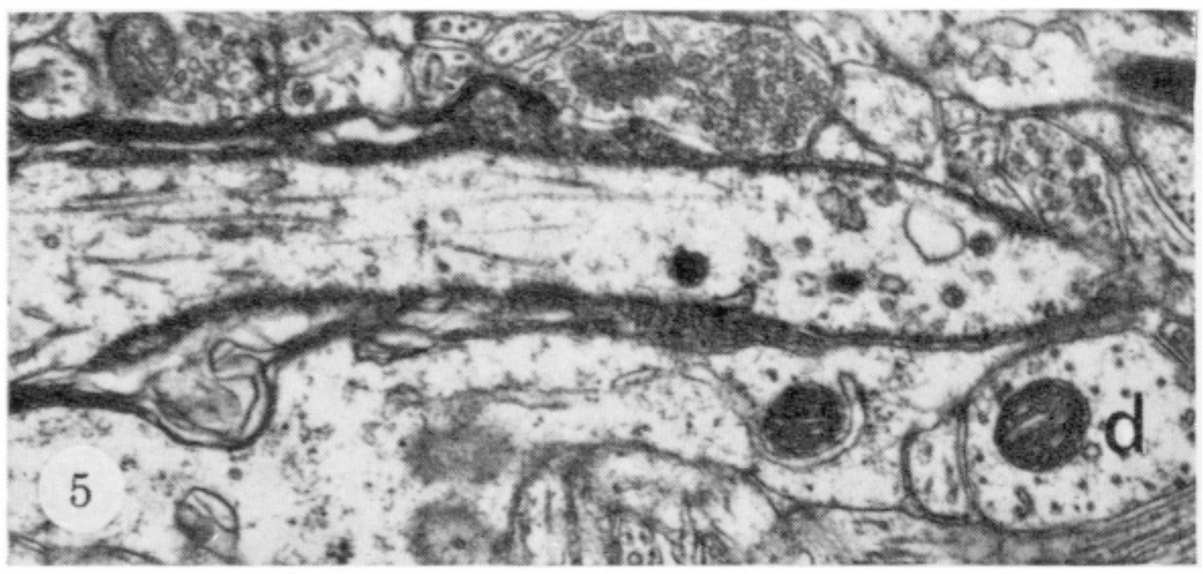

5

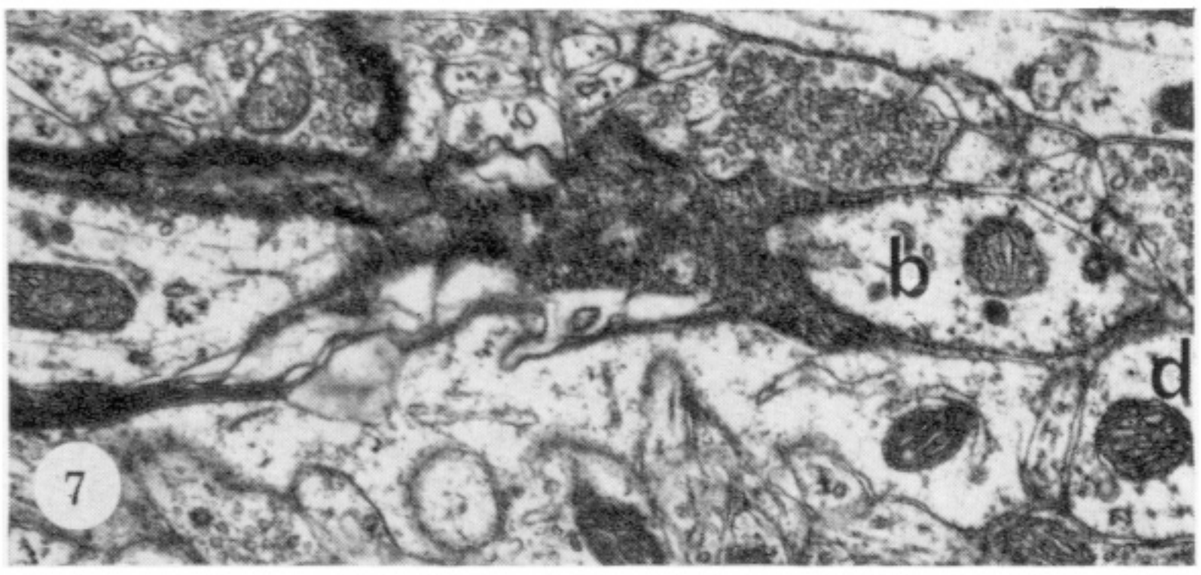

7

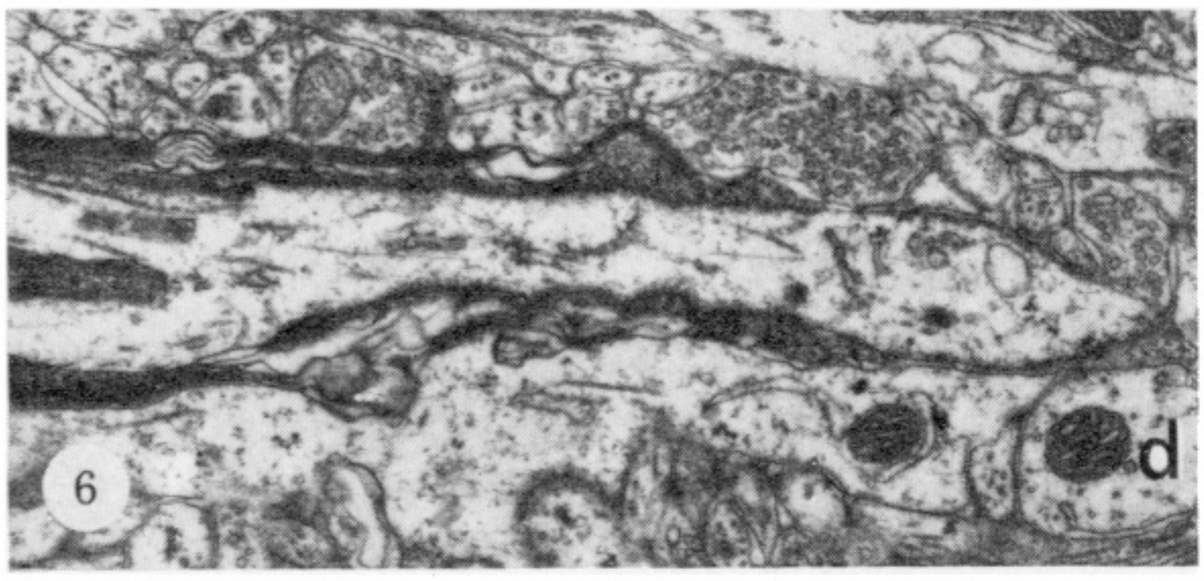

6

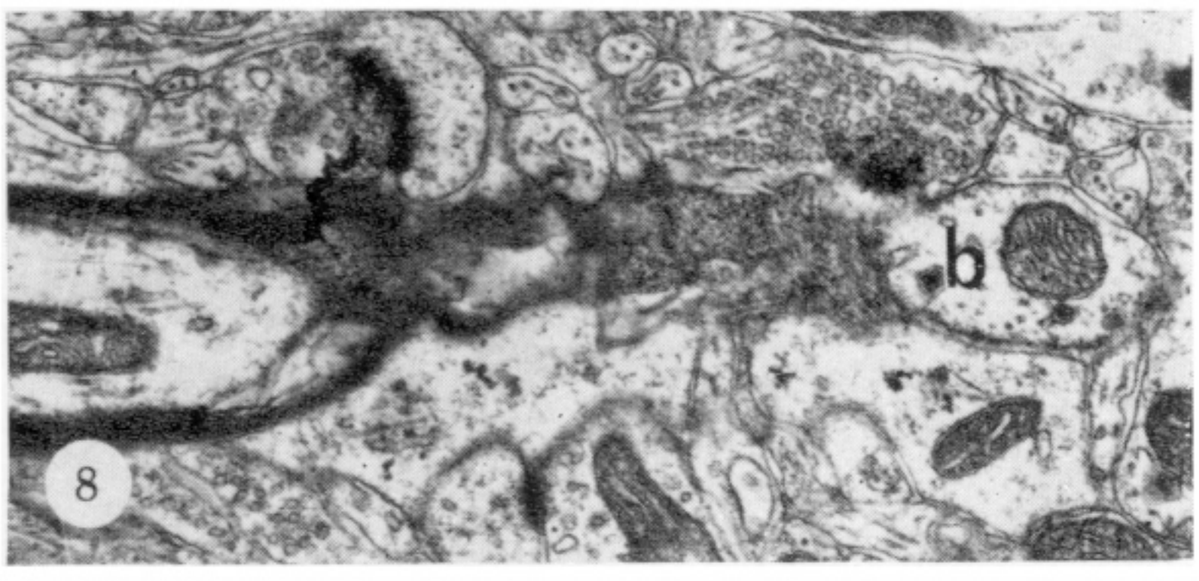

8

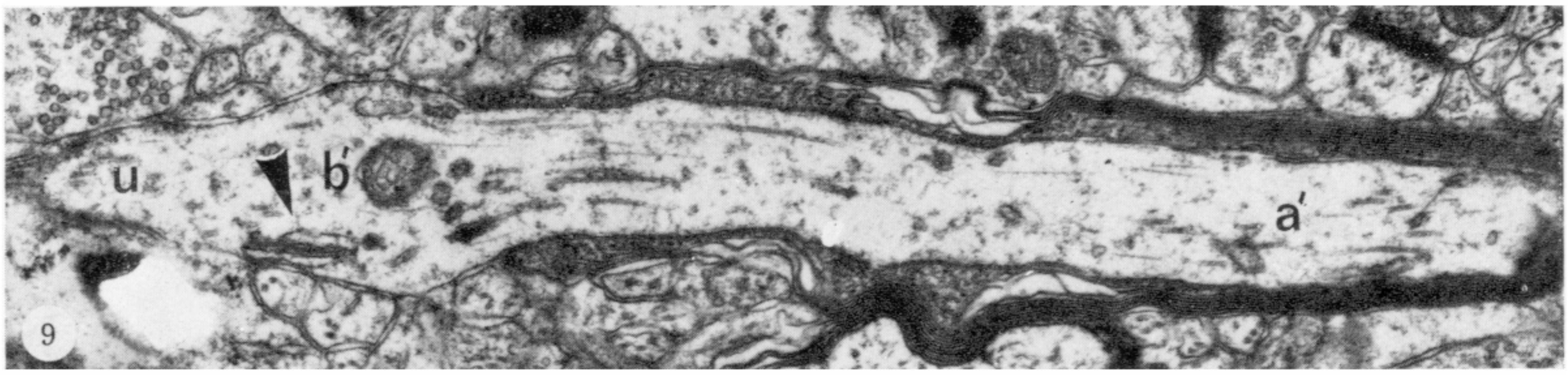

9

10

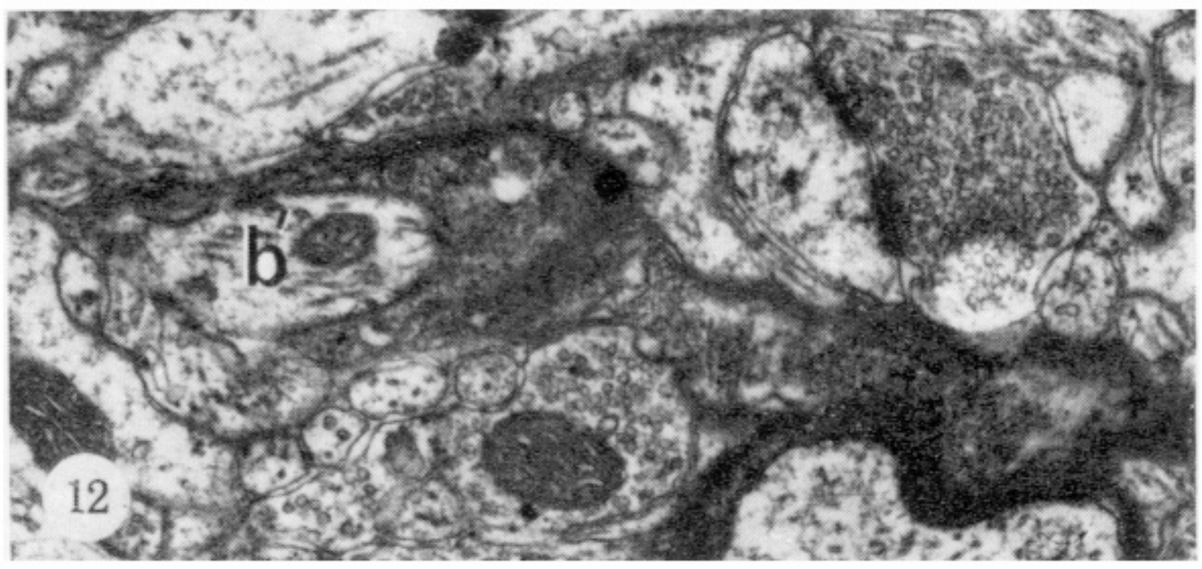

12

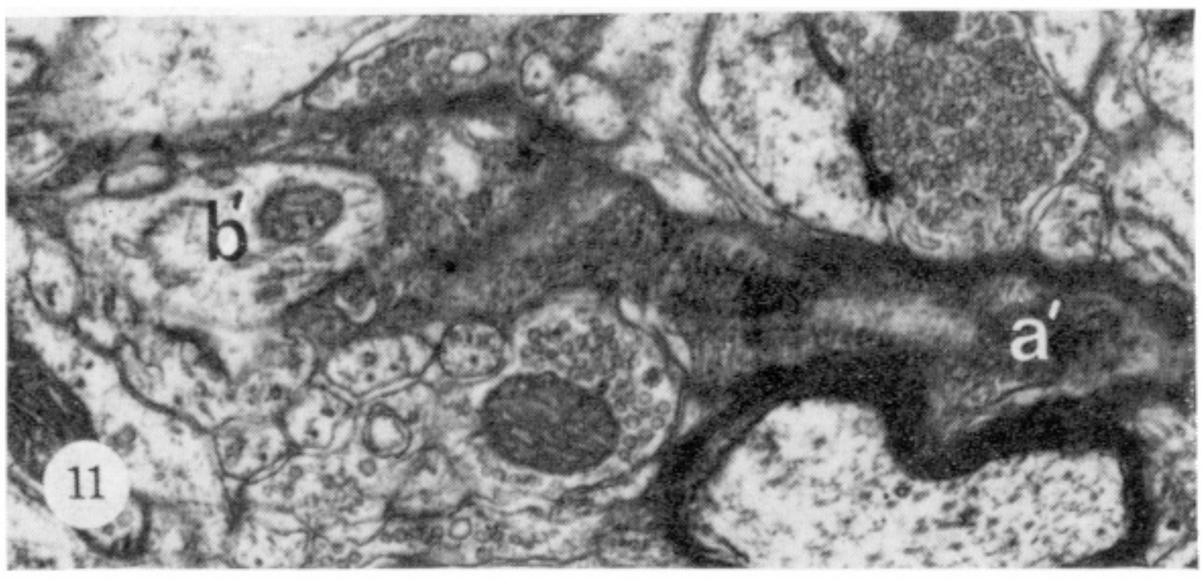

11

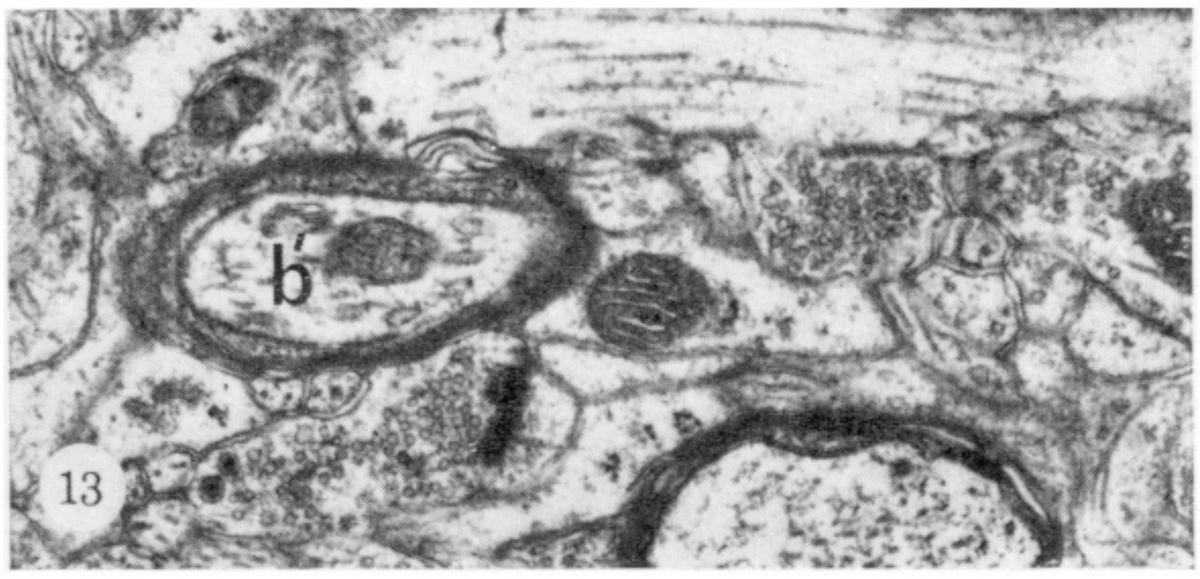

13

FIGURES 4–13. For description see page 176.

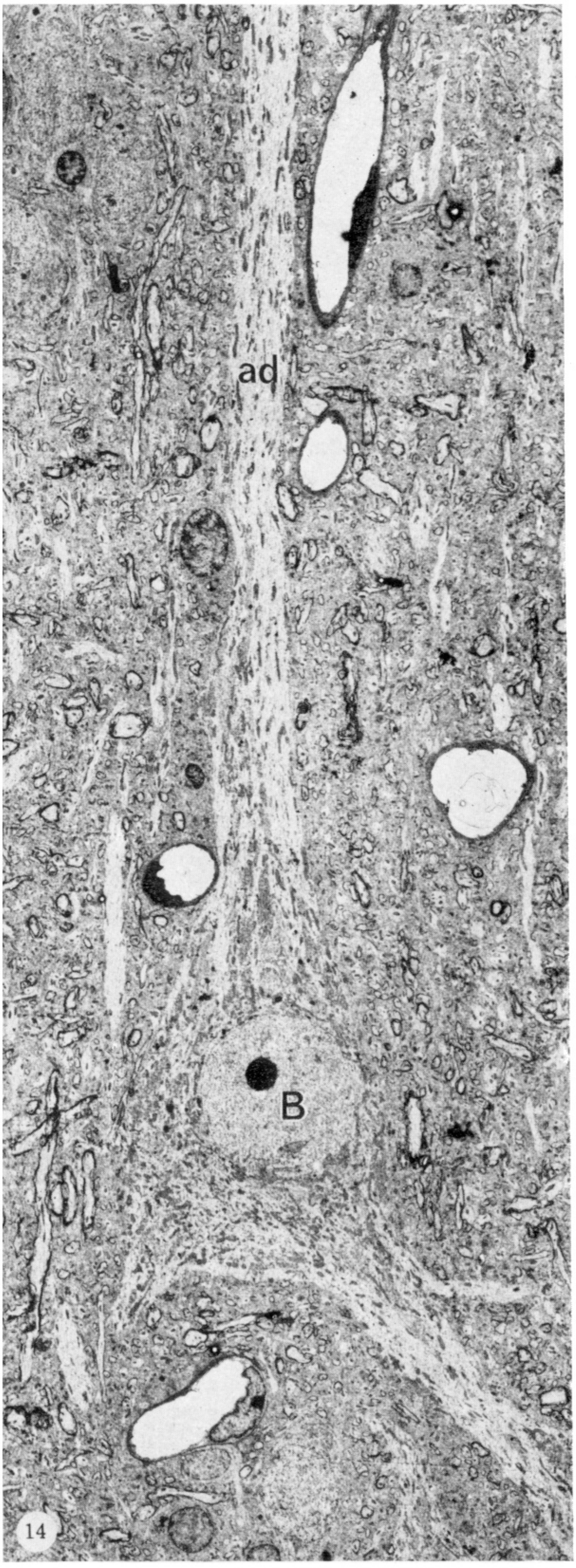

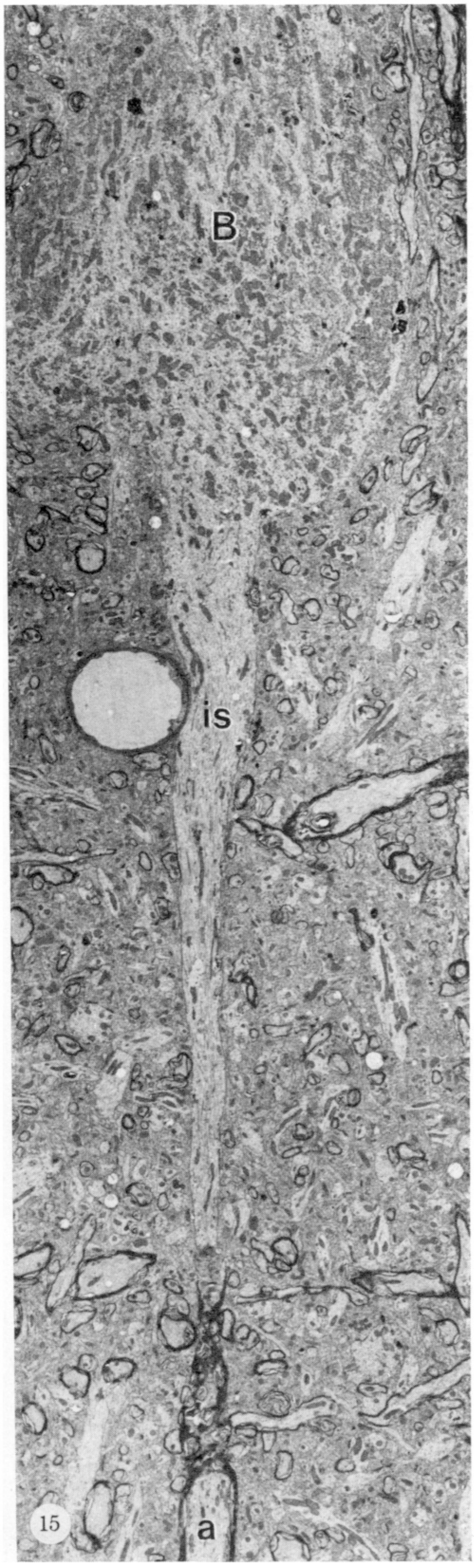

FIGURE 14. A Betz cell (B) with apical dendrite (ad) in layer V of the motor cortex. In serial sections this cell was shown to give rise to the axon initial segment of figures 15–19. (Magn. × 1300.)

FIGURE 15. Axon initial segment (is) of the Betz cell of figure 14 in a serial section. The nucleus of the cell is no longer in the plane of the section although a considerable amount of cytoplasm is still seen. Much of the apparent tapering of the initial segment is due to its not being parallel to the plane of the section. The continuity of the initial segment with the myelinated axon (a) was confirmed in serial sections (e.g. figure 19). (Magn. × 3000.)

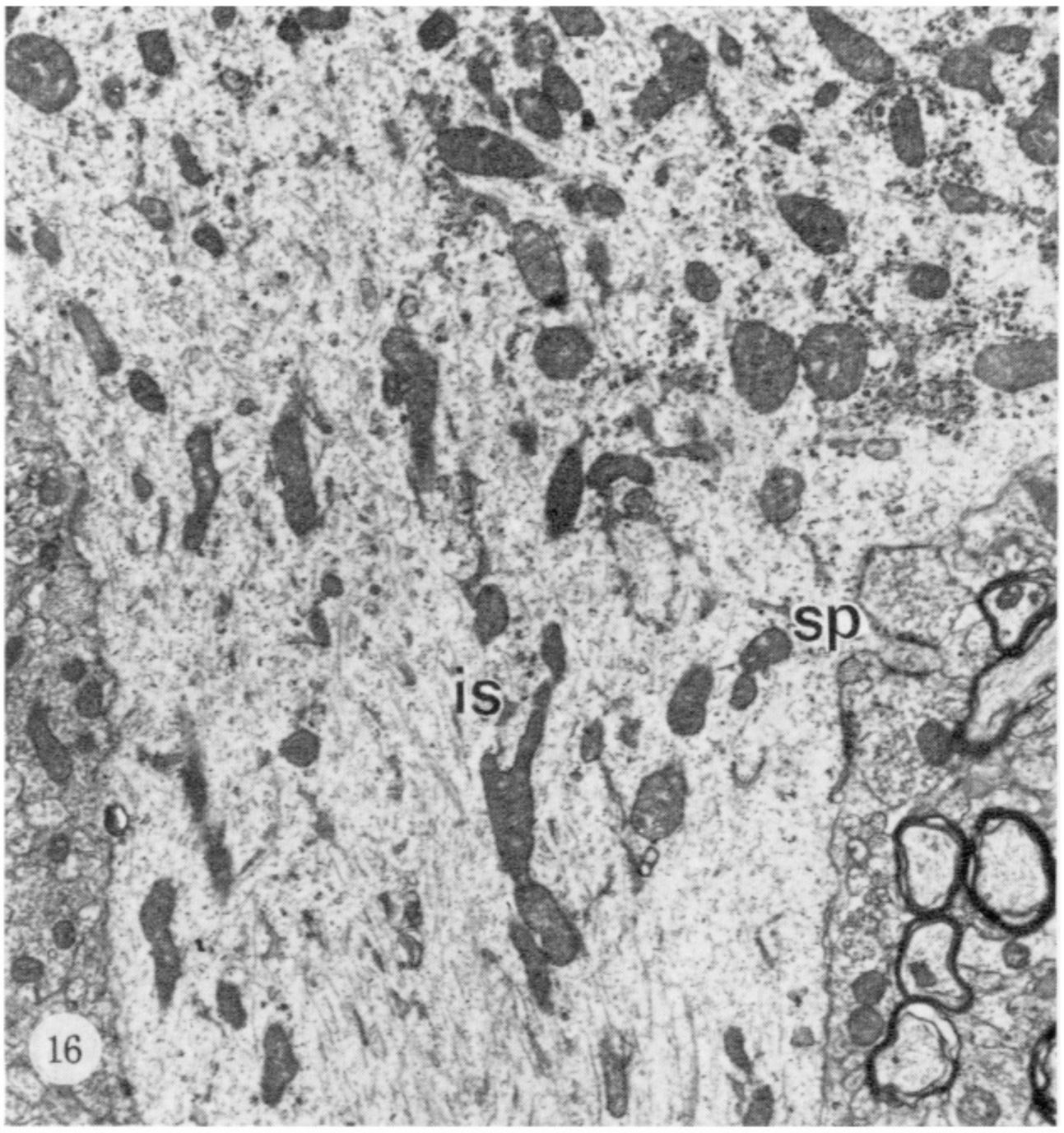

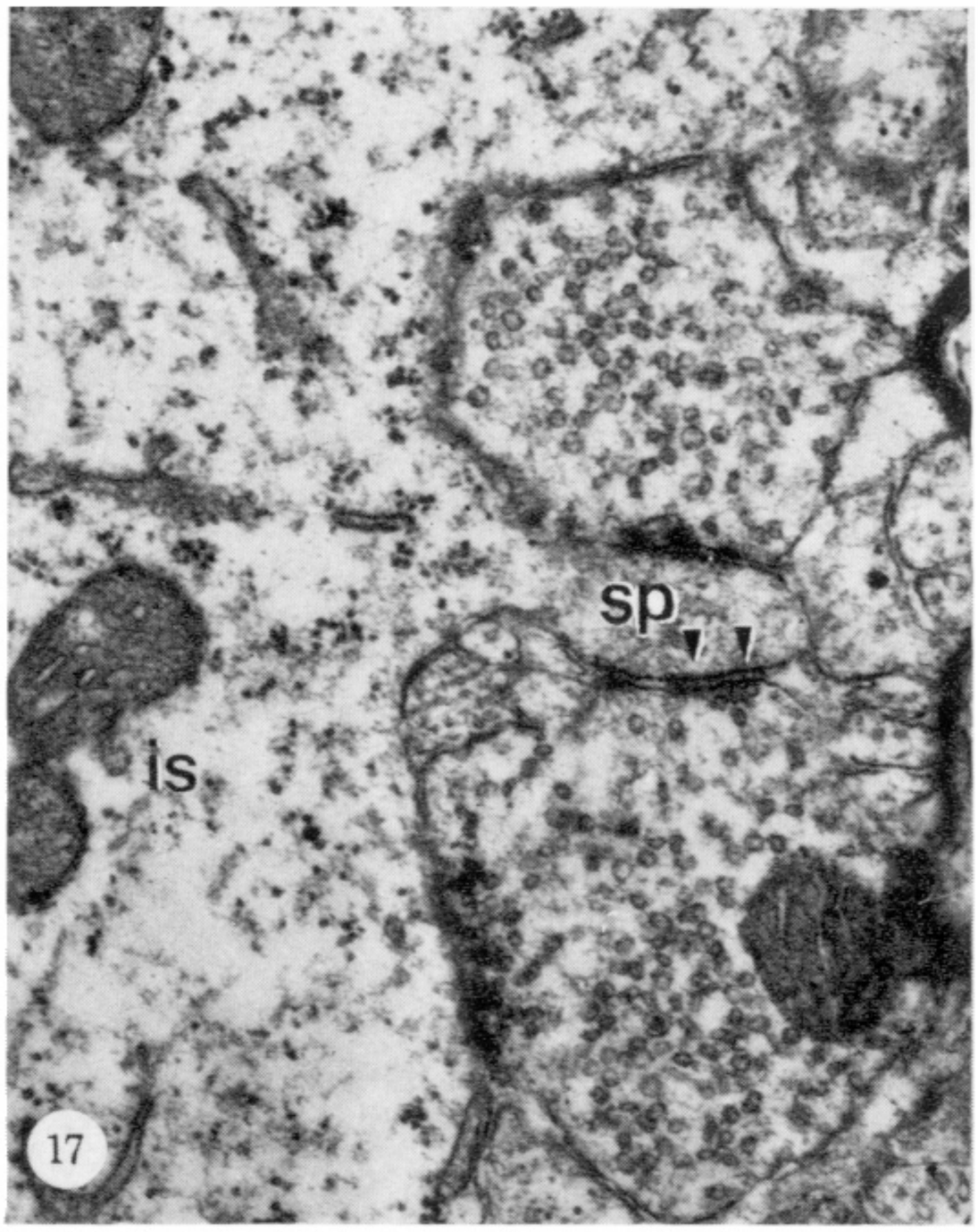

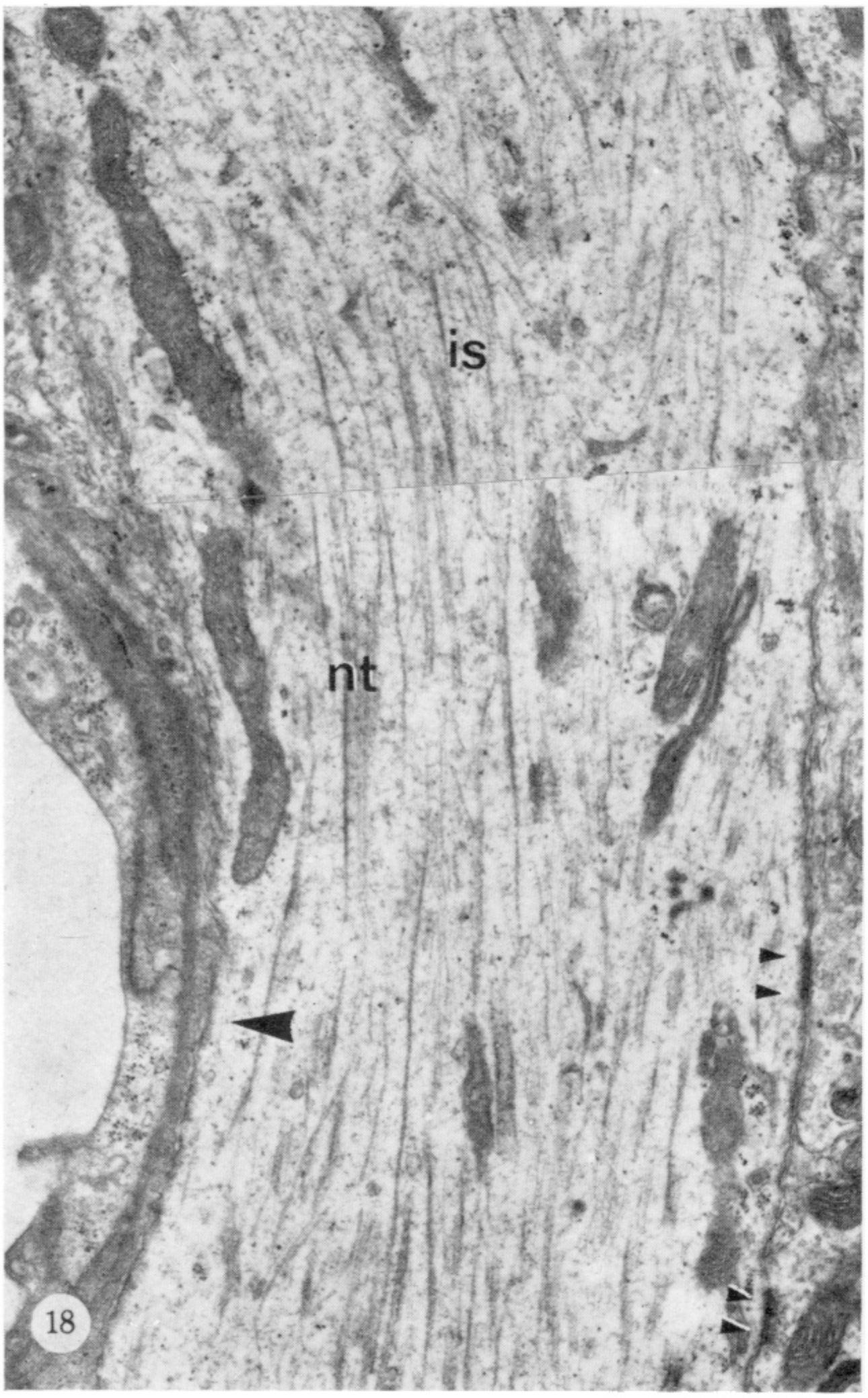

FIGURES 16–19. For description see opposite.

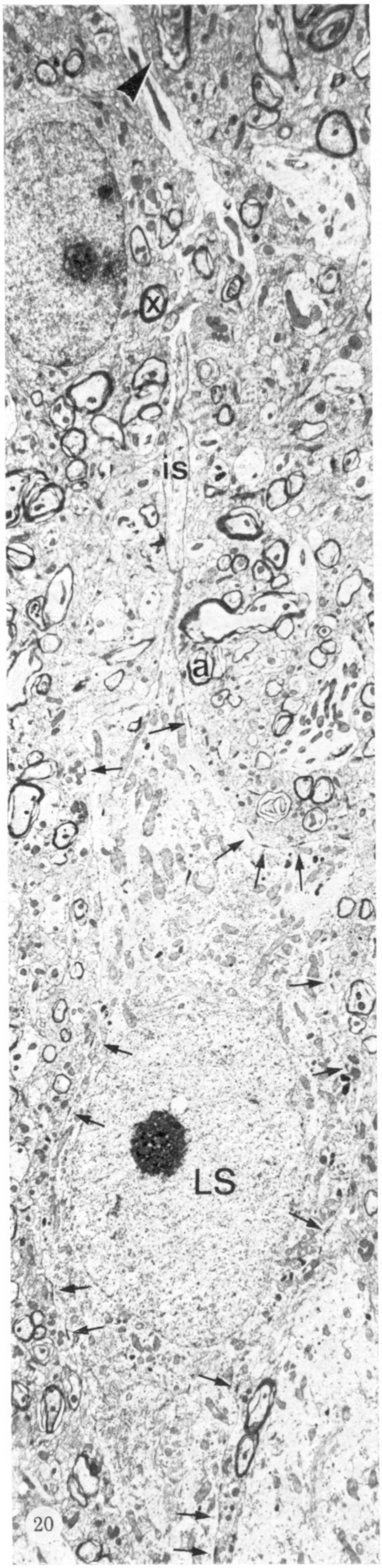

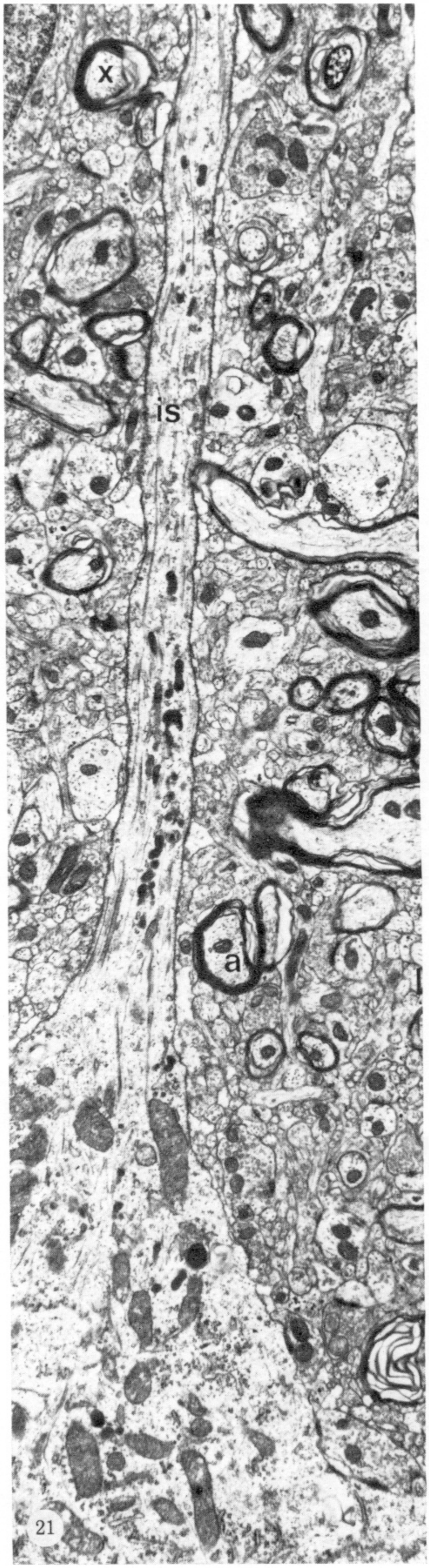

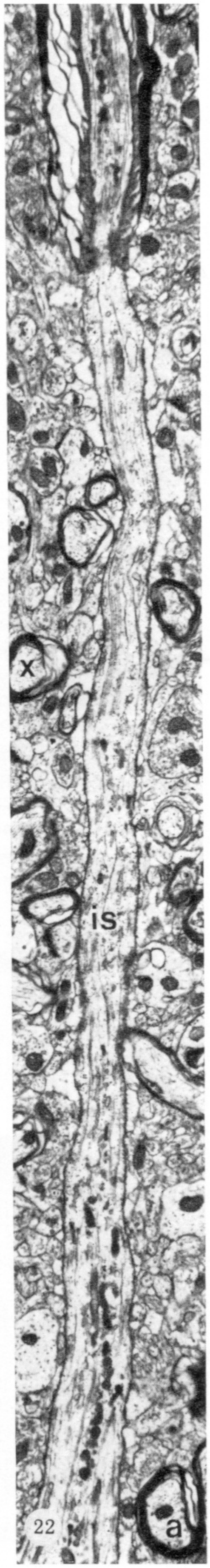

FIGURES 20–22. For description see opposite.

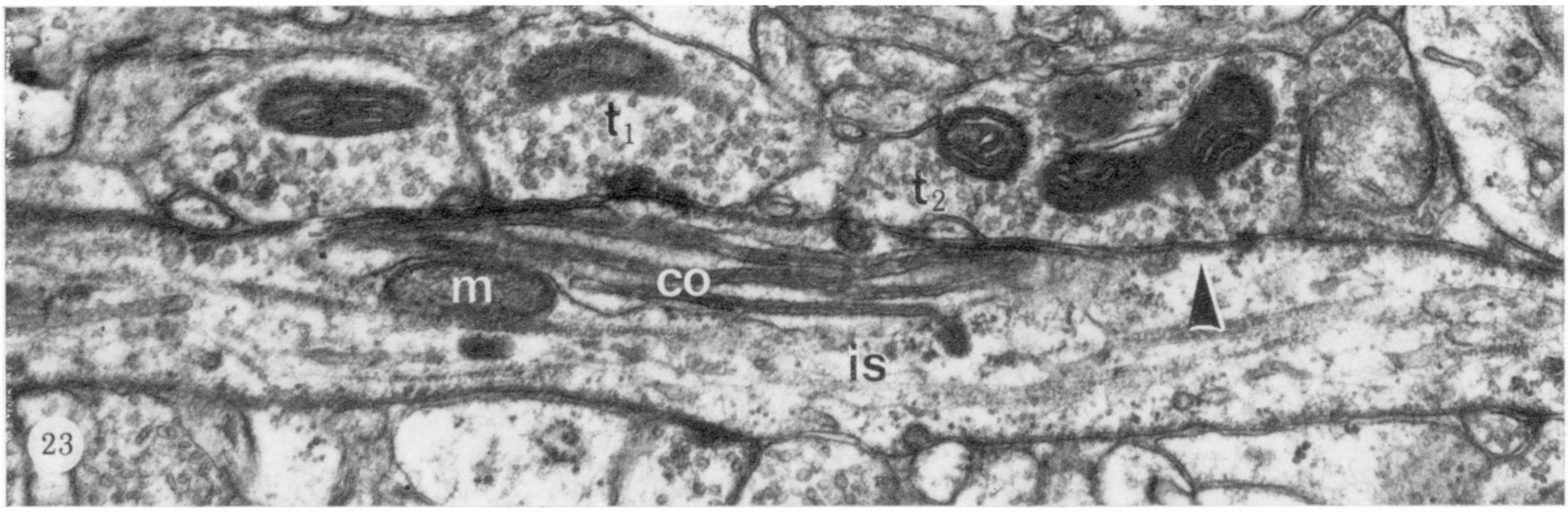

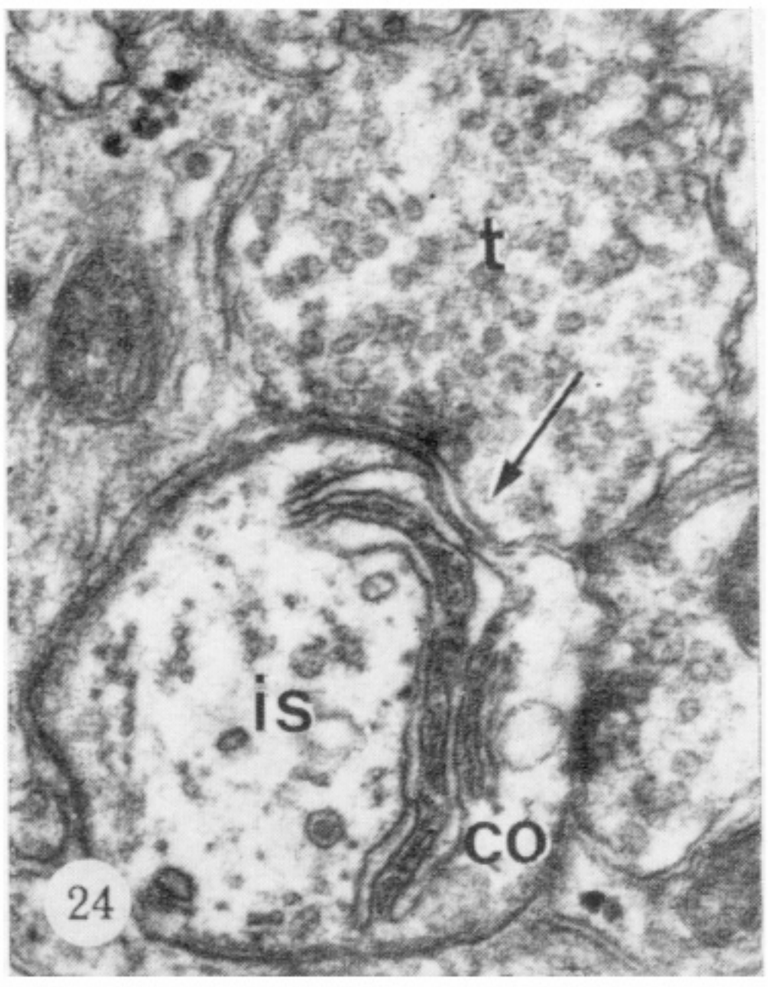

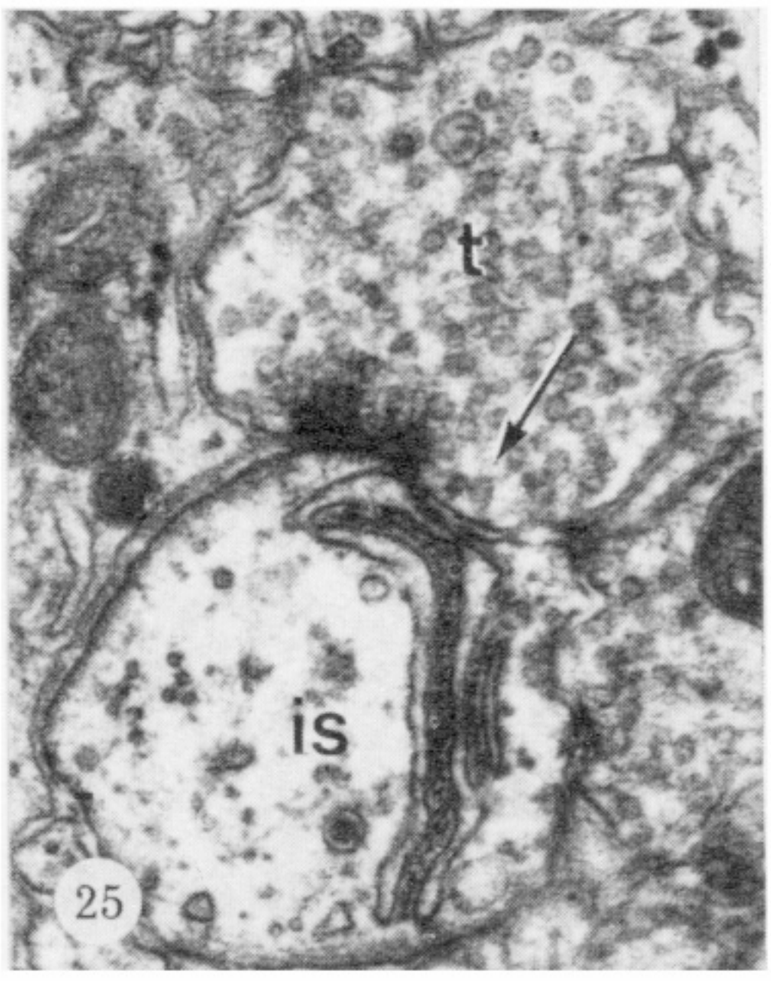

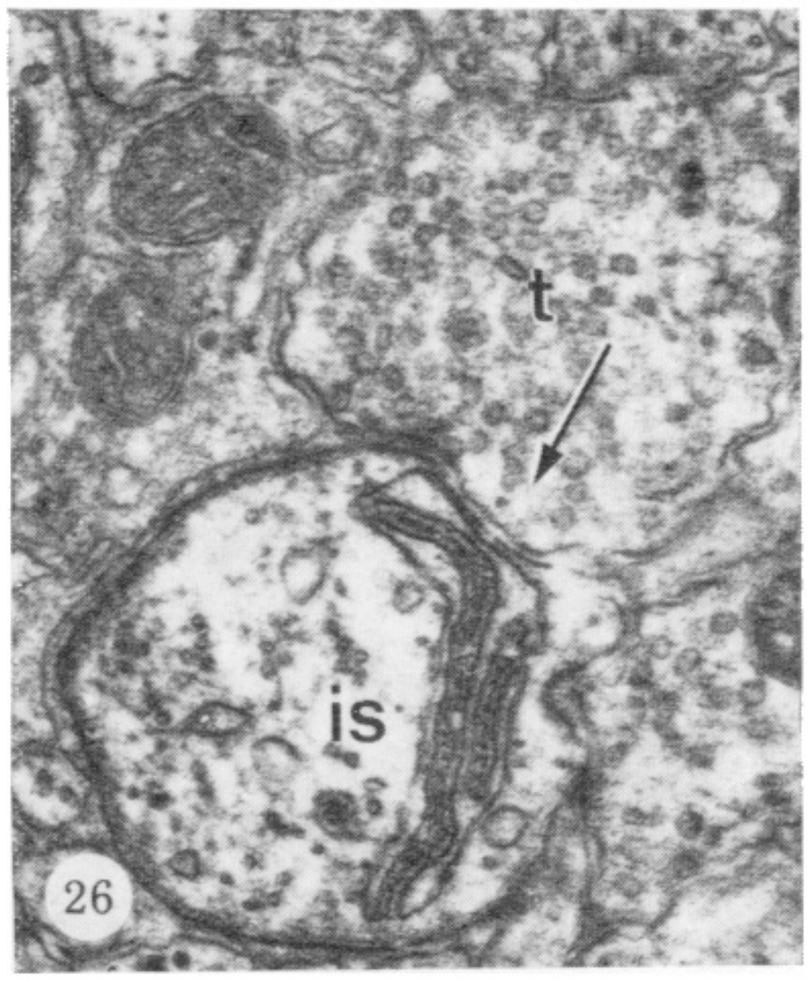

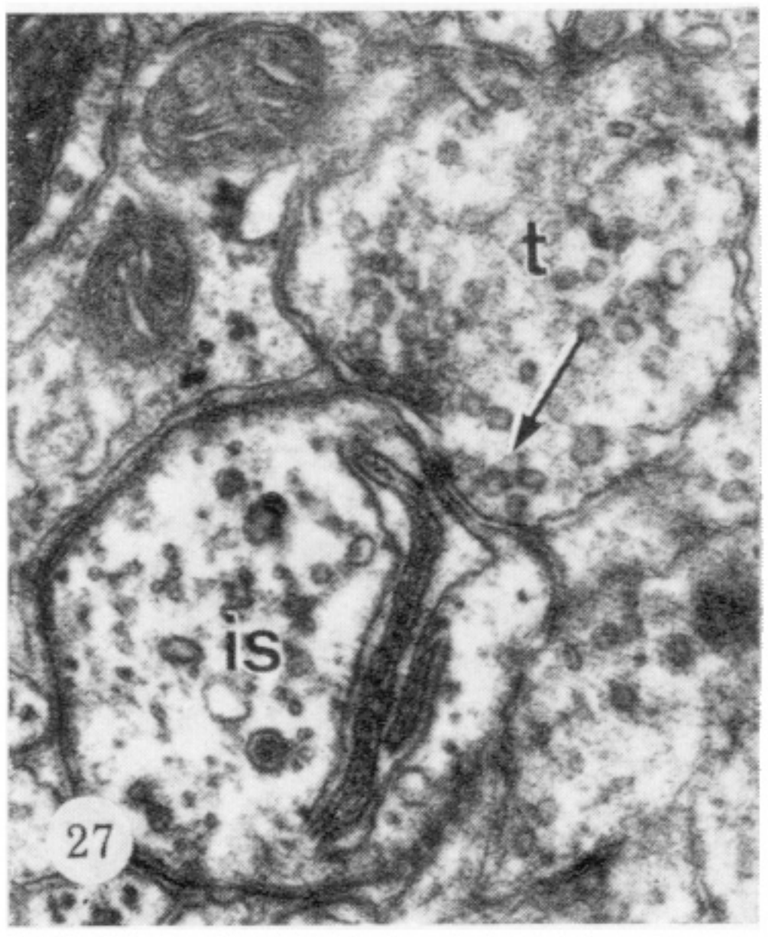

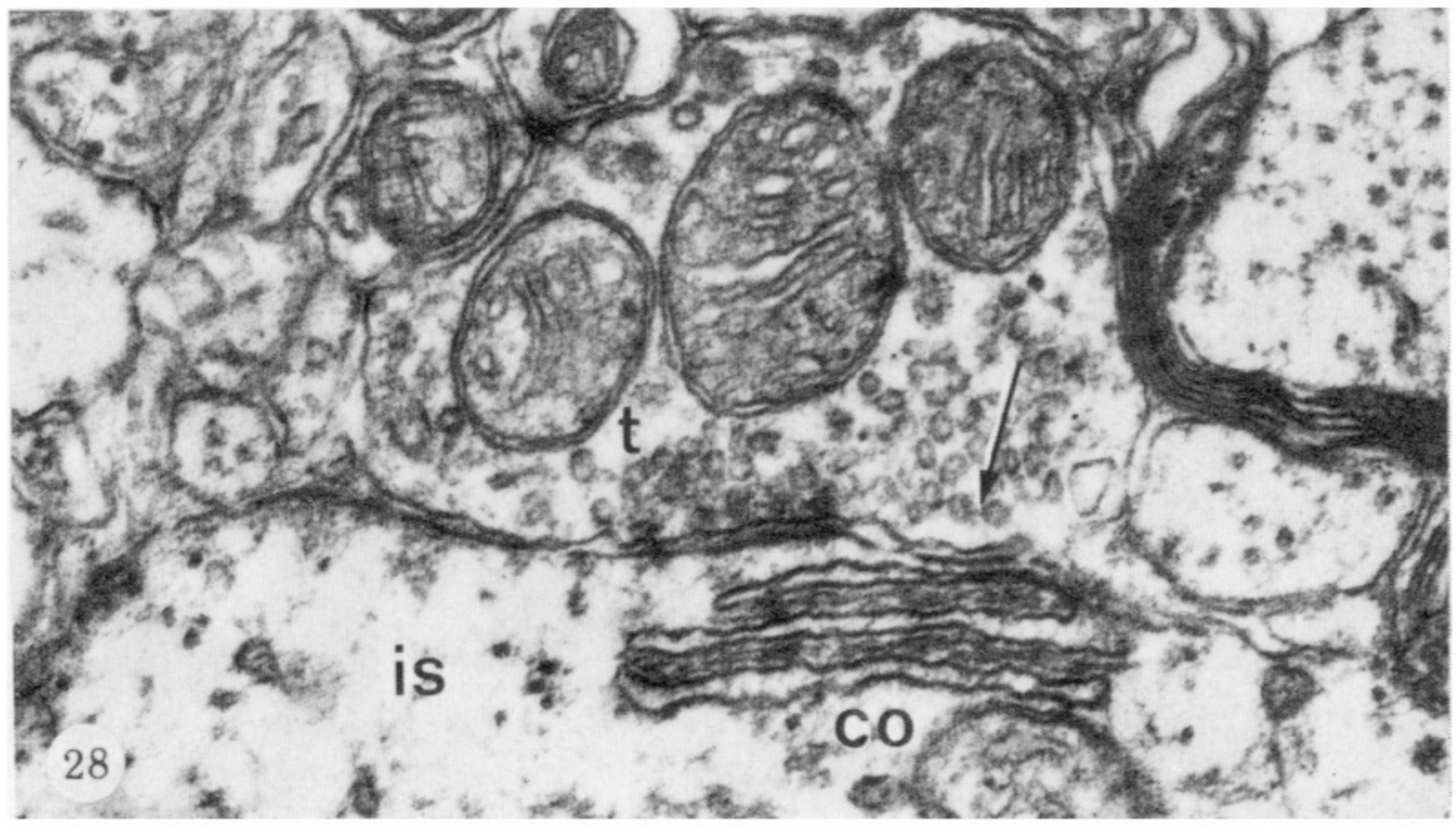

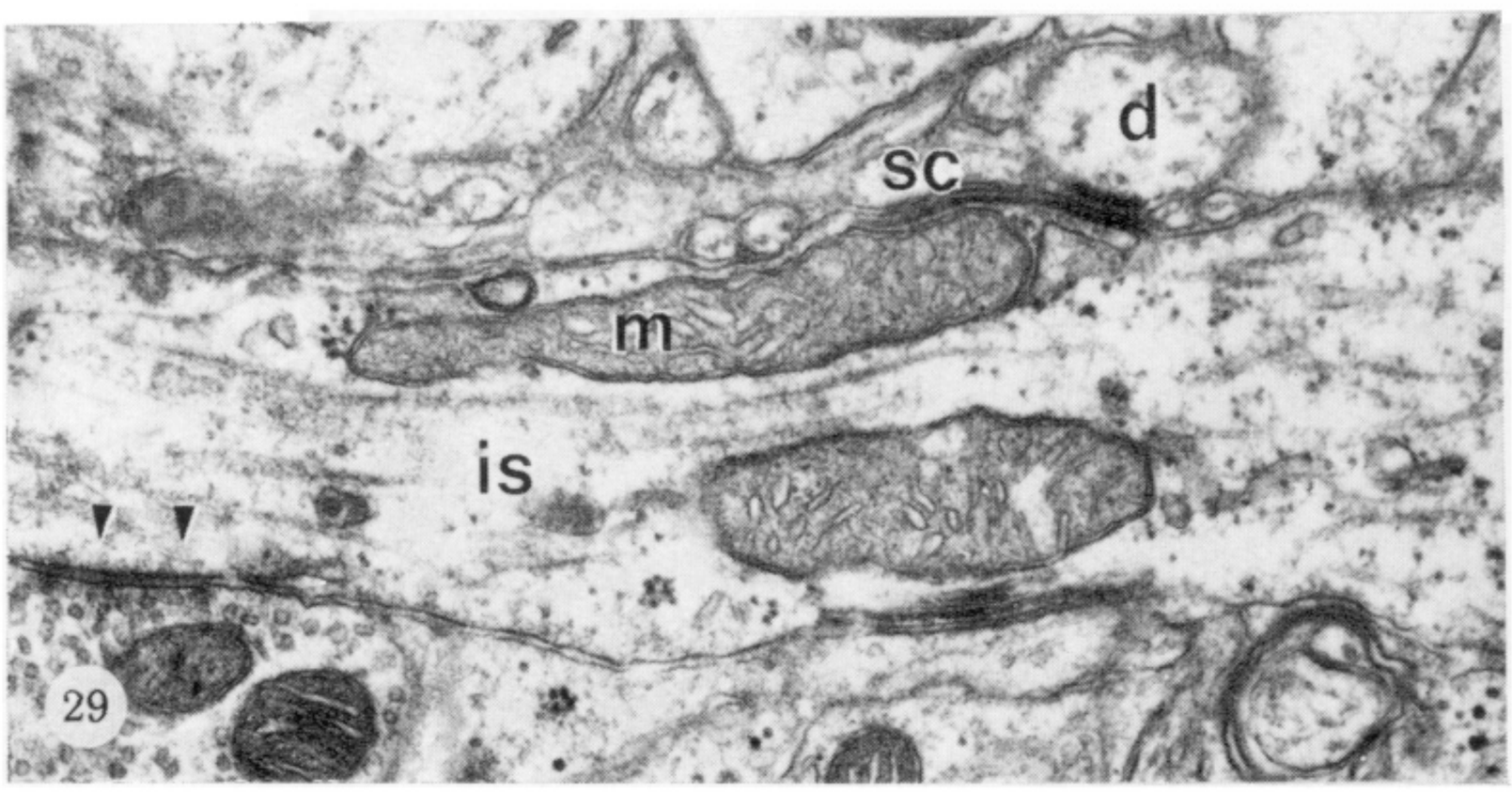

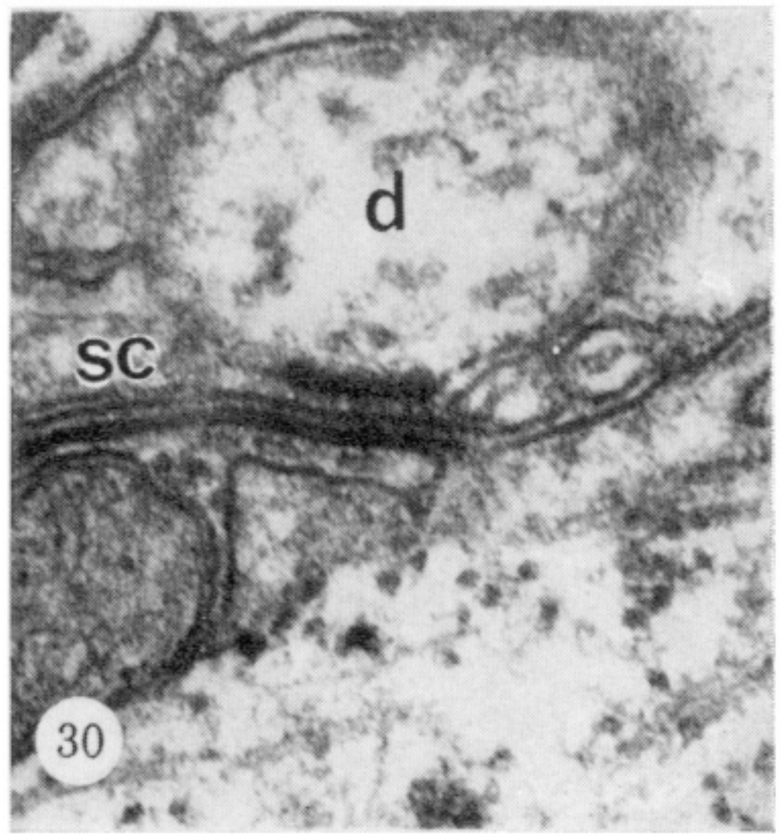

FIGURES 23–30. For description see opposite.

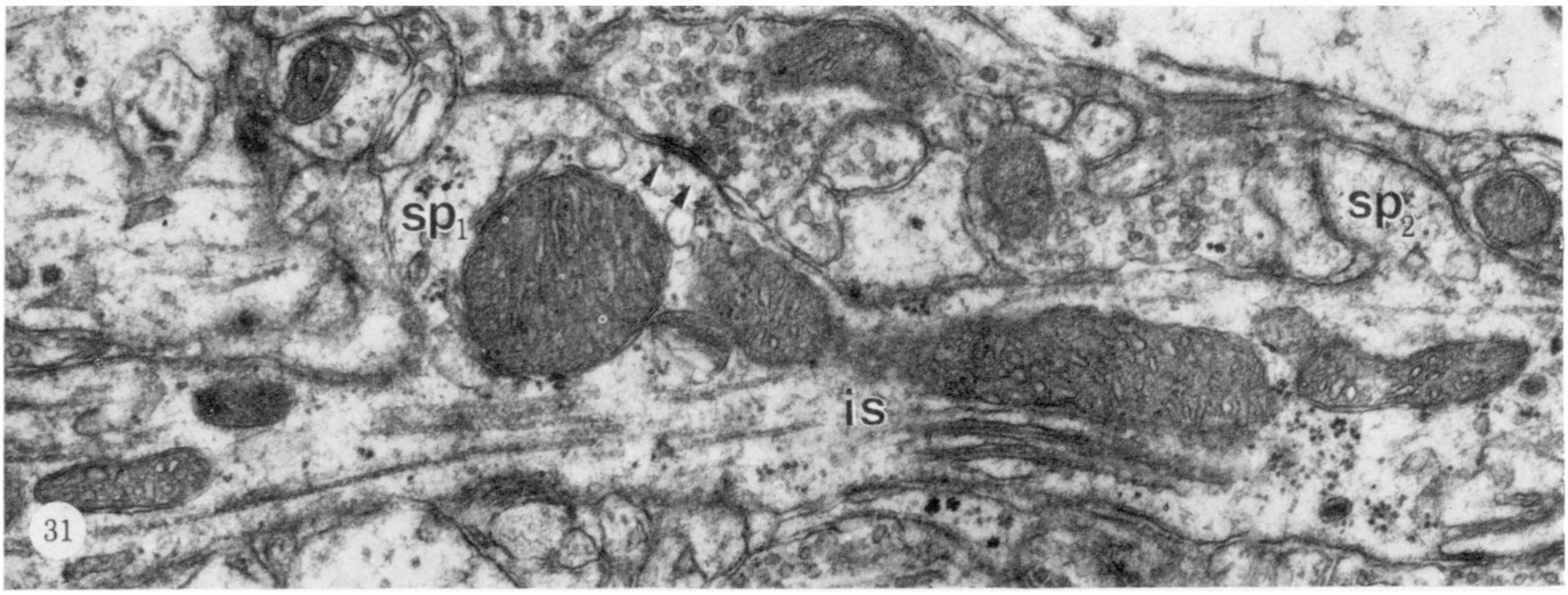

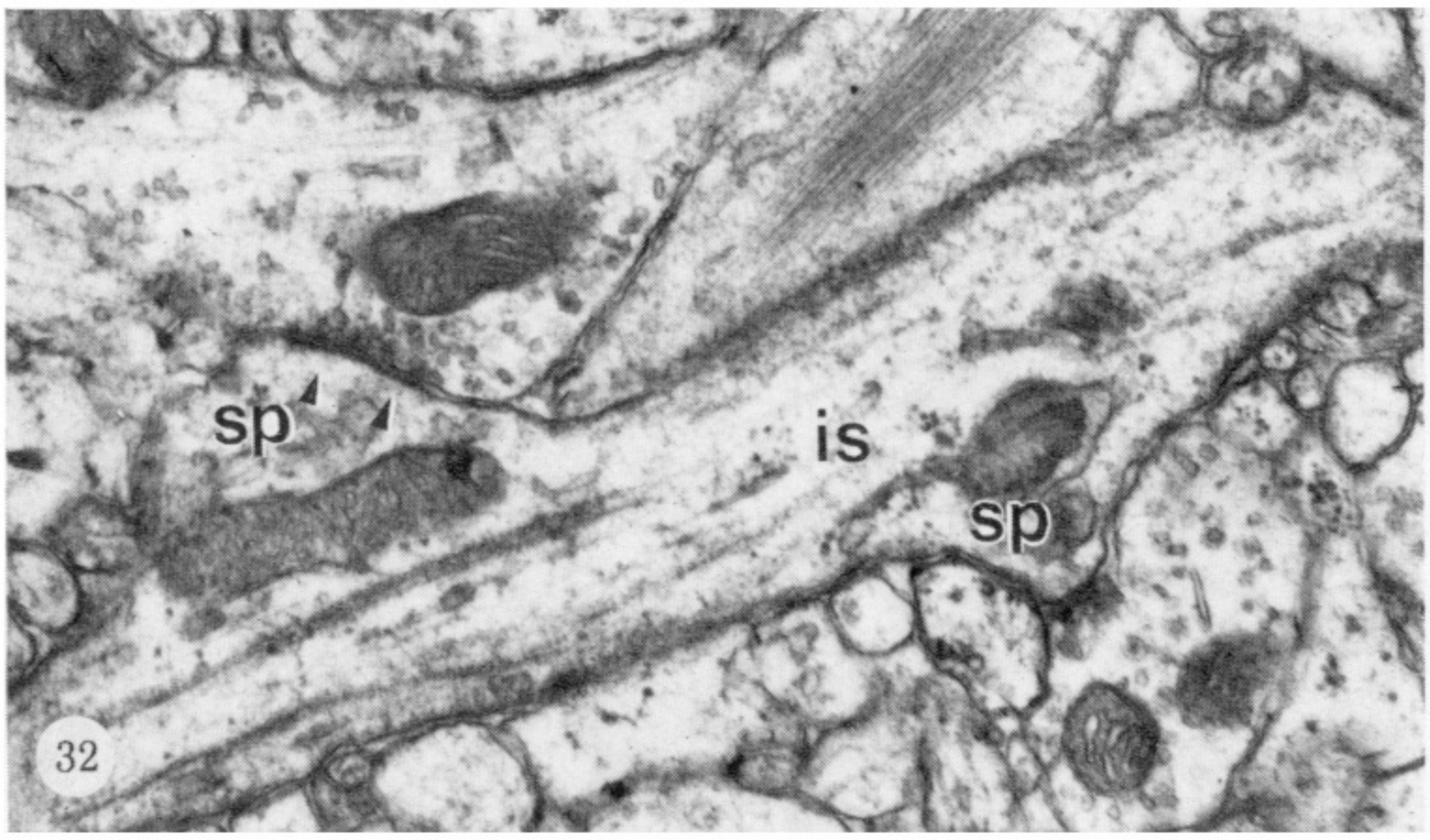

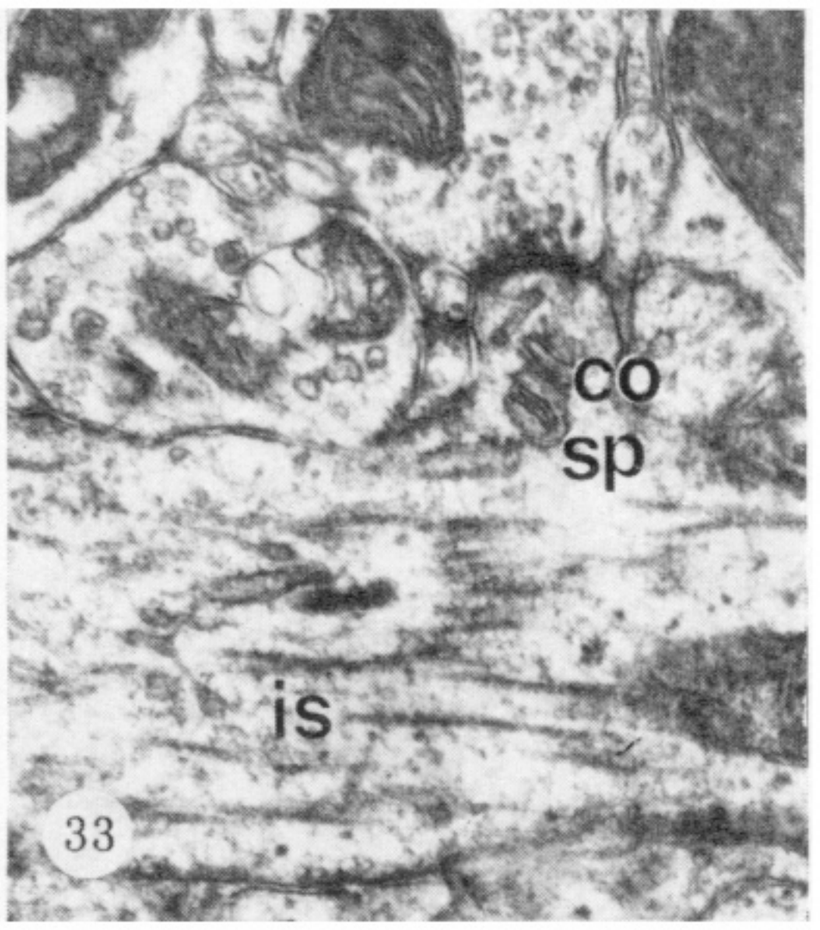

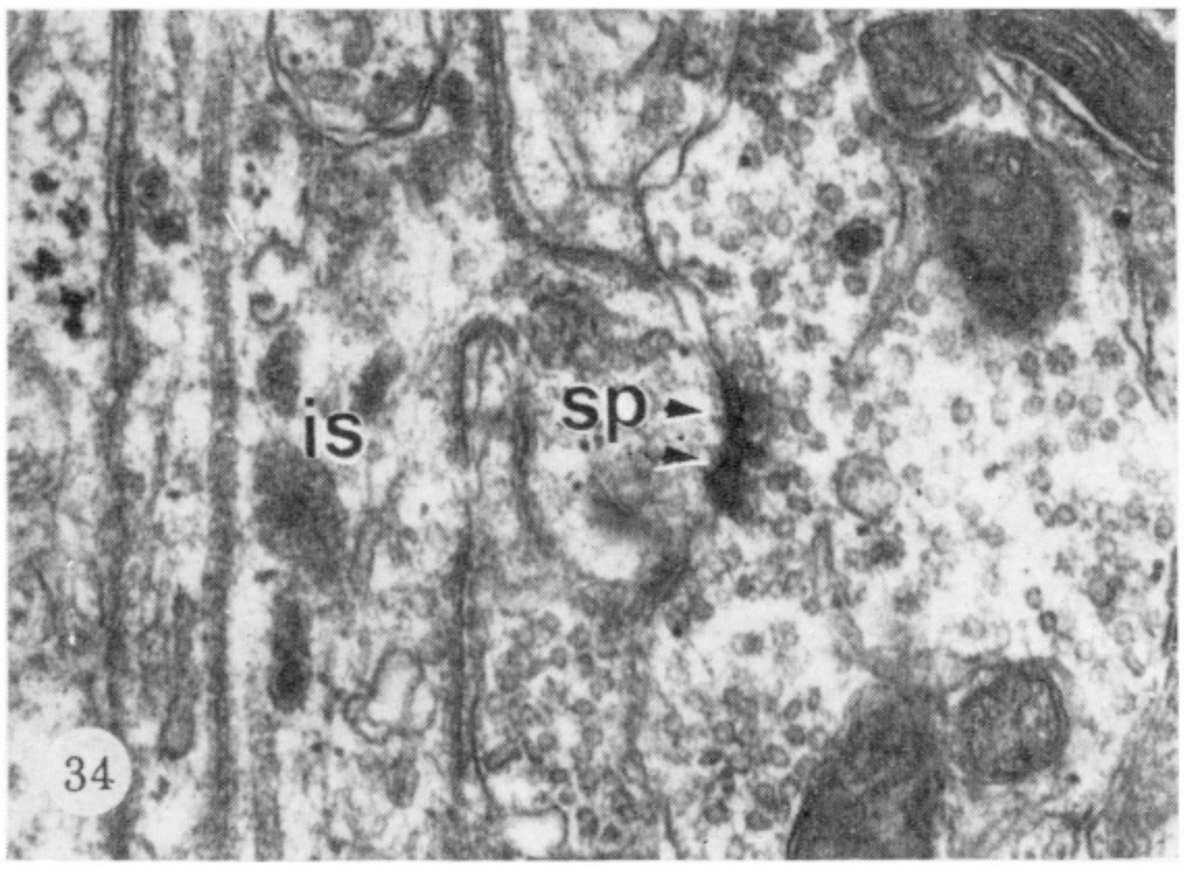

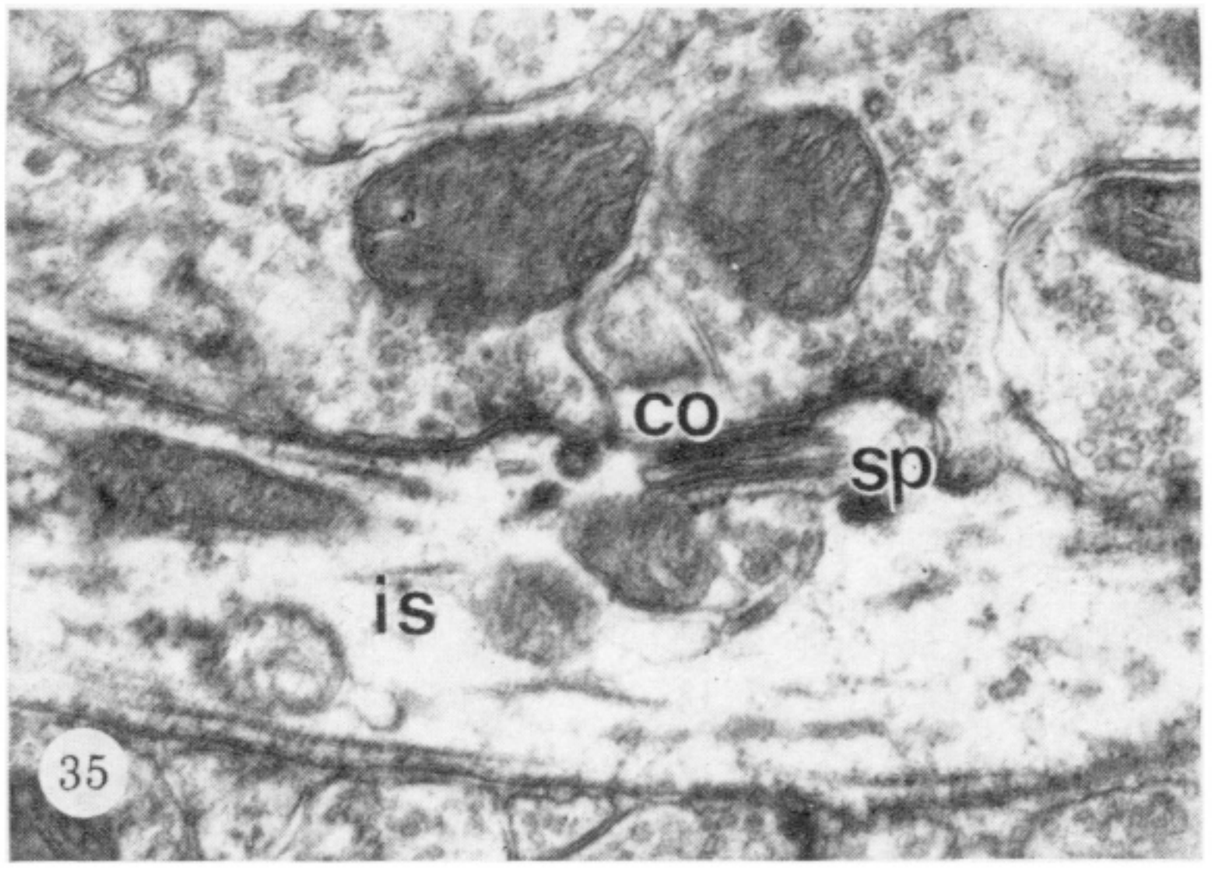

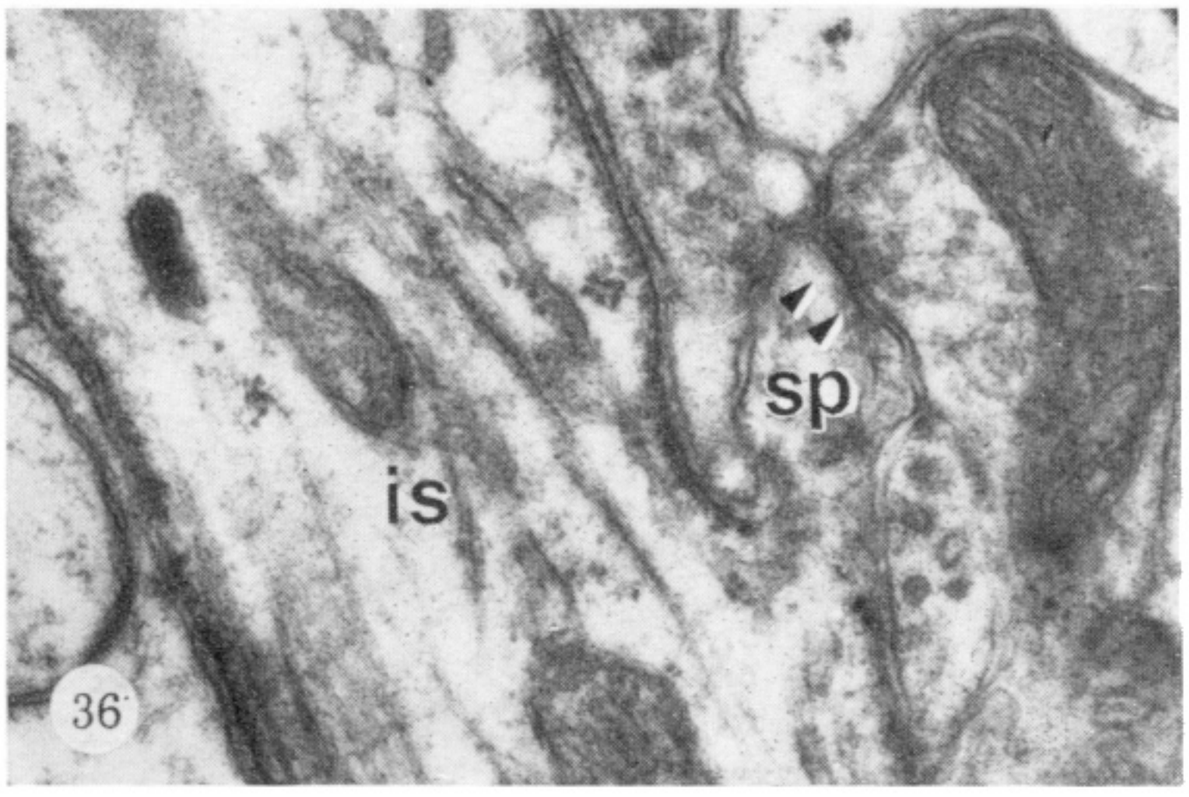

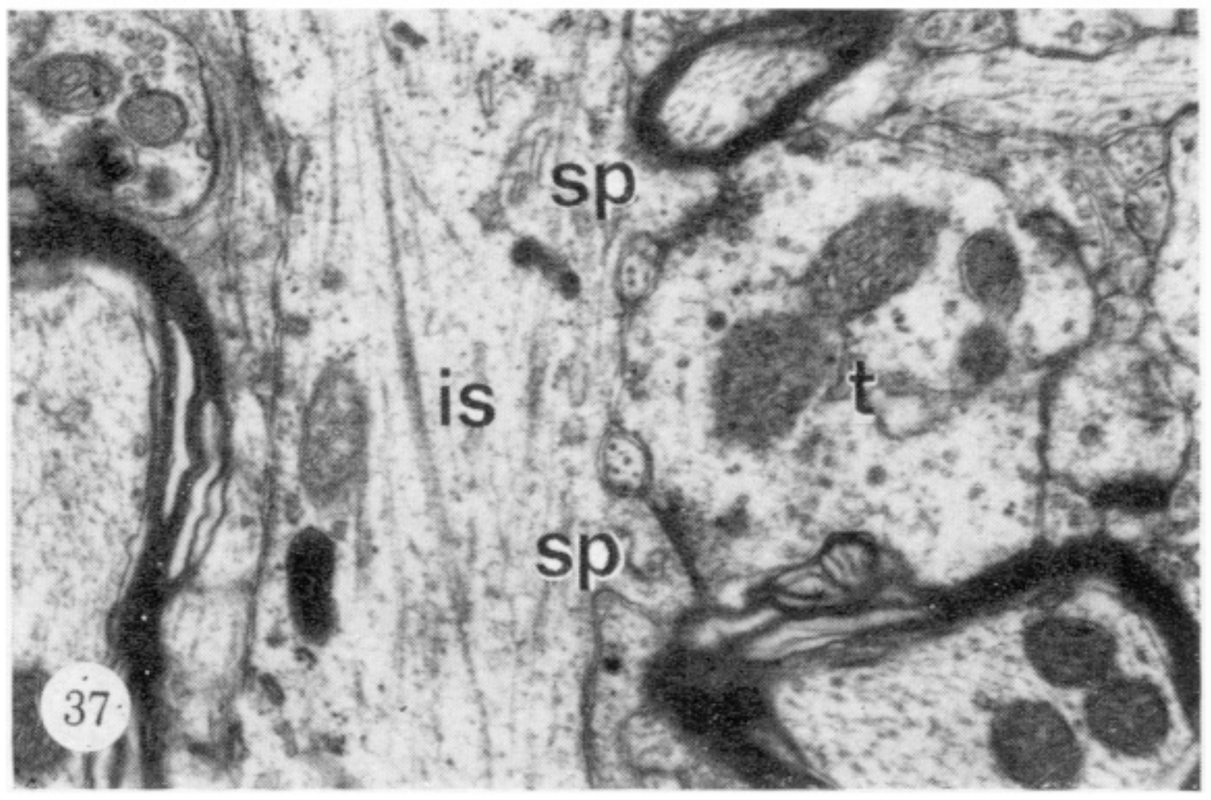

FIGURES 31–37. For description see opposite.

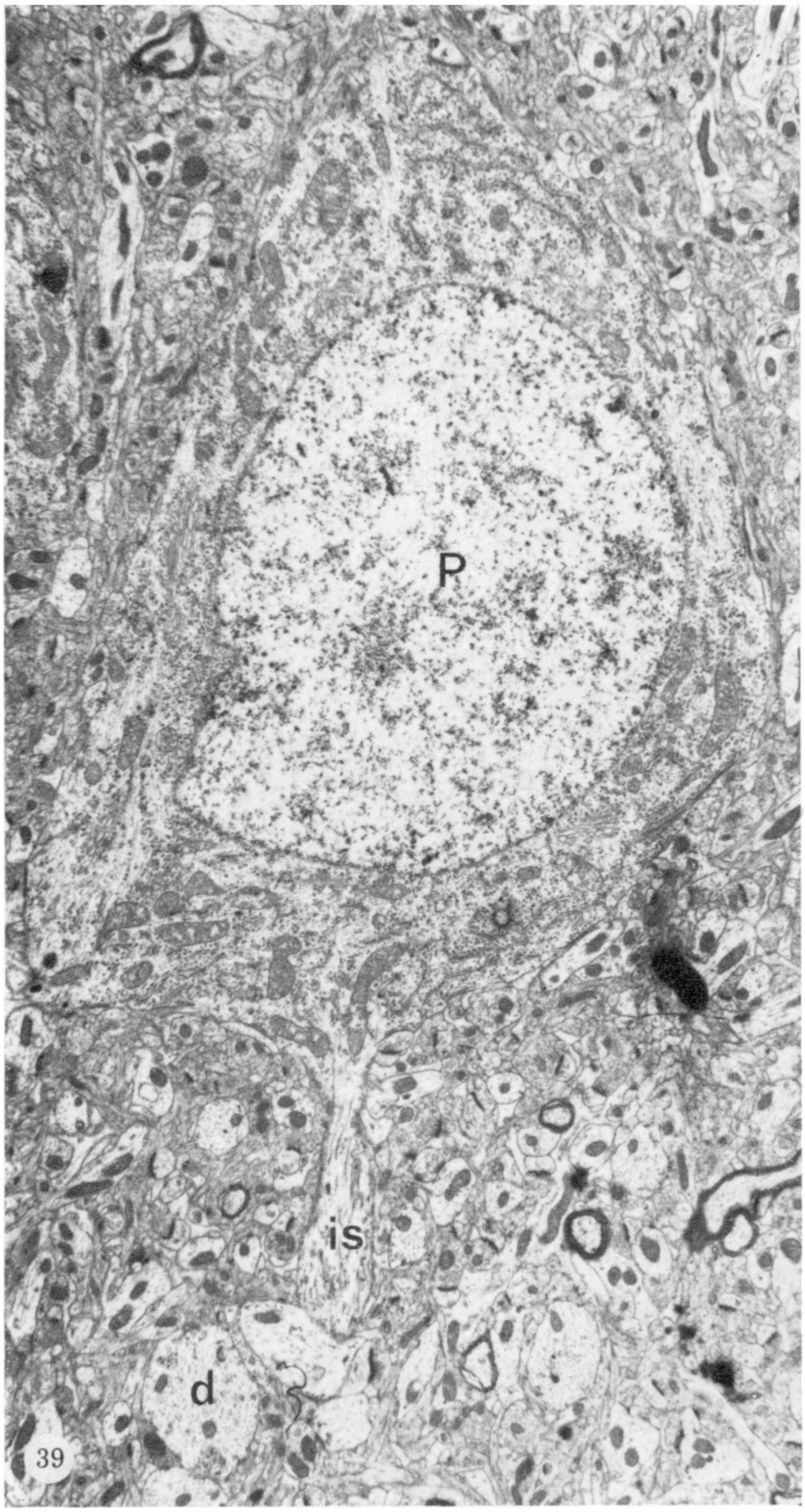

39

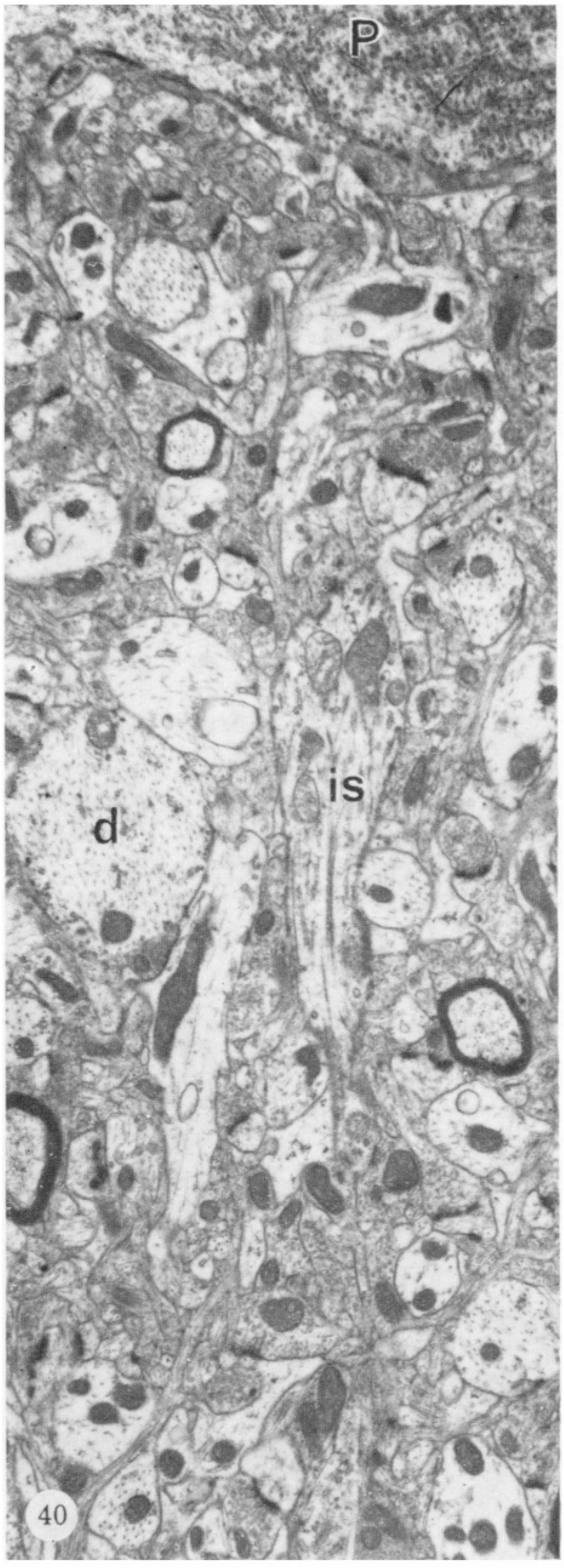

40

41

FIGURES 39–41. For description see opposite.

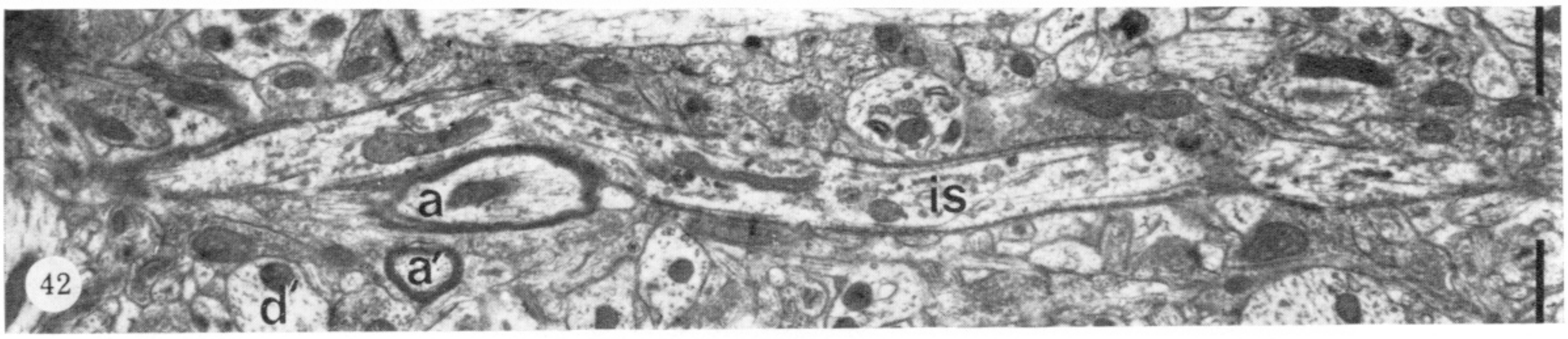

42

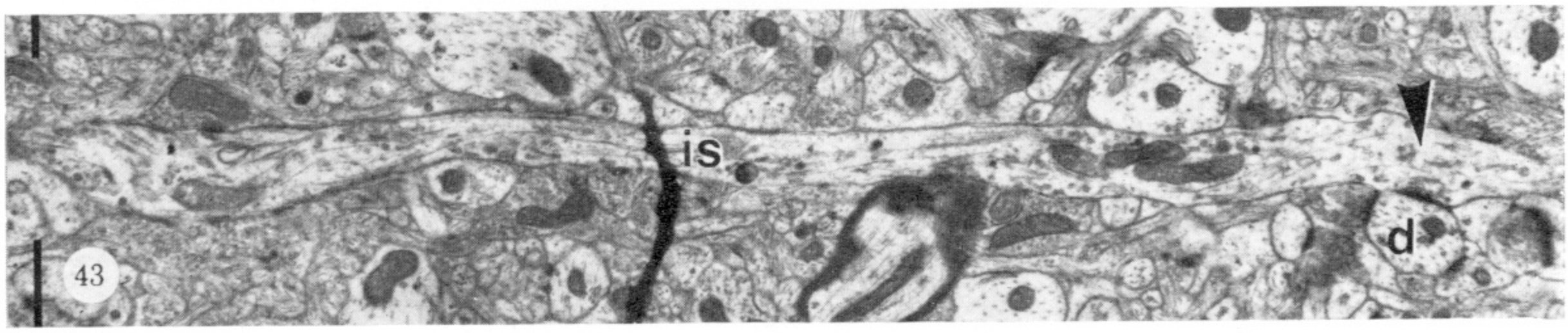

43

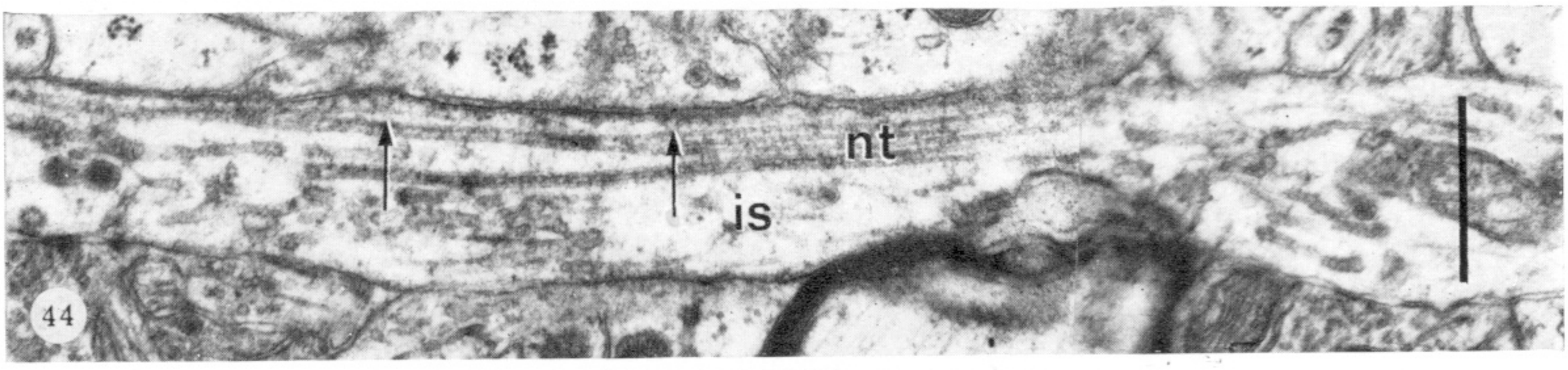

44

45

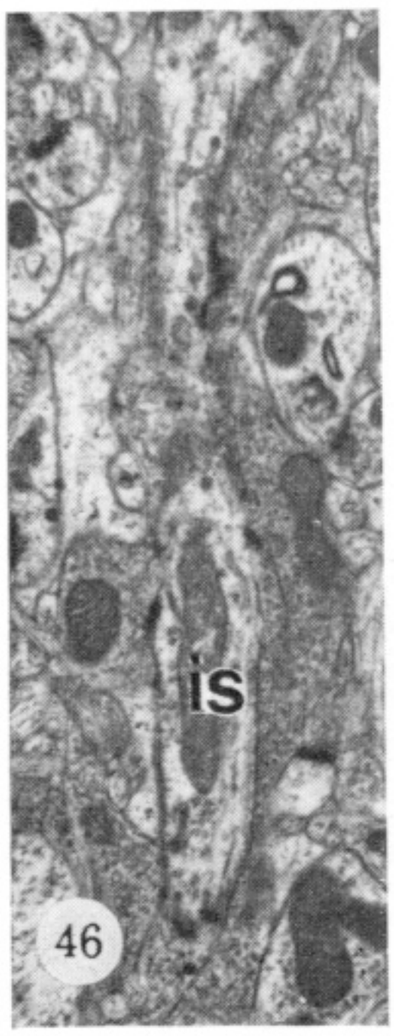

46

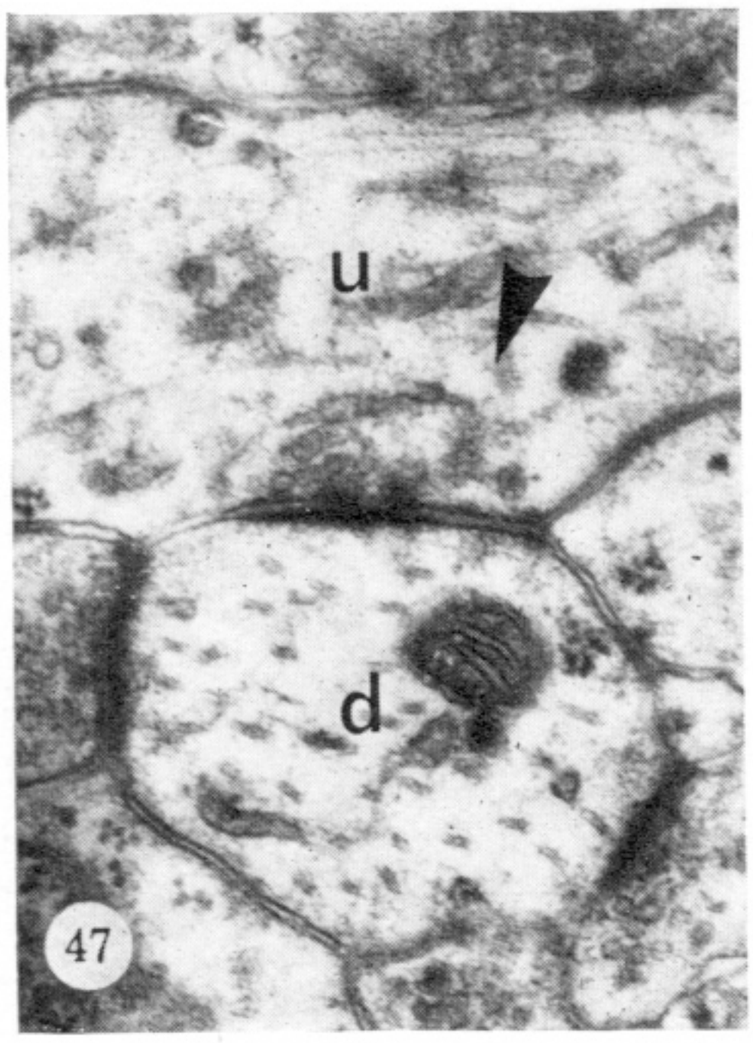

47

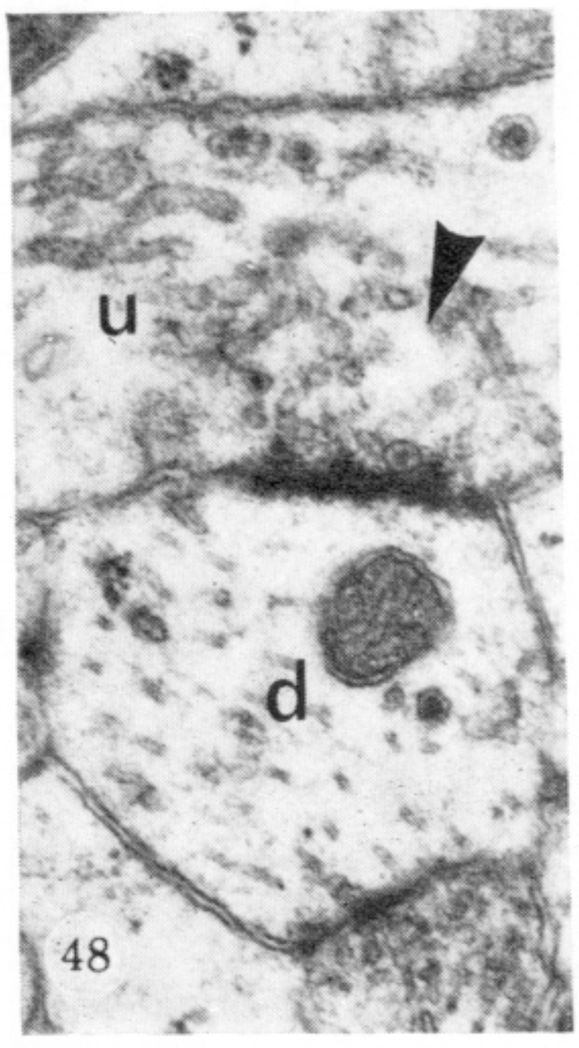

48

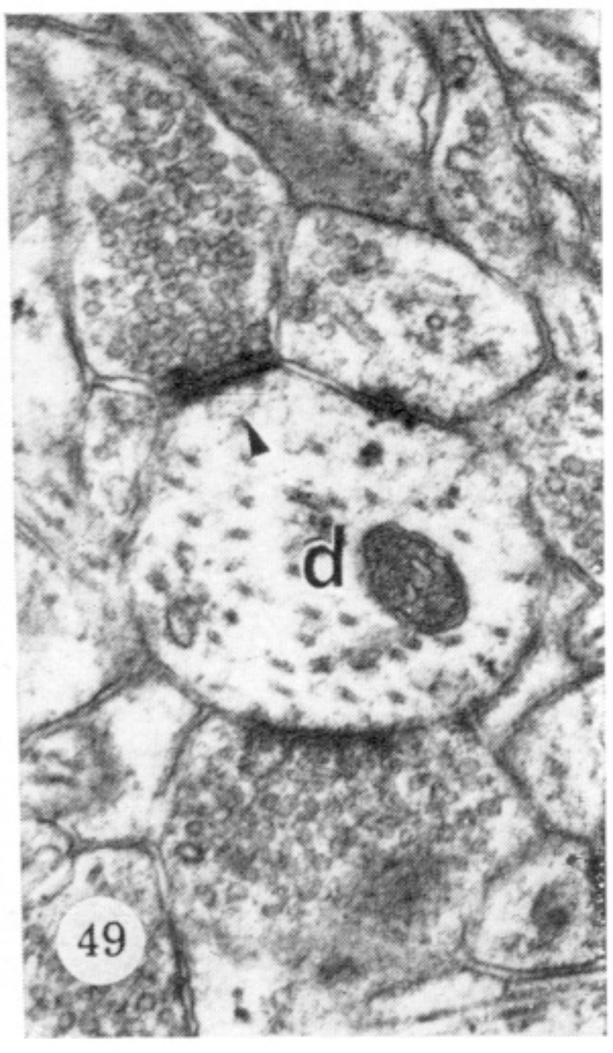

49

FIGURES 42–49. For description see page 182.

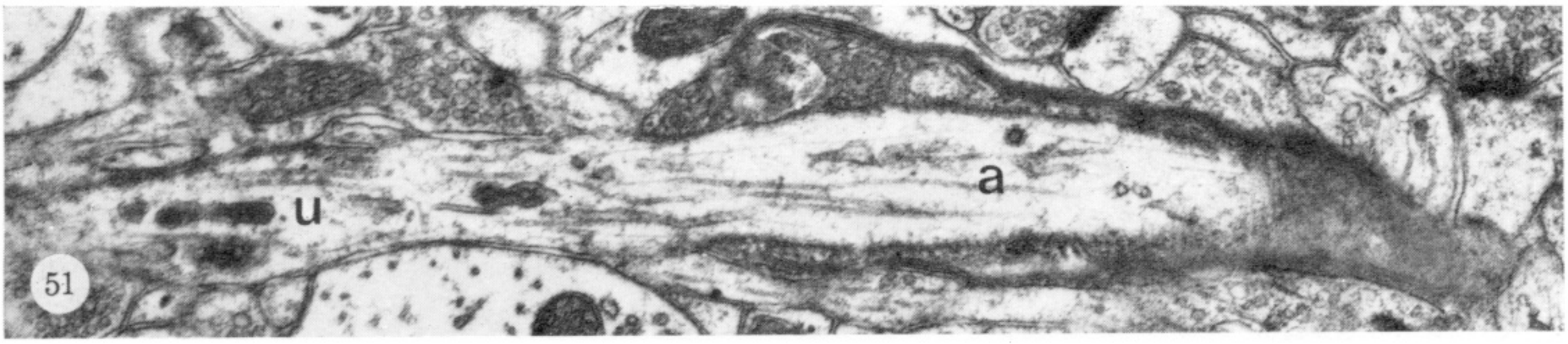

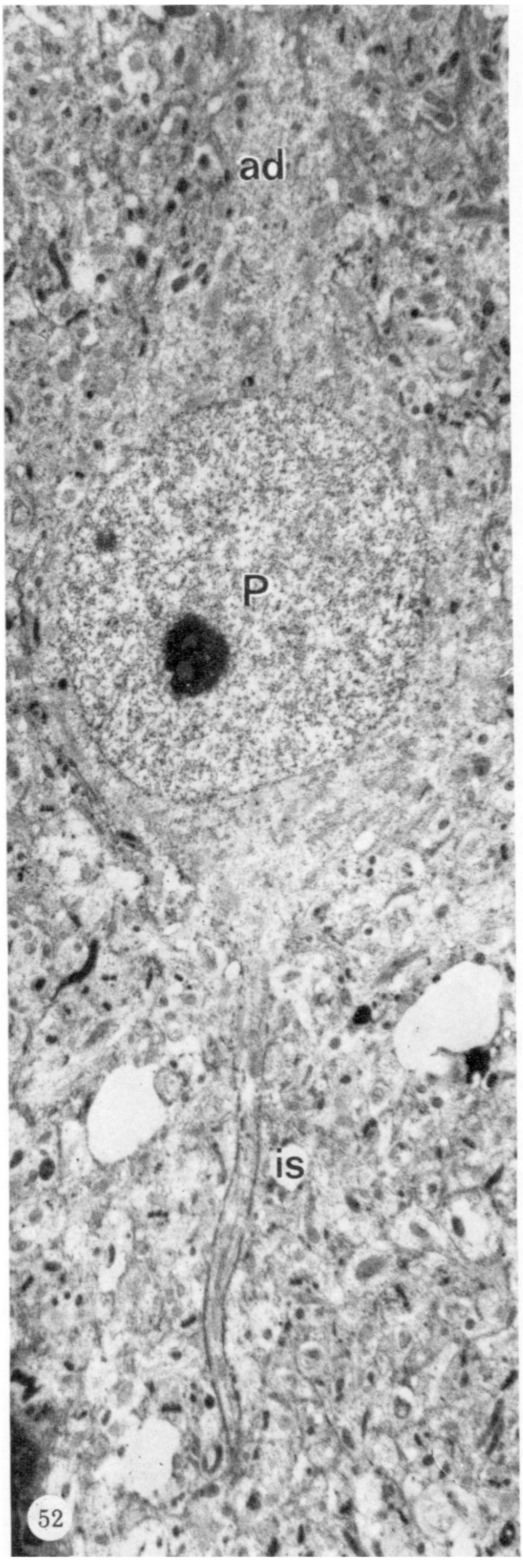

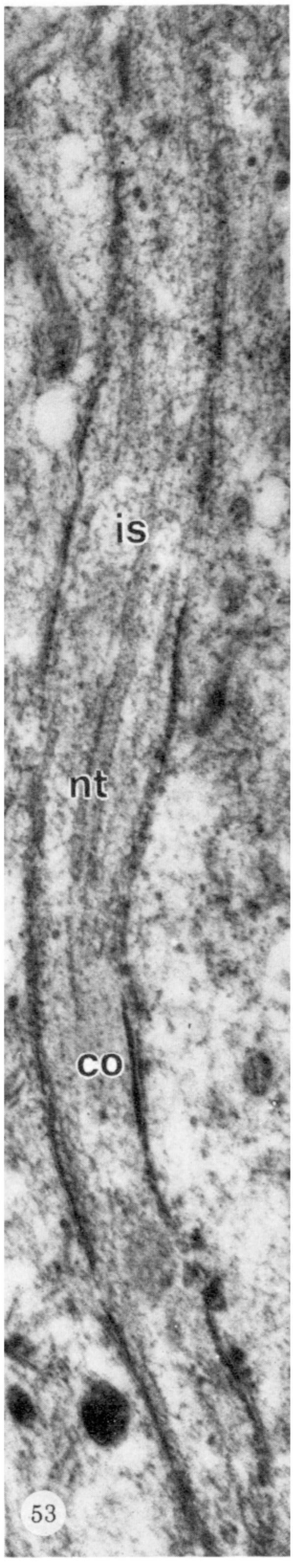

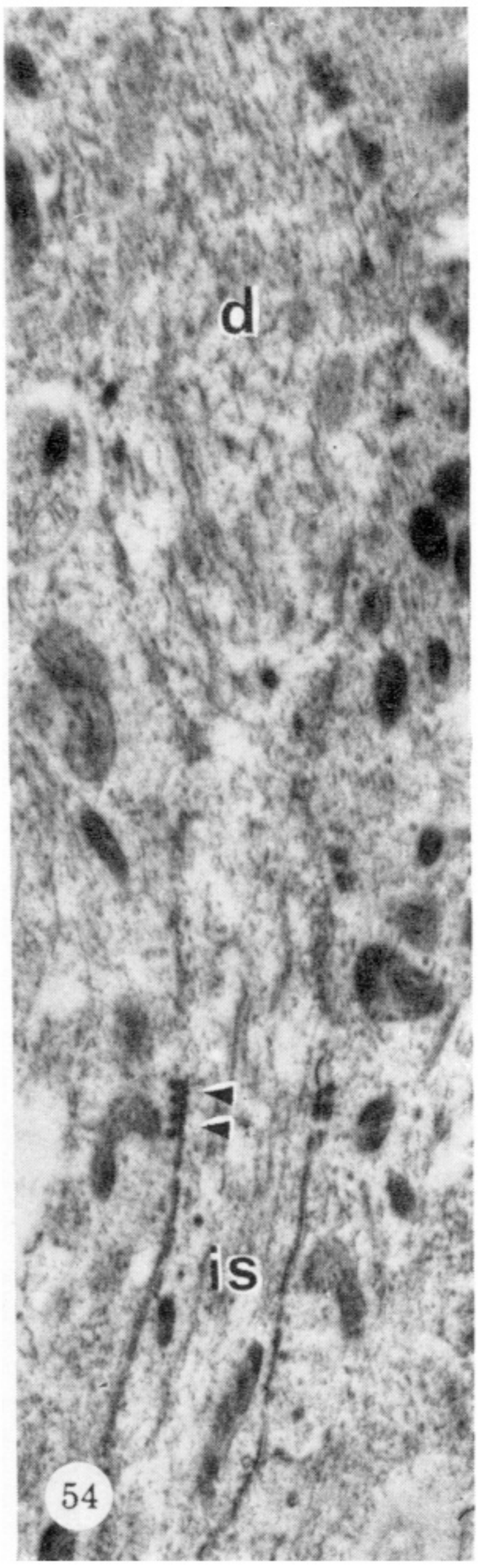

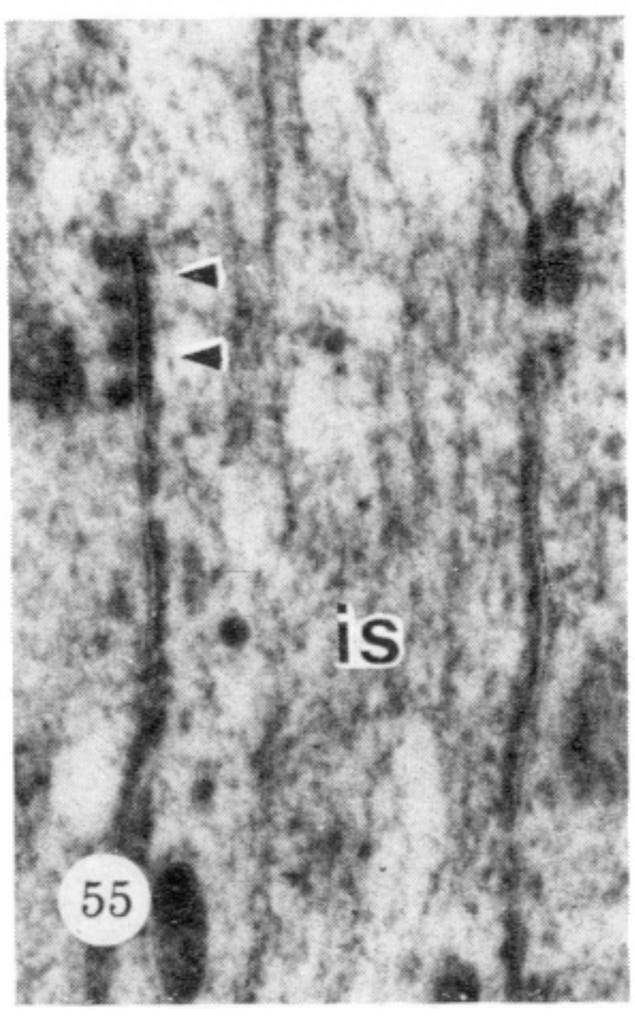

FIGURES 51–55. For description see page 183.

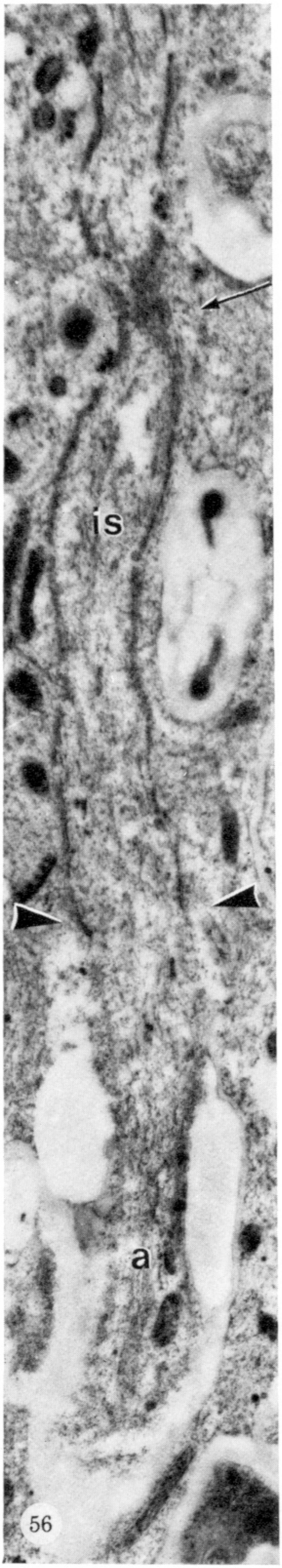

56

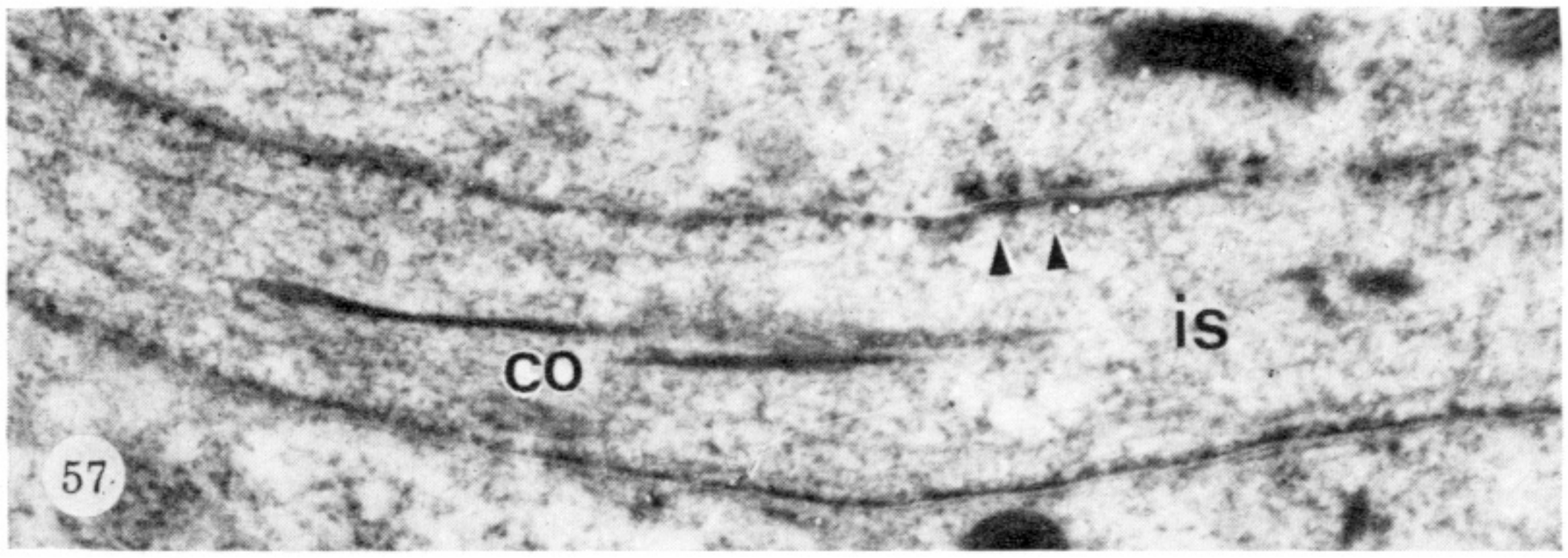

57

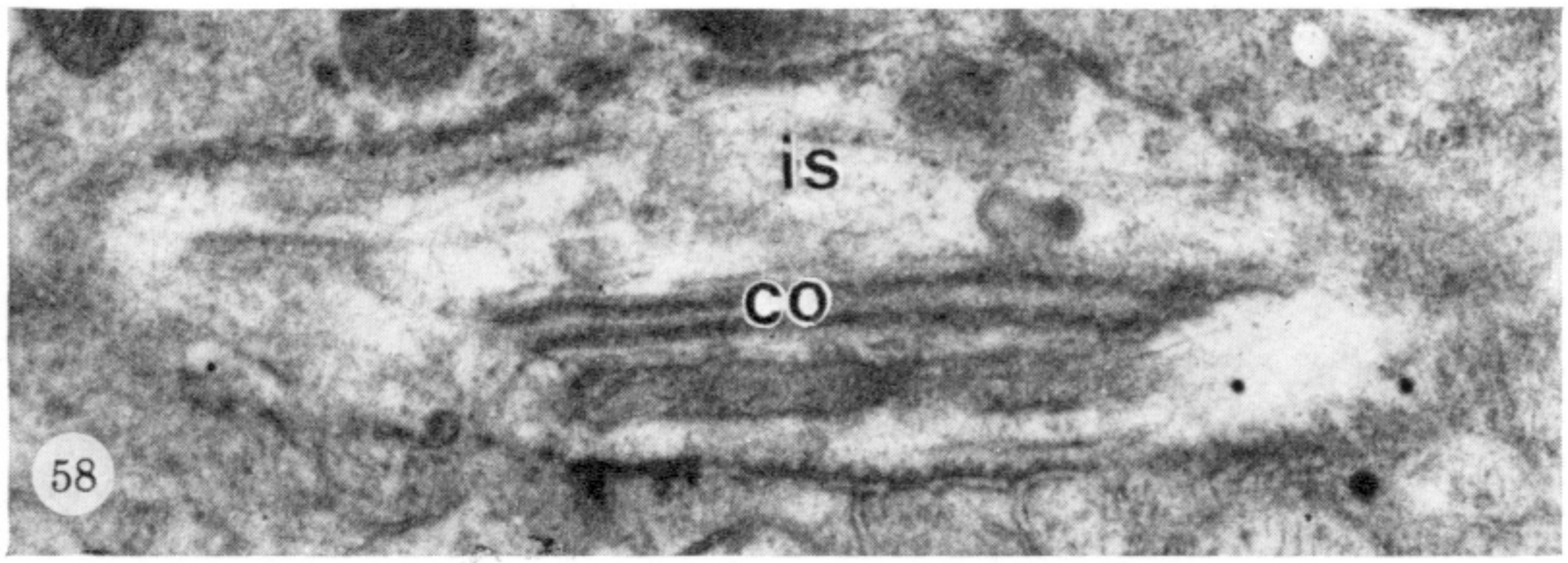

58

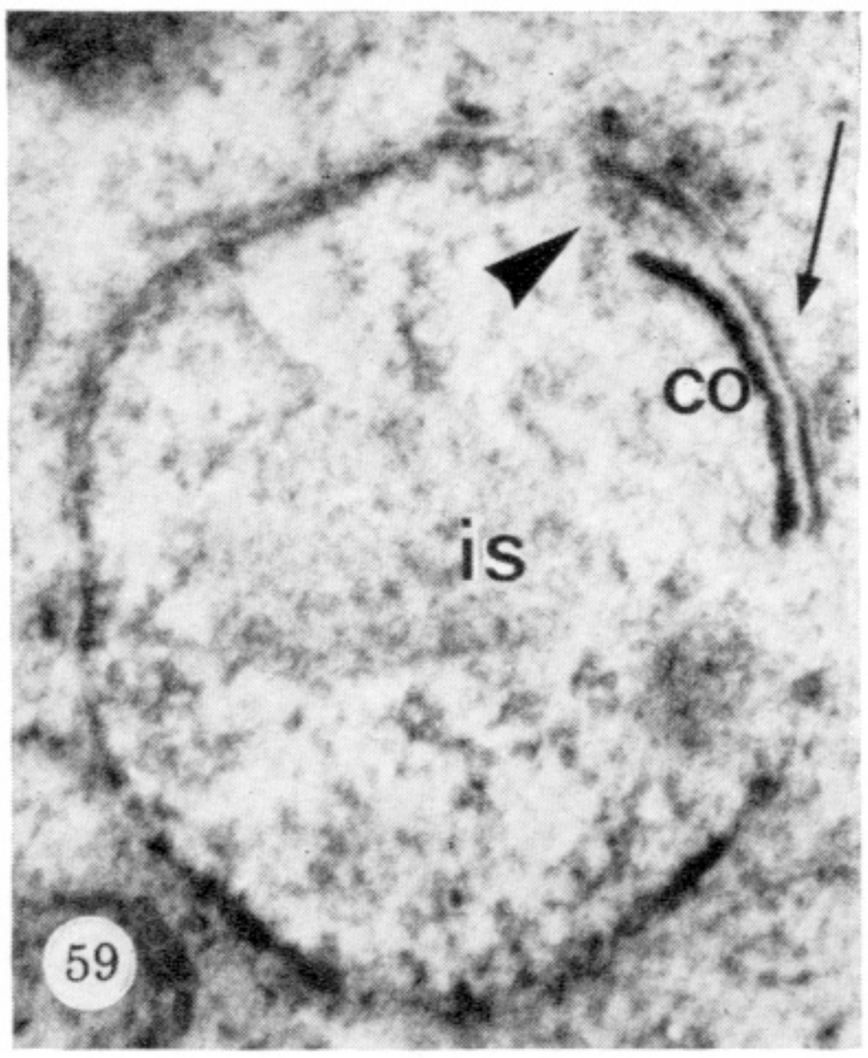

59

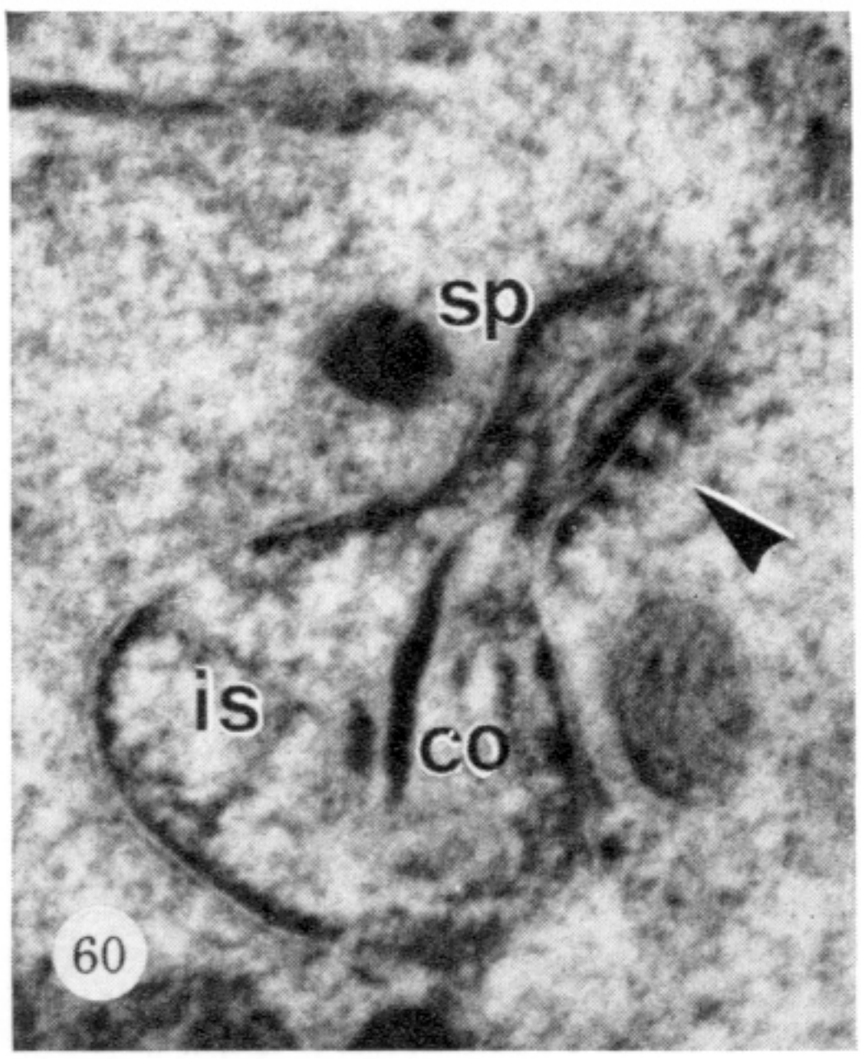

60

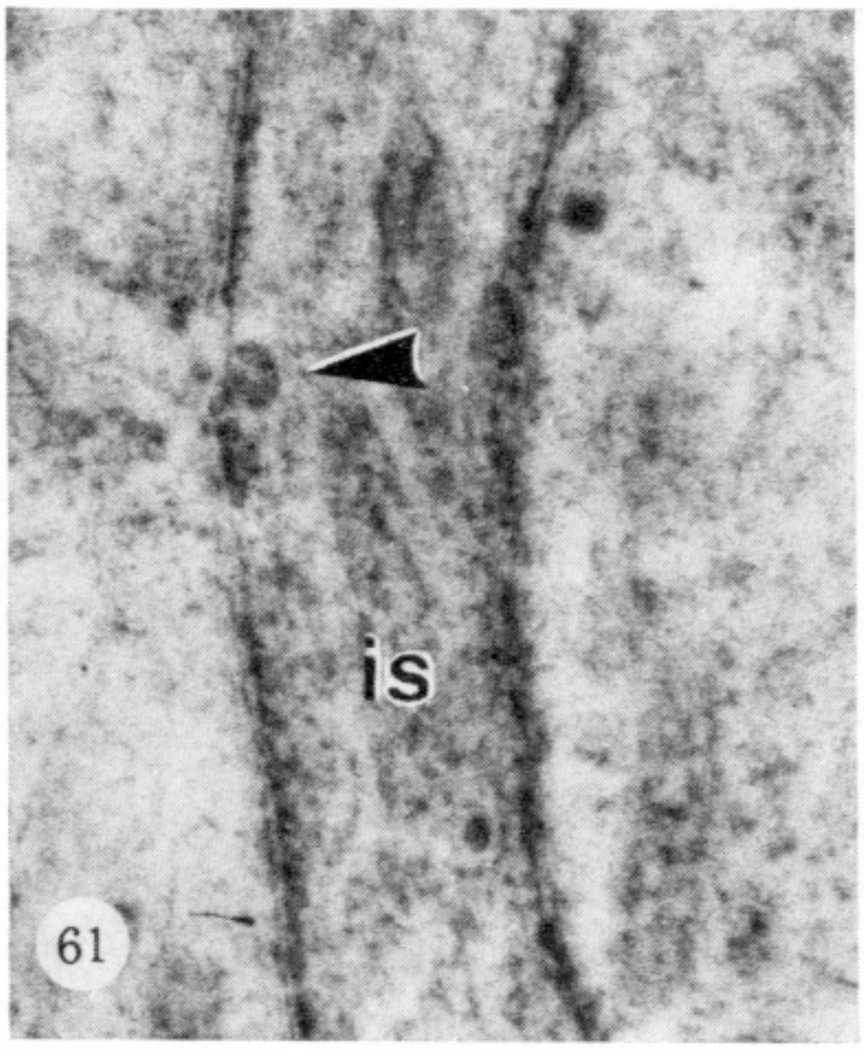

61

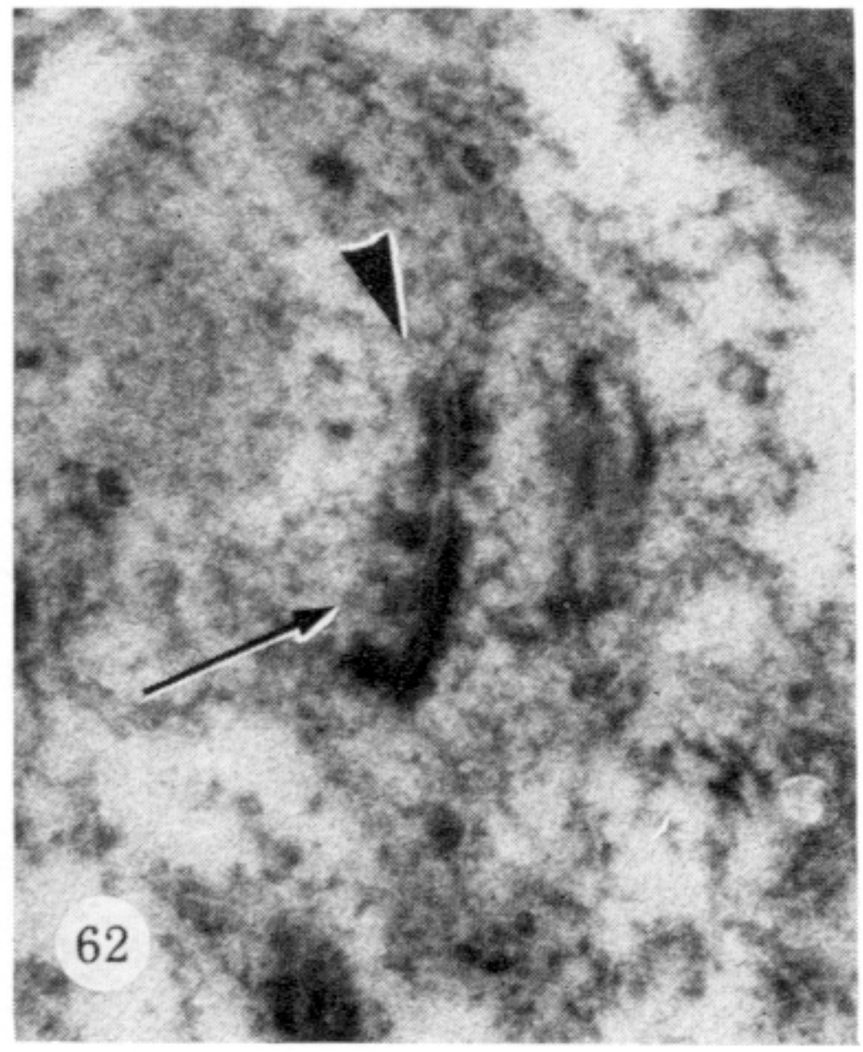

62

FIGURES 56–62. For description see opposite.